A LINK BETWEEN TGF-β SIGNALLING PATHWAYS AND NUCLEOLUS FUNCTION IN *DROSOPHILA MELANOGASTER*

ANDREIA CLÁUDIA PEREIRA CORREIA

Dissertação de Mestrado em Bioquímica

Universidade do Porto
Faculdade de Ciências
Instituto de Ciências Biomédicas Abel Salazar

2012

ANDREIA CLÁUDIA PEREIRA CORREIA

A LINK BETWEEN TGF-β SIGNALLING PATHWAYS AND NUCLEOLUS FUNCTION IN *DROSOPHILA MELANOGASTER*

Dissertação de Candidatura ao grau de Mestre em Bioquímica da Universidade do Porto

Orientador – Torcato Martins
Categoria – Investigador Doutorado Integrado
Afiliação – Instituto Biologia Molecular e Celular, Universidade do Porto

2012

A viagem não acaba nunca. Só os viajantes acabam. E mesmo estes podem prolongar-se em memória, em lembrança, em narrativa. Quando o visitante sentou na areia da praia e disse:

"Não há mais o que ver", saiba que não era assim. O fim de uma viagem é apenas o começo de outra. É preciso ver o que não foi visto, ver outra vez o que se viu já, ver na primavera o que se vira no verão, ver de dia o que se viu de noite, com o sol onde primeiramente a chuva caía, ver a seara verde, o fruto maduro, a pedra que mudou de lugar, a sombra que aqui não estava. É preciso voltar aos passos que foram dados, para repetir e para traçar caminhos novos ao lado deles. É preciso recomeçar a viagem. Sempre.

José Saramago

Agradecimentos

Enfim, mais uma viagem quase terminada. Chegou o momento em que olhamos para trás e começamos a ser invadidos por aquela nostalgia típica de quando sentimos que o tempo passou demasiado depressa, sem nos ter deixado saborear cada momento como gostaríamos...mas as memórias perduram, e a recordação do que passou e do que aprendi nestes dois anos de Mestrado é um tesouro que ficará sempre guardado.

O Mestrado de Bioquímica trouxe-me para esta cidade maravilhosa que é o Porto há precisamente dois anos. Devo bastante ao Ricardo que, mesmo na minha ausência, fez sempre força para integrarmos o Mestrado, apesar de todas as barreiras que nos foram colocadas. Assim, agradeço à Universidade do Porto e à comissão do Mestrado por nos ter acolhido, e espero sinceramente o nosso esforço e dedicação tenham de alguma forma contribuído para que seja dado maior valor aos alunos de Genética e Biotecnologia vindos da UTAD. Queria também agradecer em especial à Professora Maria João Saraiva pela sua posição como minha tutora e por toda a orientação e disponibilidade, na concretização deste projeto.

Durante o ano curricular foram muitos os momentos que nunca vou esquecer, passados com pessoas também elas inesquecíveis. Aulas, trabalhos, jantares, festas, e principalmente muitas horas de estudo no velho ICBAS. Quero agradecer muitos desses momentos a várias pessoas que de desconhecidos se tornaram amigos, como o Jorge, a Juliana, a Rita, o Bruno, o Filipe, a Diana, a Leninha e o Finger. E claro, um obrigado muito especial a vocês. À Cátia, por toda a ajuda e orientação ao início, pelas conversas e desabafos, por aquele abraço. À Je porque sendo vitoriana é uma verdadeira guerreira. Obrigado por me ouvires, obrigado por tudo. Ao Elísio, pelas palavras e pelos conselhos, pelo teu ombro. E à Andreia, pelo momento mais awkward da minha vida no 200, pelos risos, pelos desabafos, pelo atum, por todas as conversas. Adoro-vos.

Chegado o segundo ano de Mestrado voltei para a minha paixão: a Genética. E não podia ter corrido melhor. O "Developmental Biology Lab", na altura constituído apenas pelo Torcato e pelo Paulo, recebeu-me de braços abertos. Foi neste laboratório que eu dei os primeiros passos na verdadeira Ciência. E é do fundo do coração que agradeço a todos. À Lígia pela simpatia, pelas conversas, pelos conselhos. Ao safadão do Traquete pelos desabafos e pelas conversas que tanto me ajudaram, desejo-te toda a sorte do mundo no teu futuro. À Sarinha porque dá mais luz ao laboratório. Obrigado por todo o apoio, pelas palavras no momento certo, por todos os risos. Ao Paulo, por toda a disponibilidade e orientação. Pelo incomparável

raciocínio, que nos deixa sempre a pensar. Um sincero obrigado. E finalmente ao Torcato. Nunca vou esquecer tudo o que fizeste por mim. Toda a paciência, toda a dedicação, todos os conselhos. Mais do que um professor foste um amigo. Transmitiste-me essa enorme paixão que tens pela Ciência e pela Genética, ajudaste-me sempre com um sorriso, com uma palavra amiga. Obrigado por tudo, obrigado por nunca desistires de mim, obrigado por este maravilhoso projeto, obrigado por me teres contagiado com este bichinho da ciência, do querer saber, de descobrir, de questionar...obrigado por tudo o que me ensinaste, não só como cientista mas também como pessoa.

Deixo também um obrigado a todas as pessoas que de alguma forma contribuíram para a construção deste trabalho. O Rui e a Elsa que nos aturaram tanto tempo na microscopia, a Filipa, Francisco, Paula Sampaio. Também um grande obrigado à companhia de todos os dias na sala das moscas. Sofia obrigada por todo o apoio e simpatia, Joni obrigado pelas dicas nas francesinhas, Eurico e Sara, pelas histórias e pelos sorrisos.

Também à Ana e à Telma um Obrigado. À Ana viveu comigo durante estes dois anos. És uma pessoa muito especial. Simples, carinhosa, boa ouvinte. Obrigado por todas a conversas, pelos jantares à luz da vela, pelos risos, pelo companheirismo. A Telma, porque esteve sempre lá, porque continua a estar. Obrigado. E, como prometido, ao Café Vera Cruz, porque foi onde escrevi as primeiras e as últimas palavras da minha tese. Obrigado por toda a simpatia e pelas discussões futebolísticas.

Além da Ciência foi também no Porto que descobri o Pedro, tornaste-te tão importante na minha vida. Obrigado por tudo o que passámos, por cada palavra, por cada sorriso, por cada gesto. És o meu porto de refúgio. Contigo é tudo mais fácil, é tudo melhor. Obrigado por seres quem és. Obrigado por existires na minha vida e a tornares mais colorida.

Um grande obrigado a todos os meus amigos que estando longe continuam sempre por perto. Em especial à Mary pela amiga incansável e pela pessoa maravilhosa que é.

Por fim, e mais importante, à minha família. Aos meus pais. Porque sem vocês não seria o que sou. Obrigado por terem acreditado em mim, e por lutarem todos os dias pelo meu futuro. Obrigado pelo apoio incondicional, pela preocupação, pela vossa constante presença mesmo sem estarem perto. Ao Alexandre e à Inês, porque são o meu sorriso de todos os dias. Amo-vos.

Table of Contents

List of Figures

INTRODUCTION

RESULTS

DISCUSSION

Abstract

Animal organogenesis requires the establishment of a highly regulated interplay between cell growth, proliferation and differentiation. Cell growth and proliferation are critically dependent on an efficient ribosome production, to sustain high protein-synthesis levels. Ribosome biogenesis and maturation takes place in the nucleolus, a dynamic subnuclear organelle that has also been characterized as a regulatory compartment involved in important cellular processes as cell-cycle control, apoptosis and cellular stress response.

Previous studies in our laboratory have shown that the fruit fly Nol12 homologue Viriato (Vito) is a key determinant of nucleolar structure that is required for tissue growth and cell survival during *Drosophila* development. Moreover, we have identified a strong genetic interaction between Vito and TGF-β signalling pathway members, and demonstrated that Vito is required for TGFβ-dependent tissue growth and photoreceptor neuronal differentiation. These results strongly support a novel signalling branch where nucleolar events contribute positively in the transmission of TGF-β signalling.

The main aim of this work is to understand if the described function of TGF-β in tissue growth is based on a possible role of this pathway in nucleolar function. We observed that expression of a strong RNAi targeting Put, the shared type II receptor for both branches of TGF-β signalling, affects nucleolar retention of structural proteins, Fibrillarin and Nopp140, which are also crucial in rRNA processing. In addition, ribosomal proteins involved in ribosome biogenesis were found to change its nucleolar localization and levels. We also observed a strong increase in nucleolar rRNA levels, suggesting that pre-rRNA processing and thus ribosome biogenesis may be compromised. In fact, *put*RNAi-expressing salivary glands have decreased amounts of mature rRNA subunits, and a more detailed analysis by transmission electron microscopy also showed that those nucleoli display nuclear accumulation of groups of small circular structures that might represent retained pre-ribosomes. Importantly, alteration of Put levels directly affects the nucleolar architecture and salivary glans growth, therefore supporting a regulation of nucleolar function by TGF-β signalling.

Putting all together, our results unveil a new growth mechanism, in which TGF-β signalling regulates nucleolar structure and function, opening new perspectives in the understanding of the developmental networks that govern animal organogenesis.

Resumo

A organogénese animal é um processo complexo, que requer o estabelecimento de uma interação altamente regulada entre crescimento, proliferação e diferenciação celulares. O crescimento e proliferação celulares dependem fortemente de uma produção eficiente de ribossomas, de forma a suster elevados níveis de síntese proteica. A biogénese e maturação ribossomal ocorrem no nucléolo, um organelo subnuclear que também tem sido considerado como um compartimento regulador. Estudos anteriores no nosso laboratório demonstraram que o homólogo de Nol12 na mosca-da-fruta, Viriato (Vito), é um regulador chave da estrutura nucleolar, necessário para crescimento e sobrevivência celular durante o desenvolvimento. Identificámos também uma forte interação genética entre Vito e membros da via de sinalização TGF-β, que mostrou ser essencial não só para o crescimento do tecido do olho mas também para a diferenciação neuronal.

Assim, o principal objetivo deste trabalho consiste em perceber se a função da via TGF-β no crescimento de tecidos é baseada numa possível interação com a função nucleolar. Expressão do RNAi mais forte para Put, o receptor tipo II comum para os dois ramos da via TGF-β, afeta a retenção de proteínas nucleolares estruturais, também cruciais no processamento do RNA ribossomal (rRNA), Fibrilarina e Nopp140. Os níveis e localização de várias proteínas ribossomais também sofrem alterações ao nível do nucléolo. Por outro lado, expressão do RNAi resulta em acumulação nucleolar ectópica de rRNA, sugerindo que o processamento do rRNA, e consequentemente a biogénese ribossomal, poderá estar comprometido. De facto, estas glândulas salivares possuem subunidades maduras de rRNA em quantidades reduzidas, e uma análise mais detalhada por Microscopia Eletrónica de Transmissão revelou que estes nucléolos apresentam acumulação de partículas de rRNA imaturas, retidas no nucleoplasma. Alteração dos níveis de Put mostrou afetar diretamente a morfologia do nucléolo, assim como o crescimento das glândulas.

Em conclusão, os resultados obtidos com este trabalho revelam uma nova interação na qual a função nucleolar contribui positivamente para a sinalização TGF-β, abrindo novas perspetivas na compreensão da rede complexa de interações que governam a organogénese animal.

List of abbreviations

Actβ - Activin β

Ago - Argonaute

Ato - Atonal

Babo - Baboon

Ban - Bantam

BMP - Bone Morphogenetic Proteins

Brk - Brinker

Dac - Dachshund

Dad - Doughters against dpp

DAPI - 4',6' – diamidino-2-phenylindole

Daw - Dawdle

DFC - Dense Fibrillar Component

Diap-1 - *Drosophila* inhibitor of apoptosis 1

dm- diminutive

dMyc - *Drosophila* Myc

DP - Disc proper

Dpp – Decapentaplegic

dsRNA- Double-stranded RNA

dTOR- *Drosophila* target-of-rapamycin

ETS - External Transcribed Spacer

Ey - Eyeless

Eya - Eyes absent

Eyg - Eyegone

FC - Fibrillar component

FMW - First mitotic wave

Gbb - Glass Bottom Boat

GC - Granular component

GFP - Green fluorescent protein

Hh – Hedgehog

Hid- Head involution defective

hpRNA - Hairpin RNA

Hth – Homothorax

i.e.- *Id Est*

IGS - Intergenic spacer

ITS - Internal Transcribed Spacer

JAK/STAT - Activated Kinase/Signal Transducer and Activator of Transcription

Mad - Mother against dpp

Mav - Maverick

Med - Medea

MF - Morphogenetic Furrow

Myo - Myoglanin

NoD - Nucleolar detention sequence

NOR - Nucleolar organizer region

NPC- Nuclear pore complex

Omb - Optomotor-blind

PE - Peripodial epithelium

pMad- phosphorylated Mad

Pol I- RNA polymerase I

Pol II- RNA polymerase II

Pol III- RNA polymerase III

Pre-rRNA- precursor ribosomal RNA

Put – Punt

RD - Retinal determination

RFP - Red fluorescent protein

RISC - RNA-induced silencing complex

RNAi - RNA interference

Rp - Ribosomal protein

RpL - Large subunit Rp

RpS - Small subunit Rp

rRNA - Ribosomal RNA

Sax - Saxophone

Scw - Screw

Sd - Scalloped

Shn - Shnurri

siRNA - Small interference RNA

SMW - Seconde mitotic wave

snoRNA - Small nucleolar RNA

So - Sine oculis

TEM- Transmission Electron Microscopy

TGF-β - Transforming Growth Factor Beta

Tkv - Thickveins

TOP - Terminal oligopyrimidine

Toy - Twin of eyeless

UAS- Upstream activating sequence

Upd - Unpaired

UTR - Untranslated region

Vito – Viriato

Wg - Wingless

Wit - Wishful Thinking

YFP - Yellow fluorescent protein

Yki - Yorkie

Introduction

How genes drive development?

How a single cell gives rise to a collection of organs with the correct architecture to build a highly complex multicellular organism is one of the critical questions of developmental biology. Animal organogenesis demands for a tightly regulated interplay between cell growth, proliferation, differentiation and apoptosis. Extremely complex signalling networks regulate cellular genetic profiles, modifying cell behaviours to precisely arrange cells in time and space, and thus ensure a correct organ patterning and growth (Lecuit and Le Goff, 2007). Besides external signals, such as diet or temperature, also physiological (e.g., hormones) and organ-intrinsic signals are combined to manage these signalling networks (Edgar, 2006b; Neto-Silva et al., 2009).

The first observations of tissue-intrinsic regulation of growth arose from polyploid salamanders. Although tetraploid salamanders have the same organ size than diploid salamanders, their cell number is reduced by half (Fankhauser, 1945). Therefore, cell size is proportional to cell ploidy but the balance between cell growth and division is finely controlled in order to reach the correct final organ size. In other experiments in which salamander's limbs were transplanted between different sized species of salamanders, they grew until reach the donor organ adult size, suggesting the existence of an organ-intrinsic growth programme (Twitty and Schwind, 1931). Likewise, after grafting many thymus pieces on the same developing mice each graft grew independently and reached the typical adult size, suggesting that thymus growth is mainly regulated by organ-intrinsic signals (Metcalf, 1963). Conversely, spleen grafts transplanted to a splenectomised mouse grew until the total mass of transplanted tissue attained the mass of a normal adult spleen, implying that spleen growth is mainly regulated by organ-external signals (Metcalf, 1964).

Therefore, tissue growth and patterning are dependent on the proliferation rate, mass accumulation and cell survival of the composing cells. These parameters are finely coordinated by tissue intrinsic and extrinsic signals that restrict cells correctly arranged within the limits of the tissue target size. Growth and patterning are key developmental processes intimately related. Although little is known about the mechanisms that control organ growth, some conserved signalling pathways involved in patterning are also linked to growth regulation, such as TGF-β signalling.

Growth control: a complex crosstalk between different pathways

Regulation of tissue growth requires a highly complex interplay between several signalling pathways to keep the correct balance between growth positive and negative signals, thereby ensuring that the correct tissue size is achieved. An imbalance of this homeostatic process could result in impaired cell growth and tumorigenesis.

1. TGF-β signalling pathway

The transforming growth factor β (TGF-β) superfamily is highly conserved along metazoans (Padgett et al., 1987; Huminiecki et al., 2009) and comprises a group of secreted proteins that control key cellular functions during development. Members of this family are expressed in precise chronological and spacial patterns to ensure a proper organogenesis and adult tissue homeostasis, by directing cell growth, differentiation, and apoptosis (Massagué, 1998; Moustakas and Heldin, 2009).

Signal transduction is initiated by the binding of the dimeric ligand to a heteromeric receptor complex that consists in two units of each two distinct type I and type II serine/threonine protein kinases. Upon receptor complex formation, the type II receptor, which is constitutively active, phosphorylates the dormant type I receptor, activating its kinase domain. The signal is internalized with the recognition and activation by Type I receptor of a group of transcription factors known as receptor-activated SMADs (R-SMADs), which in turn assembles in a trimeric complex with a common SMAD (Co-SMAD) (Massagué, 1998; Shi and Massagué, 2003; Moustakas and Heldin, 2009). This complex, composed by two activated R-SMADs and one Co-SMAD, is translocated to the nucleus, where it associates with transcriptional co-factors to regulate gene expression (Massagué et al., 2000; Feng and Derynck, 2005).

Phosphorylation and subsequent activation of particular R-SMADs by type I receptor induces distinct transcriptional cell responses, and thus type I receptors coordinate specificity of TGF-β signal transduction (Feng and Derynck, 2005). In this way, TGF-β family is generally divided into two functional signalling

subfamilies, the TGF-β/Activin branch and the bone morphogenetic proteins (BMP) branch, depending on which type I receptor is activated.

Since the discovery of the first ligand of TGF-β signalling pathway in *Drosophila melanogaster*, Decapentaplegic (Dpp) (Padgett et al., 1987), a total of seven ligand family members were identified in this organism: Dpp, Screw (Scw) and Glass bottom boat (Gbb) belonging to BMP family, and Activin-β (Actβ), Dawdle (Daw), Maverick (Mav) and Myoglianin (Myo) belonging to TGF-β/Activin family (Parker et al., 2004). In BMP branch, Thickveins (Tkv) and Saxophone (Sax) are the specific type I receptors, which transduce the signal through phosphorylation of R-SMAD Mother against dpp (Mad). The single type I receptor in TGF-β/activin branch, Baboon (Babo) signals through Smad2 (Smox). Whereas type I receptors confers branch specificity, the type II receptors, Punt (Put) and Wishful thinking (Wit), are shared between the two branches of TGF-β signalling. R-SMADs of both branches also associate with the common Co-SMAD, Medea (Figure 1) (Moustakas and Heldin, 2009).

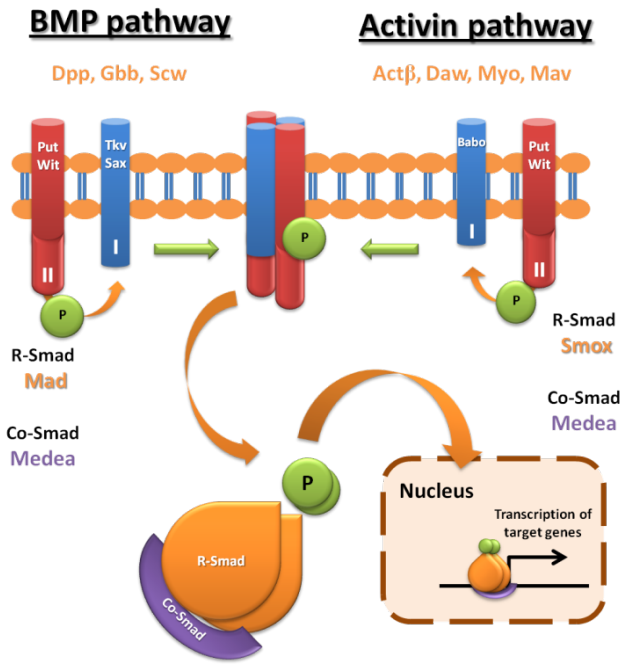

Figure 1- TGF-β signalling pathways. In *Drosophila* TGB-β signalling comprises two branches, BMP and Activin. Decapentaplegic (Dpp), Glass Bottom Boat (Gbb) and Screw (Scw) are the BMP pathway ligands, whereas Activin β (Actβ), Dawdle (Daw), Myoglanin (Myo) and Maverick (Mav) are the Activin branch ligands. After binding of the dimeric ligands to the heteromeric receptor complex, two activated R-SMADs (Mad in BMP branch or Smox in Activin branch), compose a trimeric complex with the common Co-SMAD Medea that translocates to the nucleus, and activates the transcription of target genes.

1.1 BMP (Dpp) signalling

The BMP branch of TGF-β signalling has been extensively studied, particularly the Dpp ligand. Besides its role in the establishment of the dorsal fate during embryogenesis (Ferguson and Anderson, 1992), it is well described the importance of Dpp to the Anterior/Posterior compartments organization in the *Drosophila*'s wing imaginal disc (Affolter and Basler, 2007). In this epithelial bilayer that gives rise to the adult wing, *dpp* is expressed in a restricted range of cells nearby the A/P axis, from which it diffuses throughout the wing disc in a graded concentration to perform a long-range activity (Basler and Struhl, 1994; Nellen et al., 1996; Entchev et al., 2000). This gradient is essential for the proper patterning of the wing disc, as ectopic expression of *dpp* results in adult flies exhibit abnormal wings with altered patterns, such as symmetric pattern duplications or presence of extra-tissue, the "winglets" (Capdevila and Guerrero, 1994; Zecca et al., 1995). Furthermore, ectopic clones expressing *dpp* induce the expression of Dpp target genes, such as *spalt* and *optomotor-blind* (*omb*) in the surrounding cells, opposing to the cell-autonomous behaviour observed in clones expressing the constitutively active form of the Dpp receptor Tkv (TKV^{QD}) (Burke and Basler, 1996; Nellen et al., 1996). Therefore, Dpp exerts a morphogen action in the surrounding tissue by modelling cellular behaviour in a positional-dependent fashion. In response, Dpp-receiving cells assume particular genetic profiles and acquire different cell fates depending on its distance to the Dpp diffusion point (Affolter and Basler, 2007; Dekanty and Milán, 2011).

Besides its role on patterning it was also observed that flies with a reduction in *dpp* activity in the wing display "no wing" phenotype (Zecca et al., 1995), whereas ubiquitous expression of *dpp* results in overgrowth of the wing disc (Nellen et al., 1996), supporting a strong connection between Dpp and growth. Although several models have been emerged in an attempt to explain how graded morphogenes control the uniform tissue growth, this question remains extremely controversial (Schwank and Basler, 2010). Some evidence suggests that such Dpp-induced tissue growth is positional-independent. In fact, it was demonstrated that the slope of Dpp expands together with the tissue and thus is preserved during wing development (Wartlick et al., 2011). In addition, uniform activation of Dpp pathway by expressing TKV^{QD} in the medial area of the wing disc does not prevent proliferation in the growing tissue, further indicating that the Dpp slope is not a requisite to induce proliferation in this region

(Schwank et al., 2008). Therefore, Brinker (Brk) seems to be a key mediator between Dpp signalling and growth control, by creating an inverse gradient within the wing disc, repressing transcription of Dpp target genes (Müller et al., 2003). Their complementary activity proved to be crucial to define cell fates and to ensure that the growing tissue does not exceed the expected size (Affolter and Basler, 2007; Schwank et al., 2008).

1.2 Activin signalling

In *Drosophila* the Activin signalling branch has been less characterized than the BMP branch. Nevertheless, besides the described role of this pathway in neuronal plasticity and axon guidance (Zheng et al., 2003, 2006), it was shown that *babo* mutant larvae display smaller imaginal discs, whereas the ubiquitous expression of a constitutively active form of Babo results in tissue overgrowth (Brummel et al., 1999). Importantly, loss of *babo* and *smox* increases cyclin A levels, with subsequent delay in M phase exiting during cell cycle. Thereby, *babo*/*smox* mutant larvae are not capable to undergo pupariation and die in late larval or early pupal stages, displaying small brain lobes and deficient targeting of photoreceptor's axons. These defects involve a decrease in the number of brain precursor cells, due to its impaired proliferation (Brummel et al., 1999; Zhu et al., 2008). Therefore, these experiments strongly suggest a role of Activin pathway in tissue growth, although it seems not affect tissue patterning.

Depending on the developmental context, the two branches could perform agonistic or antagonistic functions and therefore their balance would affect the organogenesis. In *Drosophila melanogaster* both branches are required during development and several reports have emerged describing cross-pathway activity. In the context of the *Drosophila*'s wing it was observed that depletion of *smox* results in the ectopic growth of vein tissue around the L5 vein, the same phenotype displayed by gain-of-function of Mad. In addition, *smox* depleted clones exhibit elevated levels of phospho-Mad (pMad), indicating an increased Dpp signalling pathway activation. Hence these experiments demonstrated a developmental context in which Mad and Smox have a epistatic activity (Sander et al., 2010). Recently, it was observed that both the *Drosophila* and the mammalian Activin type I receptors can phosphorylate Mad and Smox *in vitro*, demonstrating

a highly conserved cross-pathway activity. Moreover, studies in the *Drosophila* wing showed that ubiquitous expression of *babo* in the expression domain of a Dpp target gene, *vestigial* (*vg*), results in blistered and crumpled adult wings. This phenotype is suppressed with depletion of *mad* expression or with overexpression of *smox*, suggesting that the R-SMADs compete for Baboon phosphorylation *in vivo*. In fact, when *smox* expression is depleted, pMad levels are increased in the *babo*-expressing domains, whereas simultaneous depletion of *babo* and *smox* does not alter the normal pMad expression pattern. Therefore, Mad is phosphorylated by Babo in a Smox level-dependent fashion *in vivo*, suggesting a potential signal switching system mediated by Smox levels that mediates cross-pathway activity during developmental processes (Peterson et al., 2012).

2. Fat-Hippo pathway

In the last few years another conserved signalling network strongly related with growth control has been unveiled. Such network named Fat-Hippo comprises a set of tumour suppressor proteins that limit the activity of a growth promoter, Yorkie (Yki), retaining it at the cytoplasm by phosphorylation (Edgar, 2006a; Reddy and Irvine, 2008; Oh and Irvine, 2010). Loss-of-function mutations in these proteins results in hyperactivation of Yki and consequent tissue overgrowth. Surprisingly, it was shown that this overgrowth phenotype results not only from an increase in cell proliferation but also from a failure of cells to undergo apoptosis. Accordingly, *yki* mutant clones do not proliferate and go through apoptosis, failing to survive within the tissue (Harvey et al., 2003; Udan et al., 2003; Huang et al., 2005; Thompson and Cohen, 2006).

Many Yki targets have been identified, including cell-cycle regulators, such as Cyclin E, apoptotic inhibitors, such as the *Drosophila* inhibitor of apoptosis 1 (Diap-1) and the microRNA Bantam (Ban) (Huang et al., 2005; Thompson and Cohen, 2006). It is well described that *bantam* expression induces cell proliferation and inhibits the pro-apoptotic gene *head involution defective* (*hid*) (Brennecke et al., 2003). Nevertheless, Yki does not bind directly to the DNA, so its activity requires other DNA-binding proteins to induce target genes transcription, such as Scalloped (Sd) and Homothorax (Hth) (Halder and Johnson, 2011).

Recently, it was shown that in clones expressing Brk *ban* expression is repressed, even in the presence of Yki, and this effect is only reversed with simultaneous activation of Yki with Mad and Tkv^{QD}. Therefore, Mad can form a transcriptional complex with Yki to induce *ban* transcription, independently of Medea, whereas Brk represses *ban* expression by directly repressing its enhancer (Martín et al., 2004; Oh and Irvine, 2011). In addition, in other study has proposed the "opposing growth pathways model", by showing that uniform proliferation rates along the A/P boundary during wing development are achieved by complementary growth regulation of Dpp/Brk signalling in the wing lateral areas and Fat signal in the medial region (Schwank et al., 2011). These results unveil a new interplay between different signalling pathways, in which Dpp and Fat-Hippo modulate growth possibly through *ban* (Figure 2).

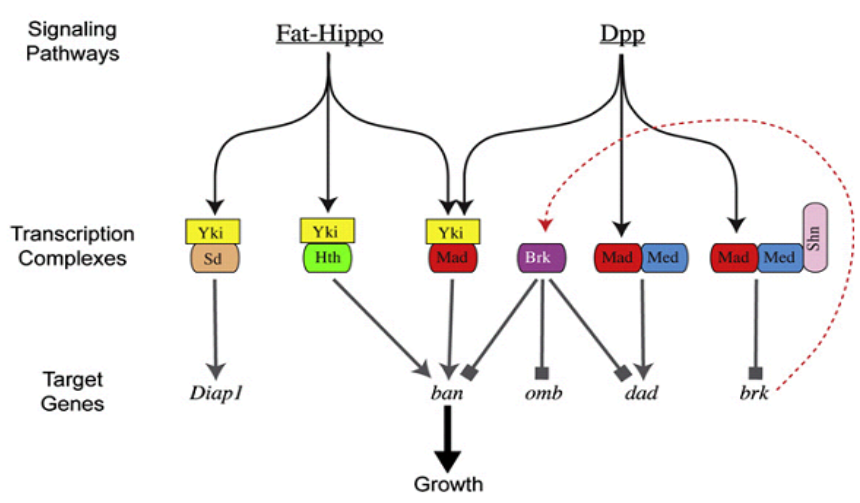

Figure 2- Fat-Hippo pathway interacts with Dpp signalling to stimulate growth. Yorkie (Yki) is the downstream target of the Fat-Hippo pathway and cooperates with different partners to induce growth by transcription of many target genes. One of those partners is Scalloped (Sd), that together with Yki induces the expression of apoptosis inhibitor Diap-1, and other partner is Homothorax (Hth). Dpp, ligand of the TGF-β pathway, activates the transcriptional factor Mad that can form a complex with Medea to directly activate the transcription of target genes, such as *daughters against Dpp* (*dad*). In addition, Mad forms a transcriptional complex with Medea and Schnurri (Shn) to repress *brk*, thereby de-repressing Dpp target genes such as *omb*. Besides their independent role in growth control, both pathways can cooperate by the formation of a transcriptional complex that comprises Yki and Mad, and subsequent activation of the microRNA bantam (*ban*). Adapted from (Schwank et al., 2011).

3. Myc induces growth through Viriato

An important player in growth regulation is the *Drosophila* Myc (dMyc), a transcription factor ortholog of c-Myc oncogene in mammals (de la Cova and Johnston, 2006). It was shown that hypomorphic dMyc mutant flies are smaller

than wild-type flies, whereas flies with dMyc overexpression are bigger than controls (Johnston et al., 1999). Additionally, null mutants for dMyc codifying gene, *diminutive* (*dm*), display a strong developmental delay in larval phases, exhibiting small nucleus that fail to reach normal DNA content in endoreplicating tissues, such as fat cells and salivary glands (Pierce et al., 2004). On the other hand, cells overexpressing dMyc reveal a large nucleus and nucleolus, with increased rRNA content and higher ploidy (Pierce et al., 2004; Grewal et al., 2005).

In vertebrates it is well known that Myc regulates several processes by controlling the expression of several genes related with growth and proliferation, including the pre-rRNAs and ribosomal proteins (Figure 3), and its action as transcription factor is mediated by chromatin remodelling. In *Drosophila*, besides its role in controlling cell cycle regulators, it was shown that dMyc stimulates rRNA synthesis, having an important advantage in the homeostatic process of cell competition (Grewal et al., 2005; Pierce et al., 2008; van Riggelen et al., 2010). Cell competition takes place when cells within the same growing tissue have different metabolic rates, originating an environmental stress in which cells interact with each other. Winner cells have a growth advantage, which is conferred by the capacity of protein synthesis. Thus, these cells continue to proliferate and survive, whereas the loser ones undergo apoptosis and are eliminated (Johnston, 2009). When clones of cells overexpressing dMyc are present in a wild-type tissue they act as super-competitors, thereby eliminating the wild-type loser cells by inducing Hid-mediated apoptosis, without affecting the target tissue size (Moreno et al., 2004; de la Cova et al., 2004; Johnston, 2009).

Other experiments have shown that in a tissue without dMyc expression Yki is not capable to induce growth, whereas clones overexpressing Yki display some increase in dMyc levels. Such clones induce apoptosis in neighbouring cells, exhibiting competitor behaviour, suggesting that Yki induces dMyc expression to promote growth. In fact, a model was proposed in which Yki and dMyc coordinate the action of each other. Thus, Yki forms a transcriptional complex with Sd to induce dMyc expression, which in turn repress *yki*, in an equilibrated network that ensure the correct tissue size (Neto-Silva et al., 2010; Ziosi et al., 2010).

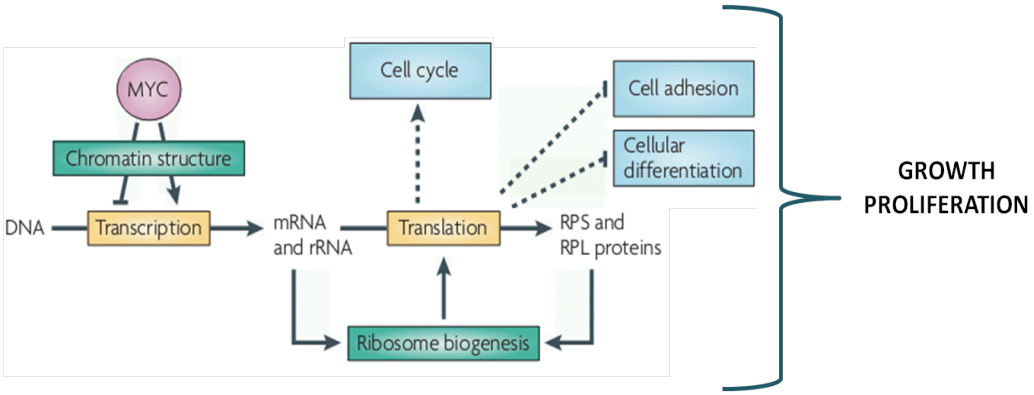

Figure 3- Myc signalling in vertebrates. Myc stimulates cell growth and proliferation by transcriptional activation of several genes, including rRNA and ribosomal proteins (RPS and RPL) (adapted from van Riggelen et al., 2010).

Recently, a study performed at the host laboratory has characterized the functional *viriato* (*vito*), a novel gene identified in a screen for genes required for tissue growth in *Drosophila*. This gene is mainly expressed in the anterior proliferating cells of the eye imaginal disc and codifies for a nucleolar protein, the *Drosophila* homologue of the conserved Nol12 protein family. Flies mutants for *vito* display a developmental delay, whereas its depletion in the eye-antennal imaginal disc results in reduction of the eye size. Moreover, *vito* was shown to regulate the recruitment of Fibrillarin to the nucleolus and to maintain proper nucleolar structure. In addition, null *dm* mutants display decreased levels of *vito*, and in salivary glands Vito was shown to be necessary for the dMyc-induced growth, although it is not needed for the transcription of other dMyc target genes. These results strongly suggest that Vito is required to mediate nucleolar response of dMyc-induced growth (Marinho et al., 2011).

Nucleolus: a sensorial centre in the cell

The nucleolus is an extremely dynamic nuclear body that surrounds the tandemly repeated ribosomal RNA (rRNA) genes assembled in nucleolar organizer regions (NORs), in eukaryotic acrocentric chromosomes. The most important nucleolar function consists in creating the appropriate environment for an efficient ribosome biogenesis, essential to maintain cell metabolism. Nevertheless, the nucleolus has been described as multifunctional, as it is involved in several cellular functions, such as cell cycle and apoptosis control, DNA repair or stress response (Raska et al. 2004; Boisvert et al. 2007).

Since the nucleolus is a non-membrane organelle, its structure is maintained by the interaction between resident nucleolar proteins and several other proteins that are in continuous exchange between the nucleolus and the nucleoplasm. This nucleolar trafficking, in which several proteins are retained and released, occurs in response to cellular demands, thereby reflecting the physiological state of the cell (Raska et al., 2004; Andersen et al., 2005). Recently, it was found that the nucleolar targeting of proteins can be mediated by intergenic spacer (IGS) regions, present between the rDNA clusters (described in detail in the next chapter). Therefore, in response to cell stress stimuli these highly repeated DNA sequences are transcribed in long non-coding RNAs that are able to capture and retain proteins containing a specific peptidic motif, NoDS (Nucleolar Detention Sequence) (Audas et al., 2012; Prasanth, 2012).

The transient nature of the nucleolar proteome ensure the sensitivity of nucleolus to external changes, making possible the interaction between different proteins with related functions in a cellular context-dependent fashion (Boisvert et al., 2007). Importantly, the highly dynamic assemble of nucleolar components provides the necessary pool of proteins in the correct stoichiometry to support ribosome biogenesis, the main function of nucleolus (Emmott and Hiscox, 2009).

1. Ribosome biogenesis

Cell growth and proliferation are critically dependent on an efficient ribosome production, to sustain high protein synthesis levels. As ribosome production is a highly energy-consuming process, it needs to be rigorously controlled.

Each rDNA cluster repeat presented in the nucleolus is composed by an array of genes codifying for rRNAs, two external transcribed spacers (ETS) and two internal transcribed spacers (ITS) (Figure 4). Therefore, ribosome biogenesis is initiated with transcription of rRNA genes by RNA polymerase I (pol I), which originates a long rRNA precursor 47S. This polycistronic rRNA goes through a stepwise processing in which is successively cleaved by endo- and exonucleases to remove the ITS and ETS sequences, and to give rise to the 18S, 5.8S and 28S pre-rRNAs. A fourth pre-rRNA 5S is transcribed at the nucleus, by the RNA polymerase III (pol III), and imported to the nucleolus to undergo maturation (Lafontaine and Tollervey, 2001; Raska et al., 2004; Xue and Barna, 2012b).

During the ribosomal maturation, small nucleolar RNAs (snoRNAs) associate with nucleolar proteins, such as Gar-1 and Fibrillarin, to form small nucleolar ribonucleoproteins (snoRNPs), which drive site-specific rRNA modifications (Wang et al., 2000; Reichow et al., 2007). Simultaneously, several ribosomal proteins (Rps) are transcribed at the nucleus by RNA polymerase II (pol II), translated at the cytoplasm and quickly imported to the nucleolus, where they assemble with the pre-rRNAs to compose the mature ribosome subunits. The large 60S subunit comprises the 5.8S, 28S and 5S pre-rRNAs and nearly 47 ribosomal proteins named RPLs, whereas the small 40S subunit is composed by the 18S pre-rRNA and about 32 RPS ribosomal proteins (Raska et al., 2004; Lam et al., 2007; Xue and Barna, 2012b) (Figure 4).

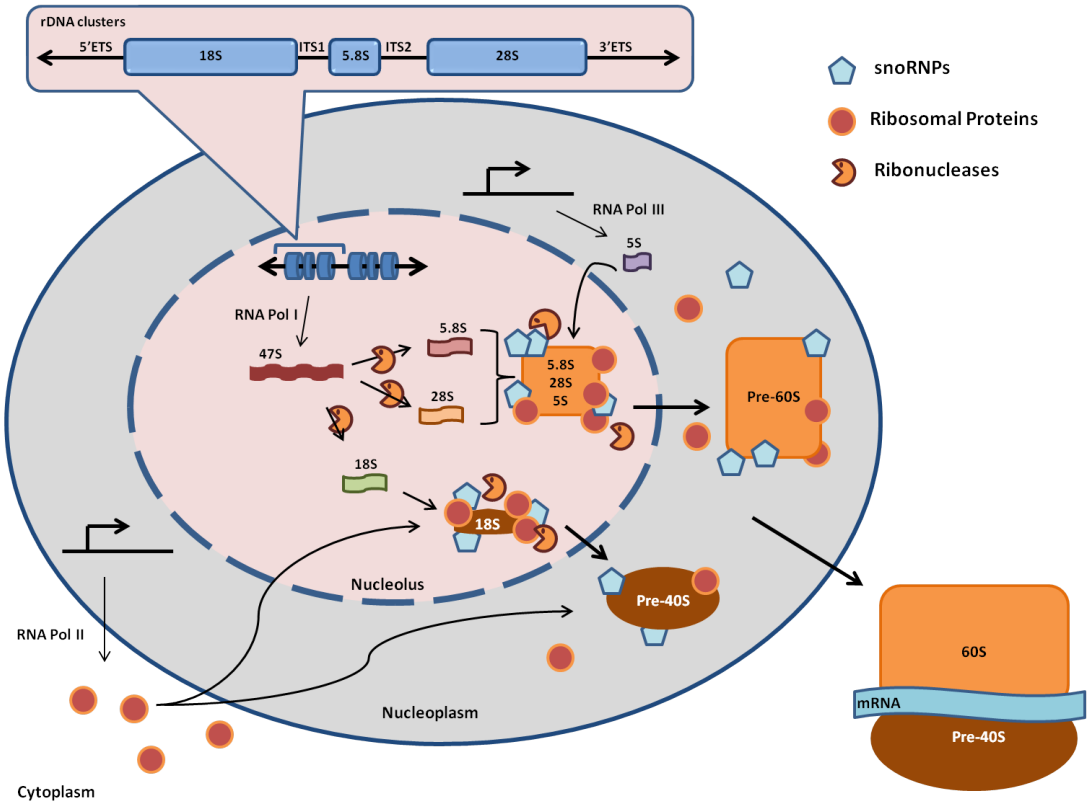

Figure 4- Ribosome biogenesis. The nucleolus comprises an array of rRNA gene clusters, which are transcribed by RNA polymerase I in the 5.8S, 28S and 18S pre-rRNAs. The fourth 5S pre-rRNA is transcribed by RNA polymerase III at the nucleoplasm and imported to the nucleolus. Processing, maturation and assembly of pre-rRNAs to form the ribosome subunits requires ribonucleases (endo- and exonucleases), ribosomal proteins, small nucleolar ribonucleoproteins (snoRNPs) and other accessory factors. Ribosomal proteins are transcribed at the nucleus by RNA polymerase II, translated at the cytoplasm and imported to the nucleolus. The mature small 40S and large 60S subunits are translocated to the cytoplasm in a late maturation process, and assemble with mRNA to form functional 80S ribosomes.

Both subunits are subsequently translocated from the nucleolus to the nucleoplasm and then to the cytoplasm, in a late maturation process involving

several ribosomal and non-ribosomal proteins that assist the nuclear export. One of these proteins is RpL10, which interacts with the non-ribosomal 60S-associated protein NMD3, to export 60S ribosomal subunit through the nuclear pore complex (NPC). At the cytoplasm the mature subunits assemble with mRNA to form 80S functional ribosomes (Gadal et al., 2001; Lafontaine and Tollervey, 2001; Tschochner and Hurt, 2003; van Riggelen et al., 2010).

In mammalian cells the distinct processes that comprise ribosomal biogenesis take place in different nucleolar regions characterized by the presence of different protein combinations. Thus, rRNA transcription occurs in the border between the fibrillar centre (FC) and the dense fibrillar component (DFC), processing mostly occurs at DFC and assembly at the granular component (GC) (Olson et al. 2000; Raska et al. 2004; Boisvert et al. 2007). In *Drosophila* this tripartite organization was not observed, being the nucleolus a homogeneous structure (Orihara-Ono et al., 2005).

Ribosomal proteins are crucial for all steps of ribosome biogenesis, and the constant flux of these proteins between the nucleolus and cytoplasm along with the constant formation of new proteins and degradation of those unassembled, provide equilibrated amounts of RPs and pre-rRNAs, required for the efficient ribosome biogenesis process (Andersen et al., 2005; Lam et al., 2007). Therefore, defects in the normal balance between RPs and rRNA amounts results in a dramatic change in the normal ribosome activity and subsequent alteration of protein synthesis. Besides their fundamental role in ensuring cellular ribosome availability, RPs have many extra-ribosomal functions, thereby enhancing their requirement for the correct cellular function (Lindström, 2009; Warner and McIntosh, 2009). One good example is the mammalian RpL11, which in normal conditions is maintained at the nucleolus, but during nucleolar stress it accumulates at the nucleoplasm and mediates the stabilization of the tumour-suppressor protein p53 (Zhang and Lu, 2009; Boulon et al., 2010). Accumulation of RpL11 at the cytoplasm is also important to prevent Myc-mediated transcription of target genes as it inhibits the recruitment of its Myc co-activator, thereby limiting Myc-induced proliferation during cell response to oncogenic signals (Dai et al., 2007; Lindström, 2009; van Riggelen et al., 2010). Accordingly, several human disorders have been linked to alterations of many RPs, including cancer. Studies point to a neoplasic transformation model in which

alterations in the normal ribosome activity results in qualitative and quantitative changes in the normal protein translation (Montanaro et al., 2008).

In *Drosophila*, loss of one copy of several RPs is sufficient to result in a phenotypic class of dominant mutations named Minute. These mutants have a developmental delay and in the adult stage are characterized for possessing poor viability and fertility as well as for displaying short and thin bristles. These phenotypic effects are a consequence of suboptimal protein synthesis, which arises from an impaired ribosome function (Marygold et al., 2007).

Drosophila melanogaster: a small fly that solves big questions

Drosophila melanogaster represents an ideal system to study the mechanisms that underlie growth. Thomas Morgan was the first biologist studying *Drosophila* early in the 20th century to explore the basis of heredity. He placed the small fruit fly in the vanguard of genetic research and since then, along with the emerging of a large range of genetic and molecular tools, *Drosophila* has been considered a powerful model organism for many reasons (Roberts, 2006; Arias, 2008a). Its small genome size, with around 14000 genes, short generation time and ease of culture and manipulation are some of the characteristics that make the fruit fly so attractive (Arias, 2008a). In addition, its genome was completely sequenced (Adams et al., 2000) and a large range of genetic tools that enables its manipulation are available. More importantly, several key developmental mechanisms and signalling pathways were highly conserved between *Drosophila* and mammals during evolution. The surprising finding that more than 70 per cent of the human disease-related genes have homologues in *Drosophila* genome (Reiter et al., 2001) revealed new perspectives for using this organism as model to study human diseases.

1. Life cycle

The duration of *Drosophila*'s life cycle critically depends on the temperature. Therefore, whereas at 18ºC the cycle takes approximately twenty days, at 25ºC an egg turns into an adult fly in no more than ten days (Figure 5). After mating, the cycle initiates with deposition of the eggs in the food. An egg develops to an embryo during the process of embryogenesis, and after 24 hours first larvae

hatch. The larval phase is divided into 3 instars separated by molts, L1 (24 hours), L2 (24 hours) and L3 (48 to 72 hours), and is characterized by a drastic accumulation of mass, by which larvae accumulate nearly 200-fold in weight. During this period larvae are feeding, and shortly before the end of L3 they leave the food source and search for a dry place appropriate to enter in pupariation (wondering phase). The final phase of metamorphosis occurs within the pupal case and takes approximately 5 days. Upon eclosion adults become receptive for mating after a few hours (Arias, 2008b).

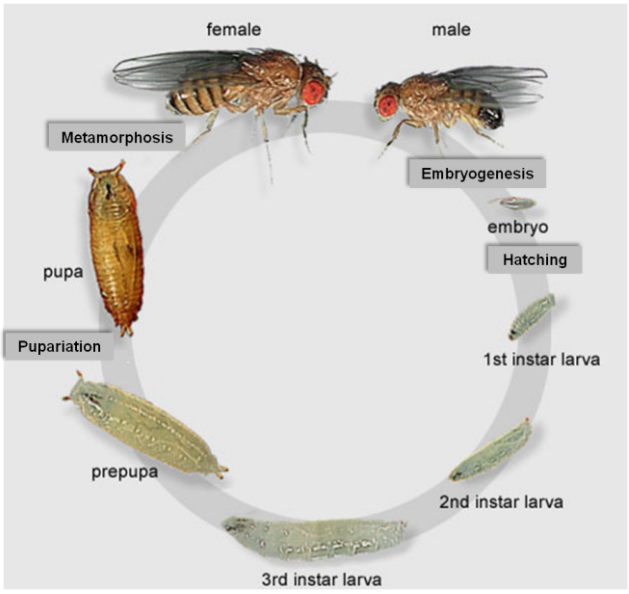

Figure 5- Life cycle of *Drosophila melanogaster*. Life cycle takes approximately 10 days at 25ºC. After mating, eggs deposited in the food undergo embryogenesis for 24 hours. The larval phase initiates after larvae hatch, and takes approximately 5 days. In the final phase larvae move to a dry place (wondering phase) and form the pupa, where metamorphosis takes place. Adapted from (Arias AM, 2008).

2. *Drosophila* imaginal discs: models to study growth

Drosophila imaginal discs comprise the epithelial sac-like tissues present in the larvae that give rise to the body appendages in the adult fly, such as eye, antenna, or wing. These structures emerge from collections of cells that acquire identity by the input of positional-dependent signals during embryogenesis, and are composed by two epithelial layers with different properties. Indeed, the main epithelium or disc proper (DP) is formed by columnar cells, and is surrounded by the squamous cells of the peripodial epithelium (PE). Such layers are separated by

a lumen but remain in close communication during development (Atkins and Mardon, 2009; Neto-Silva et al., 2009).

During larval phases these small clusters of cells undergo faster proliferation rates, and the imaginal discs suffer a dramatic increase in size. During this process, tissue growth is coordinated with tissue patterning, and differentiation occurs before the beginning of metamorphosis. Within each imaginal disc, different cell lineages acquire divergent fates, becoming progressively determined to assemble in organ-specific regions, known as compartments. These developmental fields act as independent units of growth and are composed by cells expressing the same combination of the regulatory selector genes (Domínguez and Casares, 2005; Neto-Silva et al., 2009).

Therefore, the structural simplicity of imaginal discs is transcended by the complex regulatory networks that orchestrate tissue development, which ensures the achievement of the exact organ size and shape. As a result, *Drosophila* imaginal discs provide perfect developmental models to study growth and pattern control during organogenesis.

2.1 Eye-antennal imaginal disc development

The eye-antennal imaginal disc develops into the adult eye, antenna, head cuticle and head structures, such as the ocelli and maxillary palps (Figure 6).

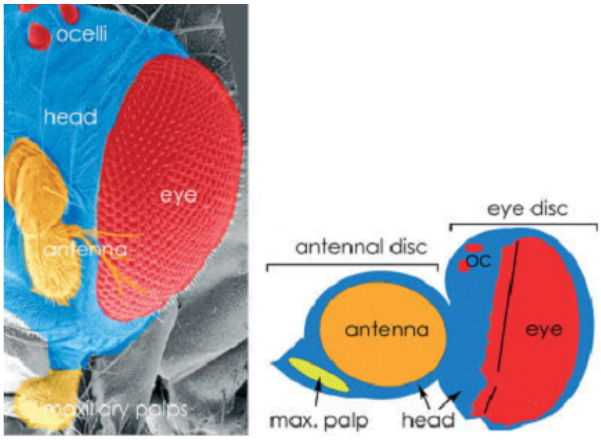

Figure 6- The eye-antennal imaginal discs develop in the fly head organs. The organs in the adult exhibit the same colours of the correspondent organ-primordia, in the eye-antennal imaginal disc. Adapted from (Domínguez and Casares, 2005).

The fly retina is composed approximately by 800 eye units, called ommatidia. Each ommatidium is a cell cluster comprising 8 photoreceptors (R1-8), and non-neuronal cells, such as clone and pigment cells.

Specification of the eye territory happens early in the first larval instar, with uniform expression of the mammal PAX6 *Drosophila* homologues, *eyeless* (*ey*) and its paralogue *twin of eyeless* (*toy*). Ectopic expression of these selector genes induces the formation of ectopic eyes, and thus *ey* and *toy* have a key role in conferring the eye identity (Halder et al., 1995; Czerny et al., 1999).

During the second larval stage, cells are proliferating asynchronously, and a range of different developmental signals emerges. At this stage, the disc has grown enough to unlock the mutual repressive action between Wingless (Wg) and Dpp, and thus, posterior cells exposed only to Dpp signal started to express retinal determination (RD) genes, *eyes absent* (*eya*), *sine oculis* (*so*) and *dachshund* (*dac*) (Kenyon et al., 2003; Domínguez and Casares, 2005; Amore and Casares, 2010). Wg, the Wnt-1 *Drosophila* homologue, is expressed in the ventral and dorsal margins of the disc and inhibits retinal specification by a repressive effect on Dpp signalling. Thus, Wg signalling restricts the retina formation to the posterior region, and maintains the cells in a proliferative state at the anterior region of the disc, by inducing the TALE-type homeodomain protein Homothorax (Hth) (Treisman and Rubin, 1995; Pichaud and Casares, 2000; Kenyon et al., 2003). Evidences suggest that Hth, in turn, sustain the anterior proliferative state by interacting with Yki and the zinc finger transcription factor Teashirt (Tsh) to form a transcriptional complex that induces the expression of *bantam* (Bessa et al., 2002; Peng et al., 2009).

The differentiation begins at the posterior margin of the disc, induced by the Dpp and the Hedgehog (Hh) signals, and cross the disc in a wave-like mode. The front of the differentiation wave is marked by the morphogenetic furrow (MF), a constriction of the epithelium in which cells arrest in G1 phase of the cell cycle, to posterior differentiation in photoreceptors (Domínguez and Casares, 2005) (Figure 7). Hh is a small-range signal secreted by the differentiated photoreceptors and directs the progression of the MF by inducing the expression of Dpp in the furrow (Greenwood and Struhl, 1999). As MF progresses in the disc, Dpp signal accompanies its movement. As Hh is also implicated in the MF progression at medial region, Dpp signal becomes essential for the progression of the MF at the margins of the disc, where it sustains its own expression.

Depletion of *dpp* in the third instar discs results in smaller discs exhibiting a delay mainly in the marginal progression of the MF. In these discs the retinal differentiation is restricted to the central area, where the Hh signal drive the furrow progression (Treisman and Rubin, 1995; Chanut and Heberlein, 1997).

At the anterior region, the progenitor cells that receive the long-range signal of Dpp from the MF enter a pre-proneural state, in which *hth* expression is lost and RD genes are up-regulated. In addition, these cells synchronize their cell cycles by going through a few rounds of cell cycle divisions, called the first mitotic wave (FMW). Following synchronization, cells arrest in G1 phase at the MF and acquire neuronal competence by expression of *atonal* (*ato*), induced by Hh. Cells expressing *ato* are selected to be the founder cells (R8), thereby successively recruiting the other neuronal and non-neuronal cells required to form the ommatidial clusters (Tomlinson, 1985; Domínguez and Casares, 2005). Cells that do not differentiate after the FMW undergo in a second mitotic wave (SMW), behind the MF. It was shown that the inhibition of *hth* expression by the Dpp long-range activity is crucial to get cells ready to cell cycle arrest and for the retinal fate acquisition (Bessa et al., 2002; Domínguez and Casares, 2005; Lopes and Casares, 2010).

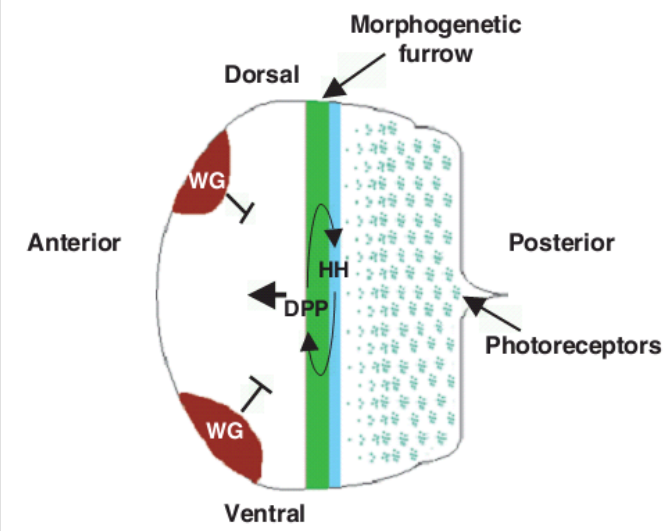

Figure 7- Development of the eye imaginal disc. During the third instar an apical constriction, the morphogenetic furrow (MF), drive the differentiation across the eye disc, from the posterior to the anterior region. With the approximation of the MF, anterior proliferating cells synchronize their cycles and arrest in G1, to differentiate in photoreceptors. Hedgehog (Hh) is a small range signal expressed by differentiated cells, inducing the expression of Decapentaplegic (Dpp) in the MF. Dpp is a long-range signal, inducing the expression of retinal determination genes in the anterior cells, thereby stimulating cells to arrest their cycles. Wingless (Wg) is secreted by the ventral and dorsal edges of the disc, in the region that develops in the head cuticle, limiting the retina formation to the posterior region. Adapted from (Silver and Rebay, 2005).

Therefore, at L3 phase the eye imaginal disc represents a highly ordered system, comprising layers of cells with different levels of commitment, which respond to distinct combinations of signals. The MF represents a changing point, dividing the anterior cells in asynchronous proliferation, from the differentiated photoreceptors at the posterior region.

3. Salivary glands

Drosophila salivary glands are polarized epithelia comprising two extended secretory tubes, composed by an epithelial layer of cells surrounding an inner lumen. Salivary glands produce and secrete several proteins, such as the salivary gland glue proteins that allow the adherence to solid substrates, essential to larvae undergo pupariation (Myat, 2005).

During embryogenesis, salivary cells invaginate from the ventral ectoderm of the embryo, by apical surface constriction. This process results in the formation of the tubular structure and is finely regulated to control the final size and shape of the salivary gland. After internalization, distal cells in contact with the visceral mesoderm migrate to the posterior region, elongating their apical membrane in the direction of the migration, along the Proximal/Distal axis (Hogan and Kolodziej, 2002; Myat, 2005).

Several genes are involved in the salivary gland development. The transcription factor Forkhead has a central role in the invagination process, whereas Hairy, Huckebein, Crumbs and Ribbon are important to the apical growth and migration. Recently it was found that the GTPase Rho1 is necessary to the apical and cell rearrangement, controlling the lumen size by regulation of the actin cytoskeleton and Moesin (Hogan and Kolodziej, 2002; Myat, 2005; Xu et al., 2011).

Terminally differentiated cells of *Dosophila* salivary glands lack the ability to divide and undergo successive cycles of endoreplication, characterized by consecutive rounds of S phases of DNA synthesis and gap phases, without occurring cell division. The resultant polyploid cells acquire a high metabolic output, which allow them to support the larval growth, thereby suffering a dramatic increase in cellular size (Smith and Orr-Weaver, 1991; Edgar and Orr-weaver, 2001). The final ploidy of these cells is regulated by external factors, such as nutritional conditions and temperature, and by growth-related signalling

pathways. In fact, loss of the *Drosophila* serine/threonine kinase, target-of-rapamycin (dTOR), a growth regulator that links the nutritional signalling with protein synthesis, decrease the ability of cells to endoreplicate (Zhang et al., 2000). On the other hand, overexpression of dMyc in salivary glands results in remarkable increase of DNA content (Pierce et al., 2004).

As tubular organs, salivary glands of *Drosophila* have been used as model to study the organogenesis of important tubular systems, such as the mammalian kidneys or lungs (Hogan and Kolodziej, 2002; Myat, 2005).

4. *Drosophila* genetic tools

4.1 GAL4-UAS system

The GAL4-UAS binary system was introduced in *Drosophila* by Brand and Perrimon (Brand and Perrimon, 1993). GAL4 is a potent transcriptional activator of *Saccharomyces cerevisiae*, being expressed in transgenic lines under the control of endogenous regulatory sequences. The upstream activation sequence (UAS) is a GAL4-responsive enhancer, and is positioned upstream of a gene of interest, regulating its expression (Arias, 2008c). The two regulators of the system, GAL4 and UAS, are maintained at separate parental lines. Therefore, when the driver line expressing GAL4 is crossed with the responsive line containing the UAS-dependent transgene, induces the interaction between the GAL4 with the UAS sequence, which activates the expression of the gene of interest in the progeny (Brand and Perrimon, 1993; Duffy, 2002).

Several GAL4 enhancer trap lines exist, to express the GAL4 transcription factor in different tissues or patterns of interest. The main advantages of this technique are the simplicity and ease of manipulate the expression of target genes, at a defined time and space (Brand and Perrimon, 1993; Duffy, 2002; Arias, 2008c).

4.2 RNA interference

The first experiments with double stranded RNA (dsRNA) and the subsequent discovery of the RNA interference (RNAi) in *Caenorhabditis elegans*

resulted in a Nobel Prize in Medicine to Craig Mello and Andrew Fire, in 2006 (Fire et al., 1998).

RNA interference consists in the mechanism of silencing specific target mRNAs as a response to its hybridization with its complementary sequence, and occurs naturally in eukaryotes (Zamore and Haley, 2005). In *Drosophila*, the RNAi can be regulated by the GAL4-UAS system, thereby making possible to down-regulate endogenous target genes in a restricted time and space. This control is achieved by expression of the UAS-dsRNA targeting the gene of interest and a specific GAL4 driver that lead to the degradation of the endogenous target gene mRNA in the target tissue (Duffy, 2002; Dietzl et al., 2007) (Figure 8).

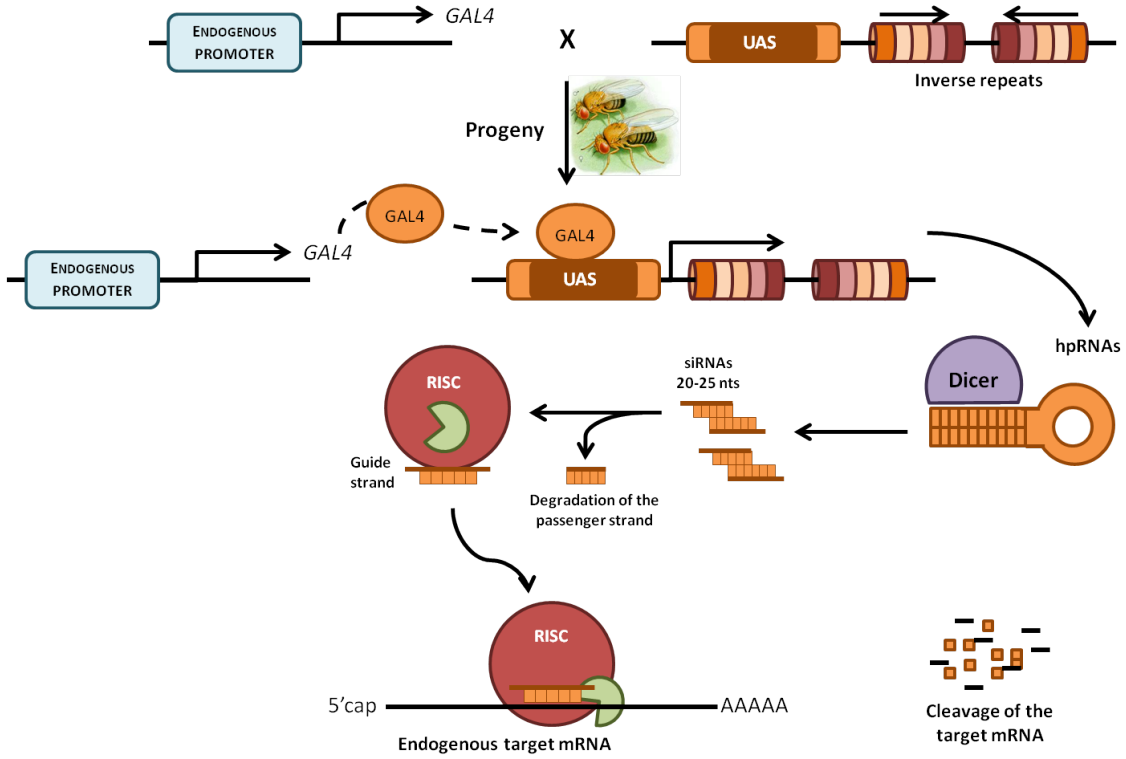

Figure 8- RNA interference approach in *Drosophila melanogaster*. A hairpin RNA (hpRNA) is expressed when GAL4 expressing lines are crossed with a UAS line. The hpRNA is recognized and cleaved by Dicer, in small interference RNAs (siRNAs). The siRNA guide strand is incorporated in the complex RISC driving it to degrade the complementary endogenous target mRNA.

In this approach, the GAL4-UAS system drives the expression of a sequence containing inverted repeats connected by a linker sequence. When transcribed, this sequence gives rise to a double stranded RNA in a hairpin structure perfectly base-paired (hpRNA), recognized by the RNase III Dicer, which cleaves it in double-stranded small interference RNAs (siRNA). One of the siRNA strand is

complementary to the target mRNA, known as the guide strand, whereas the other, named passenger strand, is subsequently degraded. The guide strand is incorporated into the RNA-induced silencing complex (RISC), driving it to the target mRNA. After base-pairing, the RISC protein Argonaute (Ago) mediates the mRNA degradation (Winter et al., 2009).

The creation of the first *Drosophila* genome-wide RNAi transgenic library has allowed the construction of several RNAi screens to study gene function (Dietzl et al., 2007). Coupling of GAL4-UAS system with the RNAi mechanism provides a simple and robust approach in which it is possible to target a specific gene in a temporal- and tissue-specific manner. Moreover, RNAi does not eliminate in absolute the target mRNA levels, thereby creating a hypomorphic condition. All these characteristics allow us to overcome the lethality resultant from mutations in the most essential genes.

The main disadvantage of this approach is the potential off-target effect, resultant from non-specific interactions of the RNAi mechanism with non-desired mRNAs. In fact, it is established that 19 nucleotides of perfect match between the dsRNA and non intended mRNAs is the critical threshold to origin pleotropic phenotypic effects and thus false-positive results (Kulkarni et al., 2006).

Aims of the thesis

Although it is well described the crucial role of TGF-β signalling in patterning, it remains very controversial how this signalling pathway regulates tissue growth.

Based on recent studies in which the *Drosophila* NOL12 homologue Viriato was shown to genetically interact with TGF-β signalling members, the main aim of this thesis is to understand whether the described function of TGF-β in tissue growth is mediated by regulation of nucleolar function.

As Put is the shared type I receptor for both TGF-β pathways, I will use a strong RNAi targeting Put to further investigate the role of TGF-β signalling in nucleolar morphology, integrity and function. Finally I will try to prove if the phenotypic effects caused by the RNAi targeting Put are, in fact, target gene-specific.

Material and Methods

Fly strains and Genotypes

The following stocks (described in FlyBase, unless stated otherwise) were used: *w*^{1118}, *ey*-Gal4, UAS-*lacZ*, UAS-*put*RNAi1 (Vienna *Drosophila* RNAi Center,VDRC, #849) UAS-*put*RNAi2 (VDRC #37279), UAS-*put*RNAi3 (Transgenic RNAi Project, TRiP, #27514), UAS-*put*RNAi4 (TRiP, #35195), UAS-*put*RNAi5 (TRiP, #35701), UAS-*put*RNAi6KK (VDRC, #107071), UAS-*med*RNAi (VDRC, #19688), UAS-*tkv*RNAi (VDRC, #3059), UAS*nopp140*RNAi (VDRC, #45583), RpS9-YFP/TM6c (CPTI-000493, Flannotator), RpL10Ab-YFP/TM6c (Cambridge Protein Trap YFP insertions, #115-462), RpL41-YFP/SM6c (Cambridge Protein Trap insertions, #115-344), Bantam sensor JB20/TM6B (gift from Marco Millan), *w*;;*ban* 5'-*lacZ* (gift from Wei Du), UASBantam (gift from Stephen Cohen), *put*^{88}*ry*/MKRS,Ser^{1}, St^{1}*put*^{135}e^{1}/TM3,Ser^{1} (#3100), *w*^{1118}; Df(3R)BSC841/mwh^{1}kni $^{1i\text{-}1}$ snk^{4}red^{1}e^{1}TL^{3}ca^{1}/TM6c,Sb^{1}cu^{1}. Hsp70GFPNopp140-True, UAS-RFPRpL26, and UASGFPRpL11 were gifts from Patrick Di Mario. All crosses were raised at 25ºC under standard conditions, unless stated otherwise.

To observe the adult eye phenotype resultant from the expression of different RNAis targeting Put, the flies were examined under a stereomicroscope (Stemi 2000, Zeiss) equipped with a digital camera (Nikon Digital Sight DS-2Mv). Representative pictures for each RNAi targeting Put were taken.

Immunostaining

Eye-antennal imaginal discs and salivary glands were dissected in cold Phosphate Buffer Saline (PBS) for 20 minutes. After that, imaginal discs and salivary glands were washed three times with PBT (PBS with 0.1% Triton X100) during 10 minutes, and immunostained during 3 hours with the primary antibodies in PBT, at room temperature. Subsequently imaginal discs and salivary glands were washed three times during 10 minutes with PBT, at room temperature, and immunostained with the secondary antibodies in PBT during 2 hours. After incubation, imaginal discs and salivary glands were washed three times during 10 minutes at room temperature, and stored in 50% Glycerol/PBS, at 4ºC.

Antibodies

Primary antibodies used were: rat anti-elav 7E8A10 at 1:100 (DSHB), rabbit anti-Fibrillarin at 1:250 (Abcam, #ab5821), rat anti-DCadherin at 1:100 (DSHB), mouse anti-AH6 (NLP, nucleolus-like particles) at 1:10 (DSHB), rabbit anti-vito 36337 at 1:250 (Abgent Europe), mouse anti-rRNA mouse at 1:500 (Novus Biologicals), anti-RpS6 at 1:200 (Cell Signalling, #2317), rabbit anti-β-galactosidase at 1:1000 (Cappel). Appropriate Alexa Fluor-conjugated secondary antibodies were from Molecular Probes. Images were obtained with the Leica SP2 AOBS and SP5II confocal system, using the 40x objective (unless stated otherwise), and were processed with Adobe Photoshop.

RNA extraction

Total RNA was isolated from salivary glands of third instar larvae, for the genotype control (*ey*Gal4/UAS-*lacZ*;+) and *put*RNAi (*ey*Gal4/+;UAS-*put*RNAi2/+), using Trizol reagent (Invitrogen) according to the manufacturer's instructions. 250ng of total RNA for each condition were run on 0,8% agarose gel, and UV photographed.

Transmission Electron Microscopy (TEM)

Dissected third instar salivary glands were fixed with 2.5% glutaraldehyde in 0.1 M sodium cacodylate buffer for 30 minutes and post-fixed with 4% osmium tetroxide. After washing, salivary glands were incubated for 30 minutes with 0.5% uranyl acetate and further dehydrated through a graded ethanol series (70% for 10 minutes, 90% for 10 minutes, and four changes of 100%). Salivary glands were then soaked in propylene oxide for 10 minutes and then in a mixture (1:1) of propylene oxide and Epon resin (TAAB Laboratories) for 30 minutes. This mixture was then replaced by 100% Epon resine for 24 hours. Finally, the Epon was replaced by fresh Epon and polymerisation took place for 48 hours at 60ºC. Ultrathin section were obtained using the ultramicrotome, collected in cooper grids and then double contrasted with uranyl acetate and lead citrate. Micrographs were taken using a Joel JEM-1400 electron microscope.

Size measurements and statistics

Salivary gland areas were measured using the Polygon selection tool of ImageJ 1.46J software (NIH, Bethesda, MA, USA). GraphPad Prism 5.0 was used for statistical analysis and for generating the graphical output. Statistical significance was determined using an unpaired, two-tailed Student's *t*-test, with a 95% confidence interval, after assessing the normality distribution of the data with the D'Agostino-Pearson normality test.

Results

Vito genetically interact with TGF-β signalling pathway during eye growth and differentiation

Since the discovery of RNAi mechanism and the creation of the first *Drosophila* genome-wide transgenic library, RNAi has been widely used for gene characterization. The establishment of RNAi genetic screens, targeting specific genes in a specific manner, has shown to be a useful approach to study gene functions and genetic interactions.

Viriato, the *Drosophila* homologue of the human Nol12, was found to be required for tissue growth in *Drosophila* eye. Eye-expression of an RNAi targeting *vito* results in a smaller eye disc, although the differentiation still occurred (Marinho et al., 2011). Therefore, in order to understand the role of Vito in eye development, a targeted double RNAi genetic screen was performed, in which flies expressing an RNAi targeting *vito* were crossed with flies expressing RNAi targeting different *ey*-induced genes (*geneX*, Figure 9A) (Marinho et al., *submitted*).

Considering the adult retina size as the readout, we decided to evaluate the observed genetic interactions, using a quantitative parameter, the Genetic interaction score (π). This parameter is defined as the deviation of the double-RNAi phenotype from the expected by the multiplicative combination of the individual single RNAis (Figure 9A).

The double RNAi genetic screen showed a strong genetic interaction between Vito and members of the TGF-β signalling pathway, unveiling a strong synergistic effect upon eye development (Figure 9B).

A

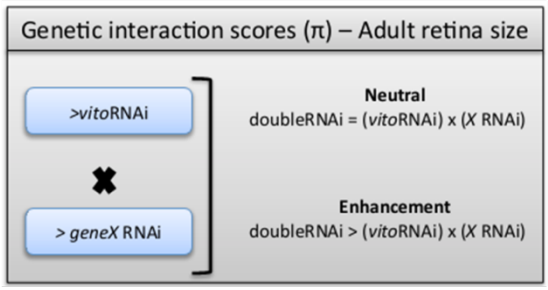

B

		Symbol	Gene name	Single RNAi (retina size)	Double RNAi *vito*RNAi X singleRNAi (expected retina size)*	Double RNAi (observed retina size)	Interaction score (π)
TGF-β signaling pathway	Dpp pathway	tkv	thickveins	0,74	0,52	0,00	**0,52**
		tkv	thickveins	1,00	0,70	0,36	**0,34**
		put	punt	0,95	0,67	0,44	**0,23**
		put	punt	0,00	0,00	Synthetic lethal	**n.d.**
		Med	Medea	0,95	0,67	0,00	**0,67**
		Med	Medea	0,92	0,64	0,00	**0,64**
	Act-β	babo	baboon	1,00	0,70	0,51	**0,19**
		Smox	Smad on X	1,00	0,70	0,51	**0,19**

Figure 9- A eye-targeted double RNAi genetic screen show a strong interaction between Vito and members of TGF-β signalling pathway. (A) Genetic interactions were classified based on the genetic interaction score (π), in which the retina size was the scored phenotype to compare the resultant phenotype with the expected by the multiplicative model. The genetic interaction score will be a direct measure of the increase in retina loss. **(B)** The interaction score is positive for several members of the TGF-β signalling pathways, suggesting a strong interaction between Vito and TGF-β in eye growth. *Expected retina sizes were calculated based on the value for *vito*RNAi retina size of 0.70; n.d. not determined.

Despite its role in tissue growth, the interaction of Vito with the TGF-β pathway seems to be necessary for photoreceptor differentiation in the eye. In fact, expression of RNAi targeting Tkv, the type I receptor of the Dpp branch of TGF-β signalling, or the Co-SMAD Med, results in a decrease in the eye disc size, accompanied by a slight delay in the marginal progression of the differentiation. However, co-expression of any of these RNAis with *vito*RNAi leads to a complete absence of differentiation in the eye discs (Figure 10A). The lack of differentiation is not a cumulative effect on disc growth, as the size of these discs is not statistically different from those of *vito*RNAi (Figure 10B), supporting a role of *vito* in the tissue differentiation induced by Dpp.

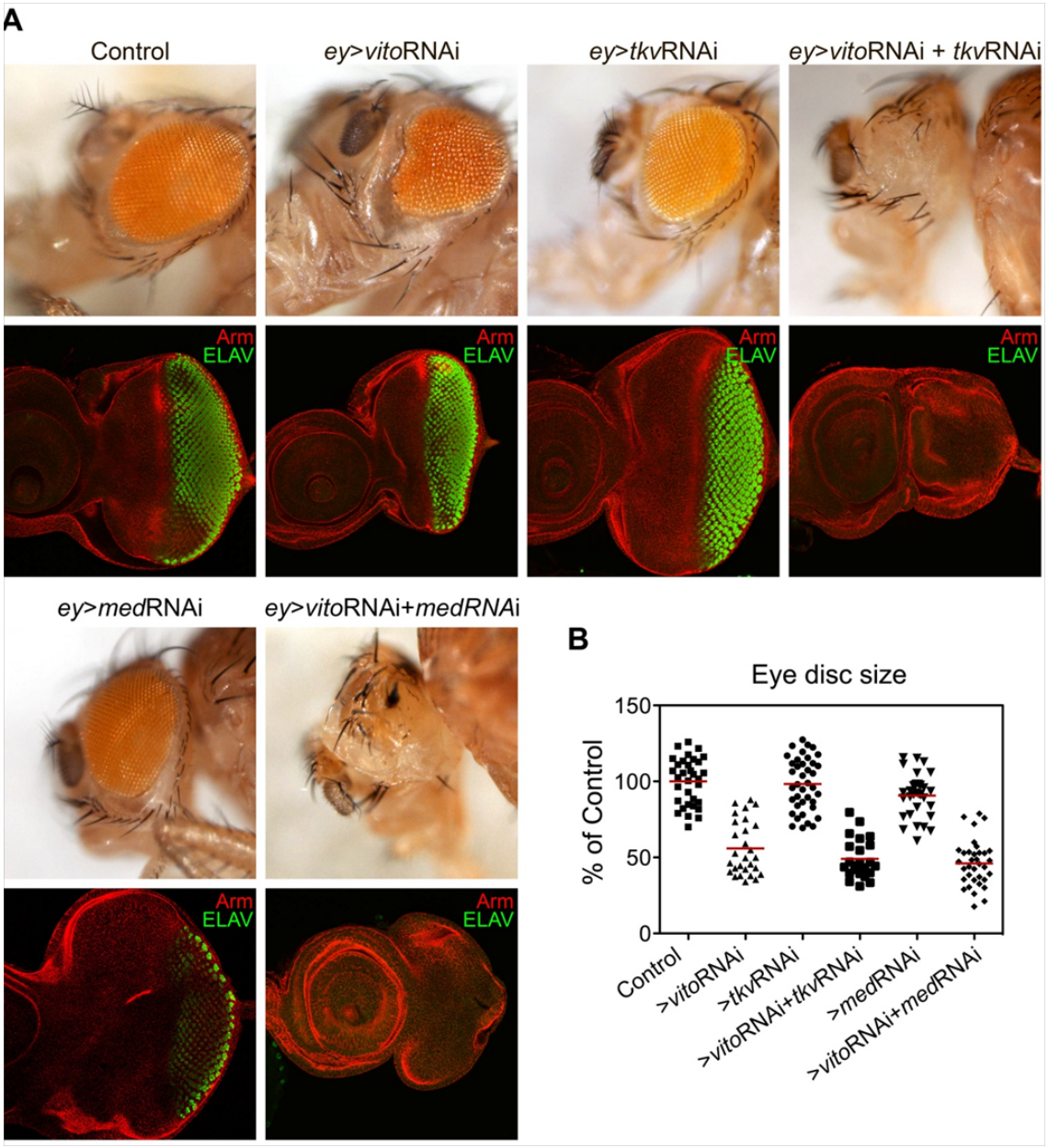

Figure 10- Vito and TGF-β signalling interaction is required for retinal differentiation. (A) Lateral images of the adult retina with the corresponding eye imaginal discs, for the indicated genotypes. Expression of an RNAi targeting Tkv or Med results in a slight reduction in the eye disc size, accompanied by a delay in the progression of the differentiation at the margins of the disc. However, when *vito*RNAi is co-expressed with any of these RNAis, the double RNAi resultant discs completely lack differentiation. The imaginal discs are stained for Armadillo (red) and Elav (green, photoreceptor-specific. **(B)** Eye disc sizes for the indicated genotypes. The size of the double RNAi eye discs is not statistically different from the *vito*RNAi eye discs size.

The progression of the Morphogenetic Furrow in the eye requires the correct nucleolar function

Given that Vito is a nucleolar protein, it was questioned if the differentiation process requires specifically Vito or the correct nucleolar function in general. To test this hypothesis, we used an RNAi targeting another important nucleolar protein, Nopp140. Nopp140 assists the snoRNPs function, acting as chaperone in their transport and assembly, thereby shuttling between the nucleolus and the cytoplasm. Therefore, its function is essential for the correct rRNA processing and assembly (Lo et al., 2006).

Expression of an UAS-RNAi transgene targeting Nopp140 in the eye, using the *eyeless* driver (*ey*Gal4>UAS*nopp140*RNAi), results in a delay in marginal progression of the morphogenetic furrow, although differentiation still occurred (Figure11A, D), resembling the partial loss-of-function of Dpp signalling (Chanut and Heberlein, 1997). Similarly to *vito*RNAi, double RNAi targeting Nopp140 and Tkv or Med result in total lack of differentiation (Figure 11B and E, C and F). Moreover, these discs display a strong growth deficit (Figure 11E and F). Antennal imaginal discs remain unaffected, ensuring that the observed phenotype is not a systematic effect of RNAi.

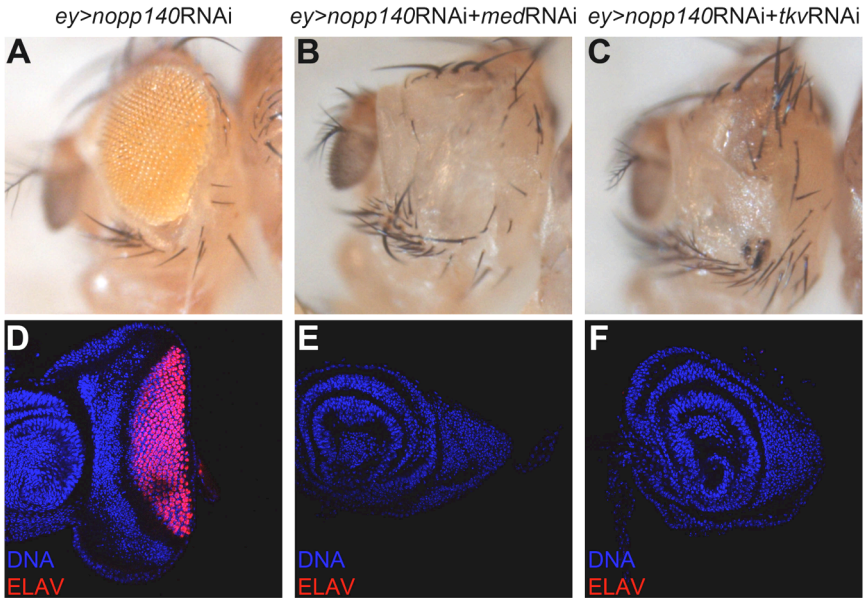

Figure 11- Expression of an RNAi for Nopp140 alters the differentiation process. Lateral views of the adult retinas and the corresponding eye imaginal discs for the RNAi targeting Nopp140 (*ey*G4/+;UAS*nopp140*RNAi/+), co-depletion of Nopp and Med (eyG4/+;UAS*nopp*140RNAi/UAS*med*RNAi) and co-depletion of Nopp140 and Tkv (*ey*G4/UAS*tkv*RNAi;UAS*nopp140*/+). Imaginal discs are stained with Elav to visualize the photoreceptor differentiation. **(A, D)** Expression of the Nopp140 RNAi results in a delay in the MF progression. **(B, E and C, F)** Double RNAi for Nopp140 and Med or Tkv results in discs strongly reduced in size and lacking differentiation.

These results suggest that the differentiation/growth drove by Dpp in the eye disc requires not only Vito but also a functional nucleolus. To investigate this interaction, we took advantage of six different RNAis of different RNAi collections to target Put, with different levels of phenotypic severity. Taking into account that Put is the type II receptor shared by both Dpp and Activin branches, *put*RNAi mimics the silencing of the TGF-β signalling. In the eye, only the expression of *put*RNAi2 blocks the retinal differentiation (Figure 12), being the strongest RNAi for Put. Therefore, we used *put*RNAi2 as the reference for the phenotypic effect of the absence of Put, and consequently disruption of TGF-β signalling.

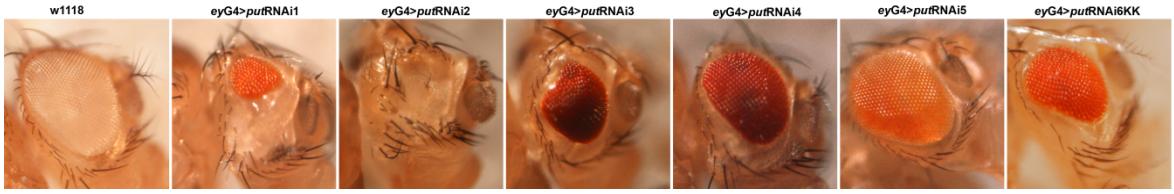

Figure 12- Severity of different RNAis targeting Put. Lateral view of the adult flies retinas expressing different RNAis targeting Put, in relation to control (w^{1118}). The RNAis were expressed in the eye under the *eyeless* (*ey*) driver.

To monitor the nucleolar behaviour in the eye disc we used a nucleolar marker, AH6. Interestingly, nucleolar structure is highly dynamic throughout the imaginal disc, large nucleoli are found in the anterior region and become progressively smaller as differentiation progresses through the eye disc (Figure 13 A and B). Interestingly, this nucleolar size reduction takes place anteriorly to the MF, suggesting that it occurs in response to a long-range signal propagated from the differentiated cells. To investigate this assumption, we decided to explore the nucleolar behaviour in early L2 eye imaginal discs, i.e. before the onset of differentiation (Figure 13 C and D). As hypothesized, when differentiation has not started yet and cells are actively proliferating, the discs display a uniform large nucleolar structure all over the eye disc. Nevertheless, we noted that as soon as differentiation takes place (Figure 13 E and F), the nearby cells change its nucleolar morphology. Once again, the nucleolar response is clearly observed abroad of the MF. To verify if the nucleolar morphology is altered in response to the Dpp signal from the MF, we decided to decrease TGB-β signalling, using the *put*RNAi2. Eye discs expressing this RNAi completely lack differentiation and display nucleolar accumulation of AH6 throughout the disc (Figure 13 G and H).

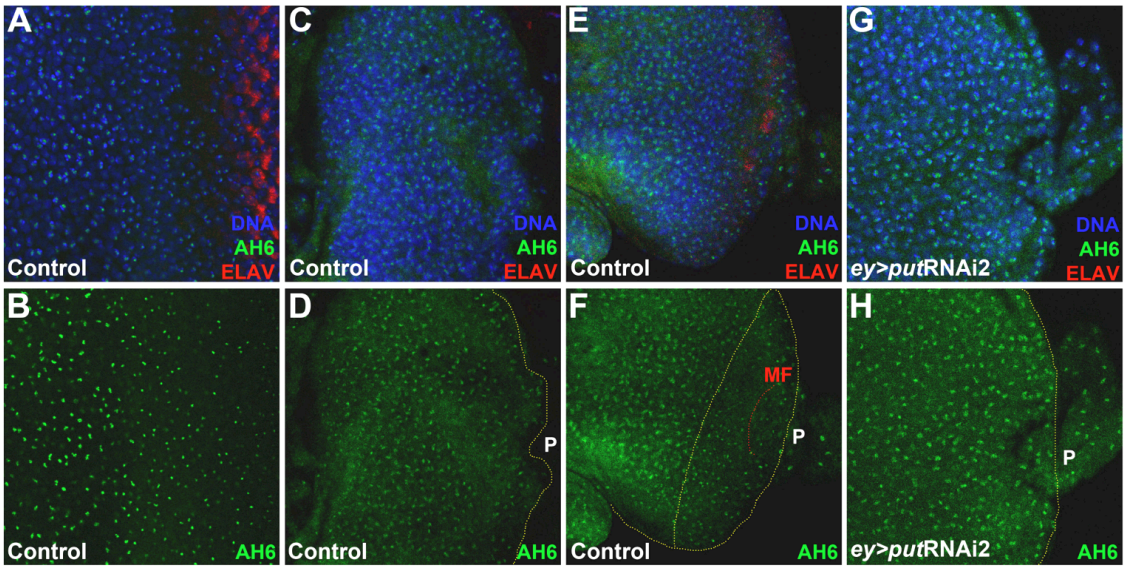

Figure 13- The nucleolar morphology is highly dynamic in response to TGF-β signalling. Eye imaginal discs are stained with for Elav (red), the nucleolar marker AH6 (green) and DAPI (DNA, blue). **(A,B)** Magnification (4x zoom) of L3 eye imaginal disc. Nucleoli become smaller with the approximation of the MF. **(C,D)** Early L2 eye imaginal disc. Before the beginning of differentiation nucleoli are uniformly expanded throughout the disc. **(E,F)** The initiation of differentiation is required and sufficient to trigger the nucleolar morphology change, ahead of the MF (red line). **(G,H)** L3 disc expressing *put*RNAi2 totally lack differentiation. P, Posterior; MF, Morphogenetic Furrow.

These results strongly suggest that TGF-β signalling regulates the function and morphology of nucleolus. This regulation seems to be essential for eye disc development, as retinal differentiation is absent when TGF-β signalling is downregulated, and nucleolar function is compromised (Figure 11).

Disruption of TGF-β signalling has a direct effect on nucleolar integrity and salivary glands growth

To further explore the effect of TGF-β in the nucleolar architecture, we made use of a YFP-trapped ribosomal protein RpL41, which has nucleolar localization (Wang et al., 2010). The YFP reporter was inserted in RpL41 exon, thereby reflecting its endogenous expression pattern. In control eye discs, RpL41 is mainly expressed at the anterior region, where the nucleoli are bigger (Figure 14, control). In accordance with the previous results, expression of *put*RNAi2 results in eye discs without retinal differentiation, exhibiting larger nucleolus uniformly throughout the disc. In these discs the RpL41 expression is detected all over the disc (Figure 14, *ey>put*RNAi).

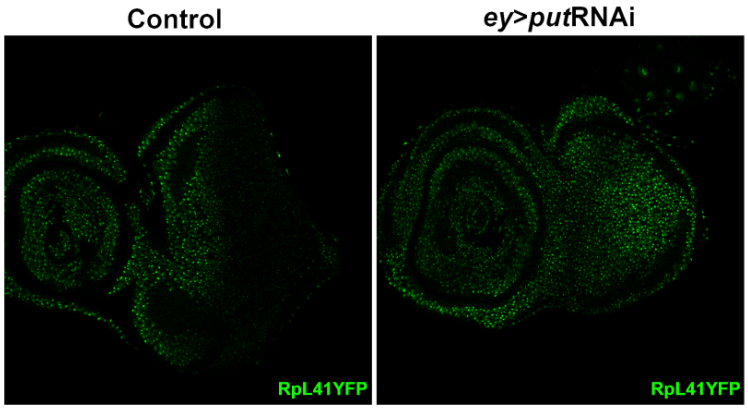

Figure 14- RpL41 expression pattern in the eye disc change with Put depletion. In control discs expressing lacZ (*ey*G4:RpL41YFP/UAS*lacZ*;+), RpL41 is only expressed in the anterior region of the eye disc. However, in discs expressing a strong RNAi targeting Put (*ey*G4:RpL41YFP/+;UAS*put*RNAi2/+) RpL41 expression is detected throughout the disc.

Due to their polyploidy, salivary gland cells display large nucleoli, allowing a more detailed analysis of nucleolar structure. In control cells RpL41-YFP is localized in low levels at nucleoli (Figure 15A, control). However, when TGF-β signalling is depleted by the expression of *put*RNAi2, this protein accumulates in abnormal higher levels (Figure 15A, *ey>put*RNAi). Interestingly, the intensity of RpL41-YFP fluorescence at nucleoli of salivary glands is proportional to the adult eye phenotypic severity of the different RNAis targeting Put (Figure 15B). Therefore, we took advantage of this correlation and used RpL41-YFP as readout of the nucleolar function and integrity.

The main function of nucleoli is to provide the adequate supply of functional ribosomes to sustain the cellular demand of proteins. Considering this, two possible explanations for the observed phenotype are plausible. It could be that *put* depleted cells have an increased metabolism, therefore requiring a higher nucleolar activity. On the other hand, *put*RNAi expression could cause impairment in nucleolar function, thereby accumulating RpL41 as a cellular mechanism of compensation. As observed for Myc overexpression (Pierce et al., 2004; Grewal et al., 2005), cells with increased metabolism display enlarged nucleoli and expanded cellular size, due to the increase in protein synthesis. However, although *put*RNAi salivary gland cells exhibit a significant increase of the ratio between nucleolar/nuclear area, the nuclear and cellular areas are significantly decreased in relation to the control (Figure 16), indicating that *put*RNAi results in an abnormal RpL41 accumulation at nucleolus that cannot be explained by an increase of the nucleolar activity for cell growth.

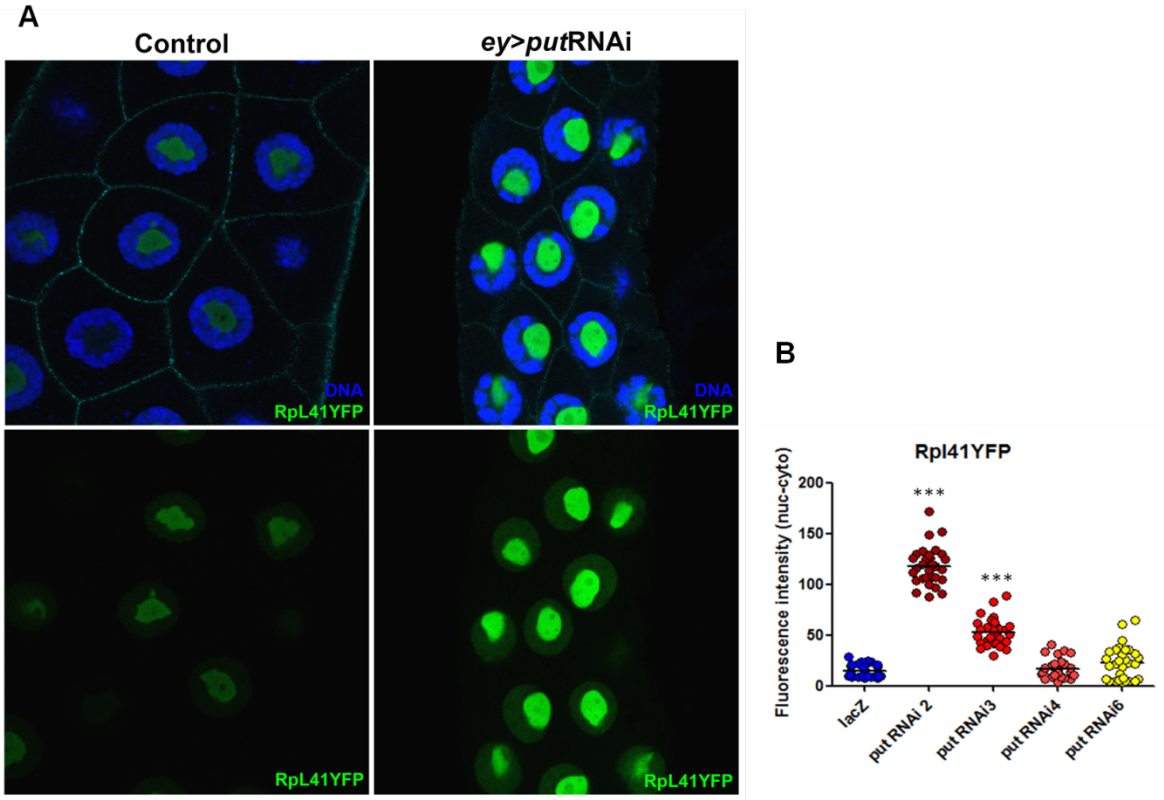

Figure 15- Absence of Put results in nucleolar accumulation of RpL41-YFP. (A) Third instar salivary glands expressing RpL41-YFP (green) and stained with DAPI (DNA, blue) are shown. RpL41 is a nucleolar protein present in low levels at the nucleolus in control salivary gland cells (*ey*Gal4:RpL41-YFP/UAS-*lacZ*;+). The absence of Put by the expression of a strong RNAi under the control of *eyeless* driver (*ey*Gal4/RpL41-YFP;UAS*put*RNAi2/+) results in an abnormal nucleolar accumulation of RpL41. **(B)** Scatter plots comparing the quantification of the fluorescence intensity of RpL41-YFP from nucleolus of the several *put*RNAis. RpL41-YFP fluorescence intensity at salivary gland nucleoli is proportional to Put RNAi severity in the adult fly eye. Statistics were done using ANOVA one way analysis (***, p<0.0001).

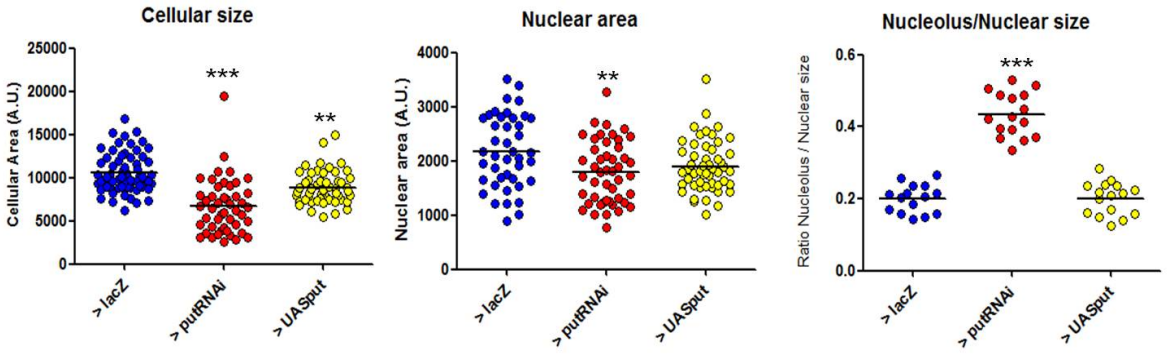

Figure 16- TGF-β signalling directly regulates the ratio between nucleolar and nuclear areas. Scatter plots comparing cellular areas, nuclear areas, and the ratio between nucleolar and nuclear areas of third instar salivary gland cells, for the control genotype (*ey*G4/UAS*lacZ*;+), *put*RNAi (*ey*G4/+;UAS*put*RNAi2/+) and Put overexpression (*ey*G4/+;UAS*put*/+). Statistics were done using ANOVA one way analysis (**, p<0.001; ***, p<0.0001).

Interestingly, overexpression of Put also reduces the cellular size, although the nuclear area and the ratio between nucleolar and nuclear areas do not change (Figure 16). In addition, we found that variation of Put levels, either by expression *put*RNAi2 or by Put overexpression, inhibits salivary glands growth (Figure 17A). Both salivary glands exhibit a significant deficit of growth in relation to control and never reach the normal size (Figure 17B), suggesting that maintenance of Put within equilibrated levels during development is crucial to the normal growth of this tissue. These results point to a key role of Put in regulating nucleolar morphology and function, and reveal a direct effect of TGF-β signalling in cellular and tissue growth.

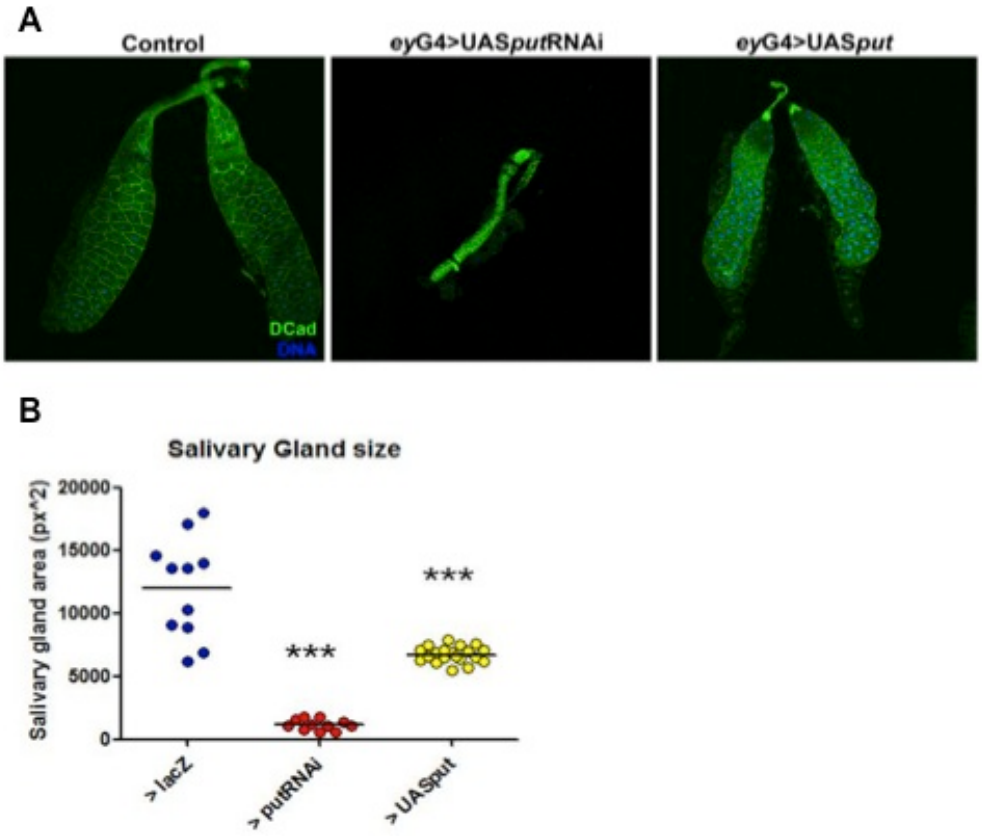

Figure 17- Put levels directly affect salivary glands size. (A) Third instar salivary glands stained with D-Cadherin (DCad, green) and DNA (blue) are shown for the control genotype (*ey*G4/UAS*lacZ*;+), *put*RNAi (*ey*G4/+;UAS*put*RNAi/+) and Put overexpression (*ey*G4/+;UASPut/+). Variation of Put levels results in a growth deficit in salivary glands. Images were taken using 10x objective. **(B)** Scatter plots comparing the salivary gland area for the indicated genotypes. Salivary gland areas are significantly reduced in Put depletion or overexpression. Statistics were done using ANOVA one way analysis (***, $p<0.0001$)

TGF-β signalling controls the recruitment of specific nucleolar components

As TGF-β signalling seems to regulate nucleolar morphology, we decided to investigate the behaviour of nucleolar specific proteins, such as Nopp140 and Fibrillarin. Both proteins are resident at nucleolus, thereby being important for the maintenance of nucleolar architecture. Moreover, Nopp140 and Fibrillarin have crucial enzymatic roles in the rRNA processing and maturation (Wang et al., 2000; Lo et al., 2006).

We made use of the GFP-tagged Nopp140-True protein, expressed from a heat-shock inducible promoter. At 25ºC this promoter has basal activity, and the protein is detected without heat-shock. In control salivary gland cells, Nopp140 is accumulated at nucleolus, being barely detected at cytoplasm (Figure 18, upper panel). When TGF-β signalling is decreased by the expression of *put*RNAi2, the levels of this protein strongly reduce at nucleolus, and are only detected in the most proximal cells of the salivary glands (Figure 18, bottom panel).

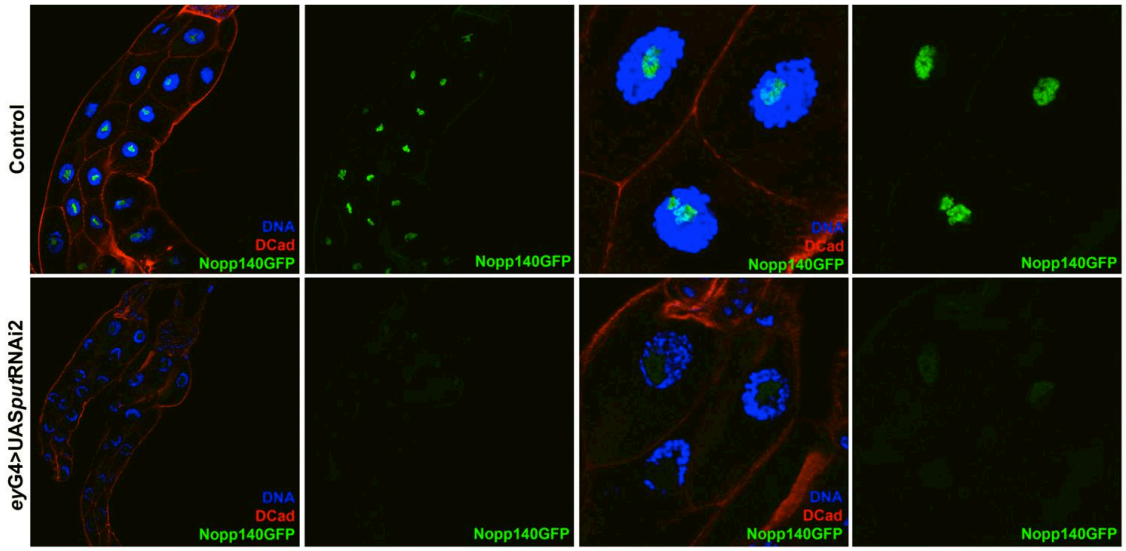

Figure 18- Nucleolar levels of Nopp140 decrease in absence of TGF-β signalling. Third instar salivary glands and correspondent magnifications (4x zoom). Expression of the Nopp140-GFP protein (green) was observed for the control genotype (*ey*G4/+;Nopp140-GFP/+) and Put RNAi (*ey*G4/+;UAS*put*RNAi2/Nopp140-GFP). DNA is marked by DAPI (blue). Whereas in control cells Nopp140 is well detected at nucleolus, its levels strongly decrease with the expression of *put*RNAi2.

Fibrillarin also localizes in higher levels at nucleolus of control cells, being barely detected at cytoplasm and nuclei (Figure 19A, left panel). Contrary to Nopp140, when *put*RNAi2 is expressed in these cells Fibrillarin levels increase and this protein strongly accumulates at nucleolus, where it becomes arranged in

a “hollow” structure, more concentrated at nucleolar peripheral regions (Figure 19A, middle panel). Moreover, overexpression of Put in salivary glands induces a reduction in Fibrillarin accumulation at nucleolus (Figure 19A, right panel).

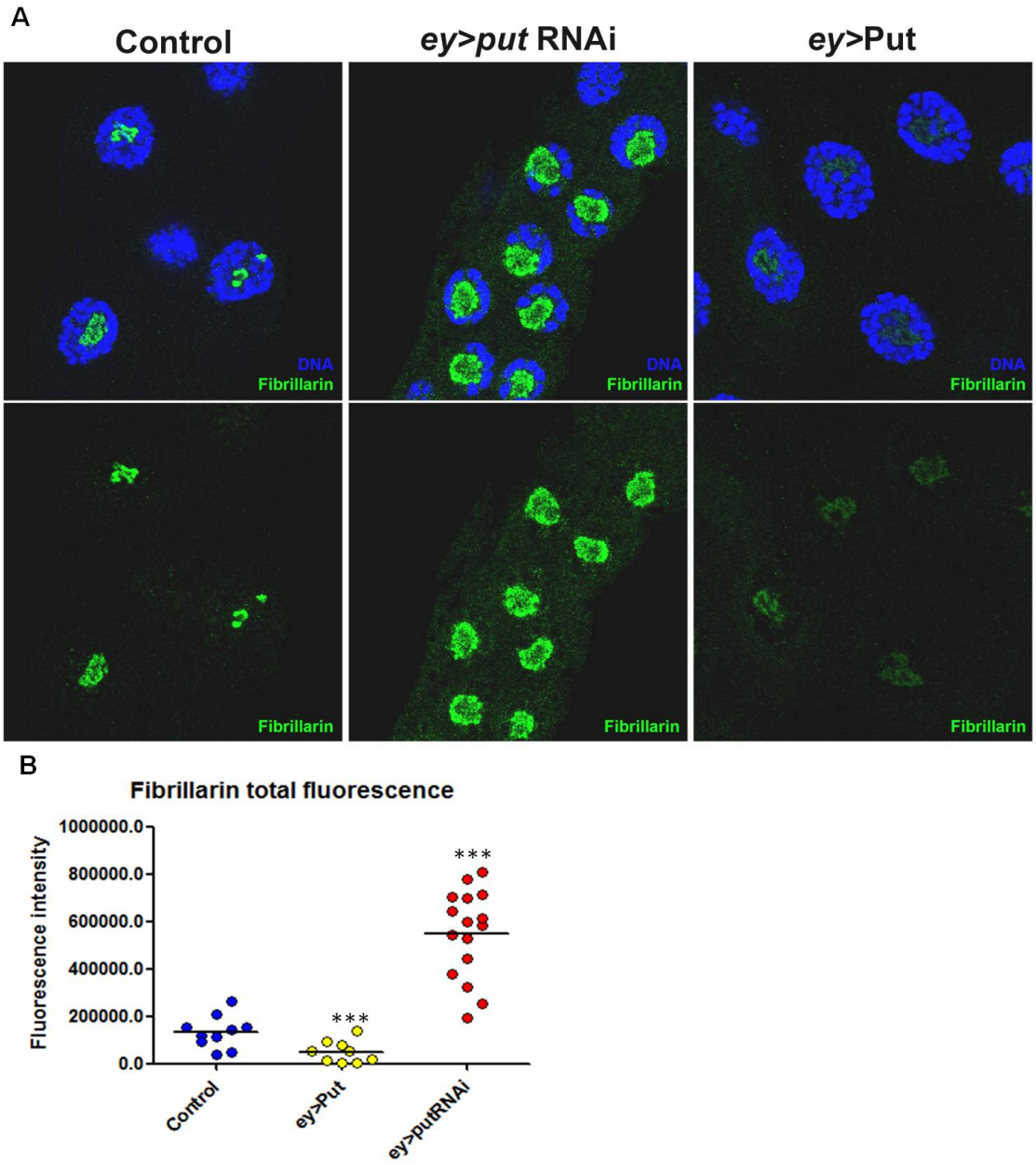

Figure 19- TGF-β signalling regulates the recruitment of Fibrillarin to nucleolus. (A) Magnifications (4x zom) of third instar salivary glands stained for Fibrillarin (green) and DNA (blue) are shown, for the control genotype (*ey*G4/UAS*lacZ*;+), *put*RNAi (*ey*G4/+;UAS*put*RNAi2/+) and overexpression of Put (*ey*G4/+;UASPut/+). **(B)** Scatter plots representing the quantification of total Fibrillarin fluorescence intensity from third instar salivary glands nucleoli, for the same genotypes. In relation to control, Fibrillarin levels are significantly increased in the absence of Put, and significantly decreased when Put is overexpressed. Statistics were done using ANOVA one way analysis (***, p<0.0001).

In fact, quantification of the Fibrillarin fluorescence intensity at nucleolus has shown that in absence of Put, Fibrillarin levels are significantly increased, whereas overexpression of Put significantly decreases the protein levels, in relation to control cells. Thus, Put levels control the recruitment of Fibrillarin to nucleolus (Figure 19B).

These results demonstrate that absence of TGF-β signalling alters the nucleolar morphology and enzymatic activity (rRNA processing and maturation) by mis-localization of specific structural components of nucleolus, such as Nopp140 and Fibrillarin.

Disruption of TGF-β signalling results in mis-localization of ribosomal proteins

Besides resident proteins, the nucleolar structure is composed by several ribosomal proteins, translocated from the cytoplasm to be assembled in the nascent immature rRNA particles (Boulon et al., 2010). Once disruption of TGF-β signalling has shown to modify the retention of nucleolar resident proteins, and induces nucleolar accumulation of RpL41, we decided to investigate the behaviour of other RPs belonging to both ribosome subunits.

To monitor ribosome small subunit proteins, we stained salivary gland cells with anti-RpS6 and made use of the YFP-trapped protein RpS9. RpS6 is only detected at the cytoplasm of control salivary gland cells (Figure 20, upper panel). However, in the absence of *put*, it was observed a slight decrease in cytoplasmic levels of RpS6, accompanied by an ectopic accumulation of this ribosomal protein at nucleoli (Figure 20, bottom panel).

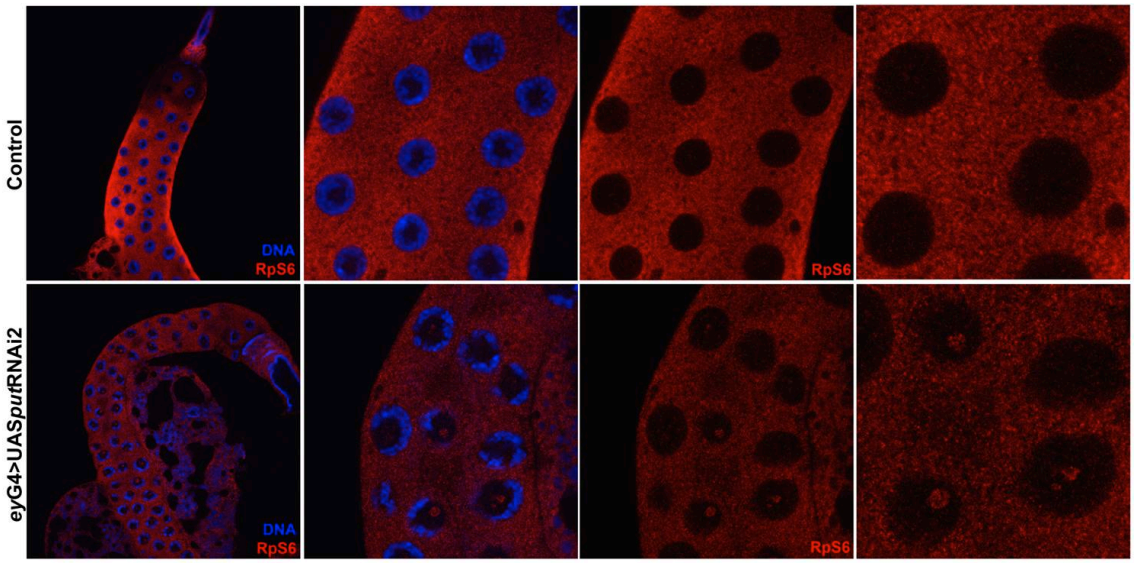

Figure 20- Absence of TGF-β signalling results in ectopic accumulation of RpS6 at nucleolus. Third instar salivary glands and correspondent magnifications (4x zoom) were stained with anti-RpS6 (red) and the DNA marker DAPI (blue), for the control genotype (*ey*G4/UAS*lacZ*;+) and for Put RNAi (*ey*G4/+;UAS*put*RNAi2/+). Whereas in control cells RpS6 is only present at cytoplasm, depletion of *put* results in ectopic accumulation of RpS6 in nucleolar aggregates.

The other ribosomal small protein analysed, RpS9, is detected at high levels in the cytoplasm and at low levels at nucleoli (Figure 21, upper panel). Disruption of TGF-β signalling strongly decreases RpS9 levels, although it may still be detected in cytoplasm and nucleoli of proximal cells (Figure 21, bottom panel).

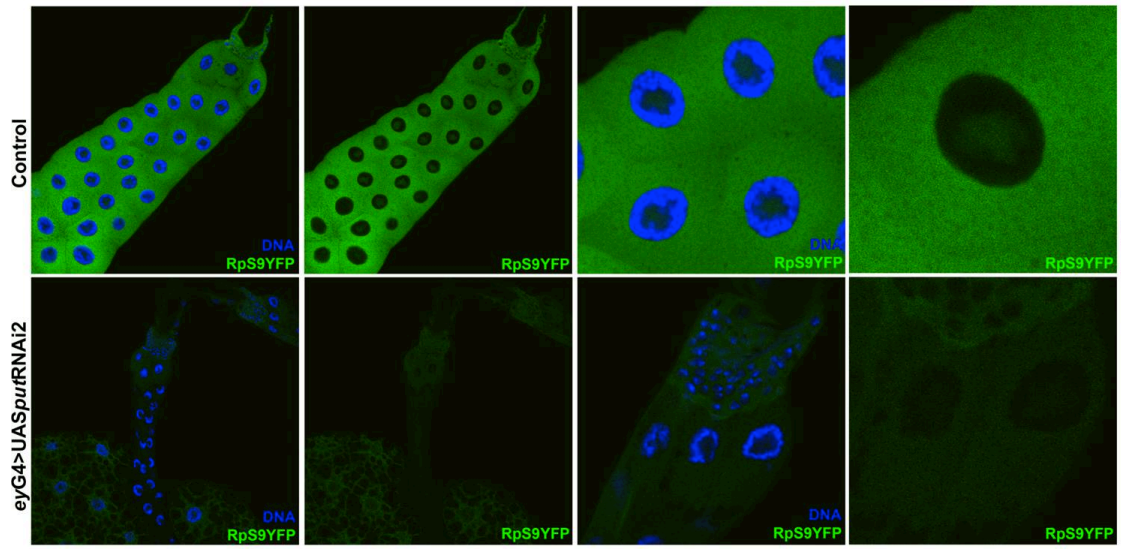

Figure 21- RpS9 levels in salivary gland cells decrease when TGF-β signalling is disrupted. Third instar salivary glands and correspondent magnifications (4x zoom). Expression of the YFP-tagged RpS9 protein (green) was observed for the control genotype (*ey*G4/+;RpS9-YFP/+) and Put RNAi (*ey*G4/+;UAS*put*RNAi2/RpS9-YFP). In control cells RpS9 is present at cytoplasm and nucleoli. Put depletion by the expression of *put*RNAi2 in these cells results in a strong decrease of RpS9 levels. Salivary glands were stained with DAPI (blue) to mark DNA at nuclei.

To further investigate if the large ribosome proteins behave in the same way, we analysed the expression of the YFP-tagged RpL10Ab protein, which reproduce the endogenous expression of RpL10Ab. In control salivary gland cells RpL10Ab is detected in similar levels at cytoplasm and nucleoli (Figure 22, upper panel), but expression of *put*RNAi2 results in a slight increase in nucleolar levels.

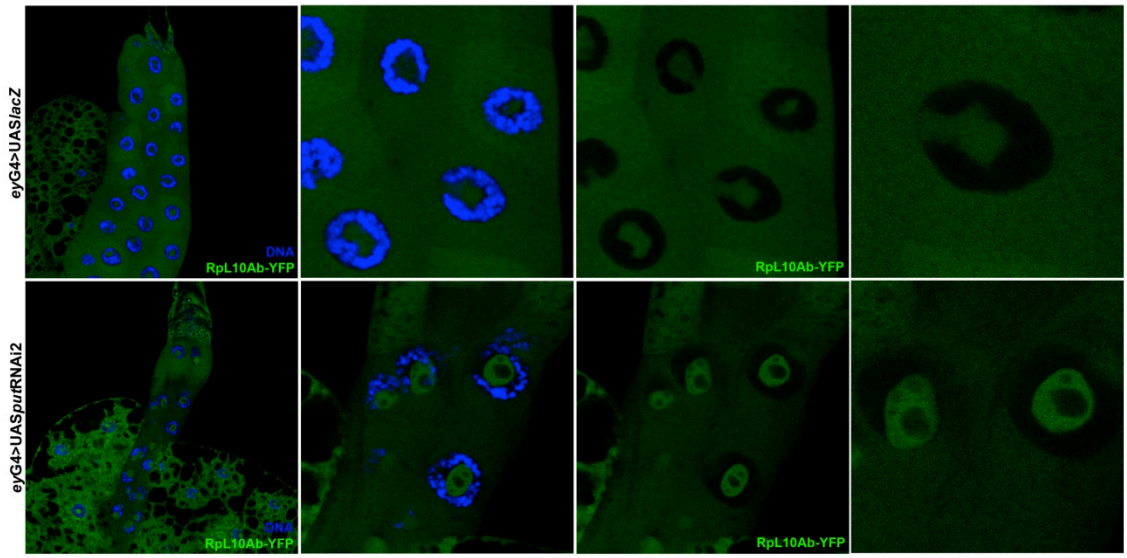

Figure 22- RpL10Ab levels are changed when TGF-β signalling is depleted. Third instar salivary glands and correspondent magnifications (4x zoom). Expression of the YFP-tagged RpL10 protein (green) was observed for the control genotype (*ey*G4/+; RpL10-YFP/+) and Put RNAi (*ey*G4/+;UAS*put*RNAi2/RpL10-YFP). DNA is marked by DAPI (blue). RpL10-YFP is detected in similar levels at cytoplasm and nucleoli in control cells, but its levels and localization at nucleolus become altered with the disruption of TGF-β signalling by the expression of *put*RNAi2.

Moreover, whereas in control cells this protein accumulates at nucleolus in a uniform condensed structure, in *put*RNAi cells RpL10Ab assembles in compact structures that are more intense at peripheral regions, surrounding vacuolar structures, in which RpL10 is occasionally present in low levels (Figure 22, bottom panel).

Besides RpL10, we also analysed the nucleolar localization of the ribosomal large subunit proteins RpL11-GFP and RpL26-RFP. In control salivary gland cells, RpL11 is present at cytoplasm and accumulates in higher levels at nucleoli (Figure 23, upper panel). When *put*RNAi2 is expressed in these cells, RpL11 levels strongly decrease and the protein is no longer detected in most nucleoli. Nevertheless, at nucleoli where it was still present RpL11 is in similar levels at nucleoli and cytoplasm, a behaviour that differs from the controls (Figure 23, bottom panel).

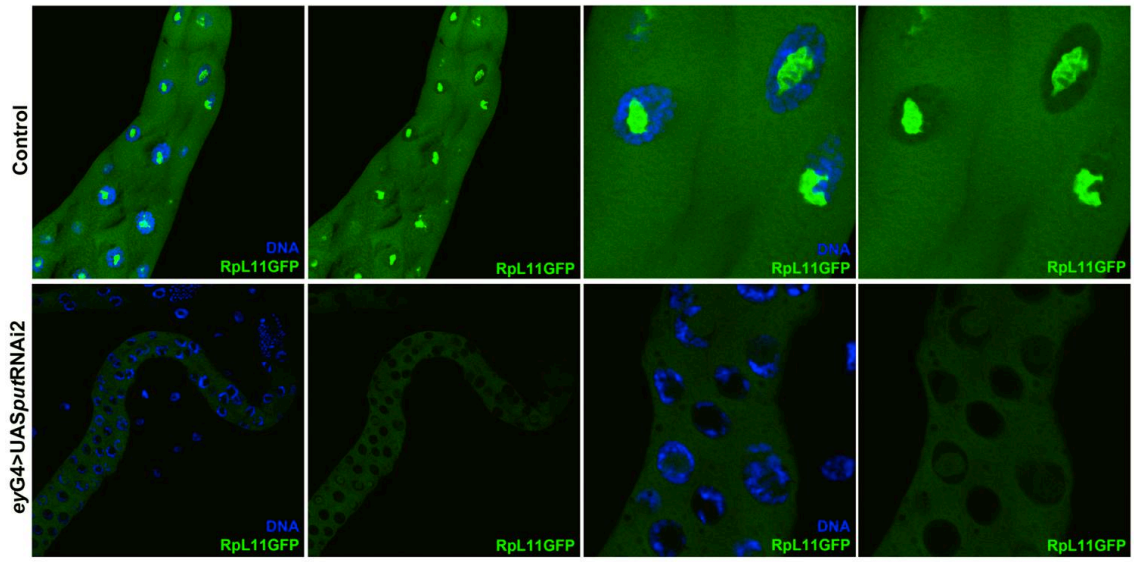

Figure 23- RpL11 levels in salivary gland cells decrease in absence of TGF-β signalling. Third instar salivary glands and correspondent magnifications (4x zoom). Expression of the RpL11-GFP protein (green) was observed for the control genotype (*ey*G4/UASRpL11-GFP;+) and Put RNAi (*ey*G4/UASRpL11-GFP;UAS*put*RNAi2/+). DNA is marked by DAPI (blue). In control cells RpL11 is accumulated in higher levels at nucleoli, but its levels strongly decrease with depletion of TGF-β signalling.

RpL26-RFP is detected at cytoplasm and slightly accumulated at nucleoli (Figure 24, upper panel). When *put*RNAi2 is expressed, RpL26-RFP becomes more dispersed and spreads to nuclei in similar levels to cytoplasm. However, conversely to RpL11-GFP, cytoplasmic and nucleolar levels do not considerably change in these cells, in relation to control (Figure 24, bottom panel).

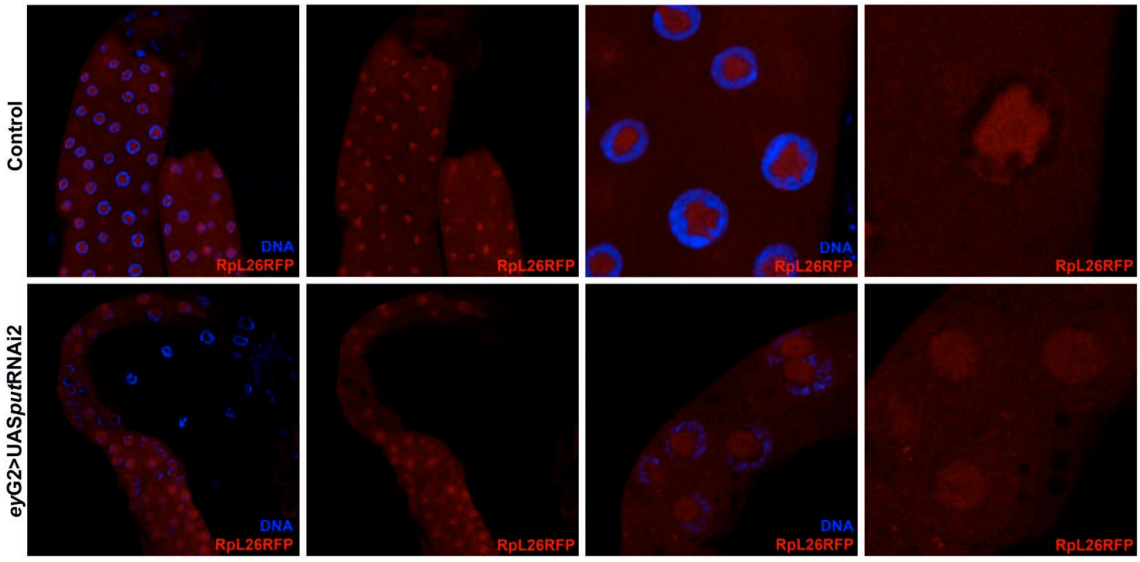

Figure 24- RpL26 intensity in salivary gland cells is not altered in the absence of TGF-β signalling. Third instar salivary glands and correspondent magnifications (4x zoom). Expression of the RpL26-RFP protein (red) was observed for the control genotype (*ey*G4/+;UASRpL11-GFP/+) and Put RNAi (*ey*G4/+;UAS*put*RNAi2/UASRpL26-RFP). DNA is marked by DAPI (blue). In control cells RpL26 expression is detected in cytoplasm and in bigger levels at nucleoli. When putRNAi2 is expressed this protein is also diffused in nuclei, but its levels at cytoplasm and nucleoli remain similar to control.

Interestingly, a general decrease in expression levels is observed for almost all analysed proteins in *put*RNAi-expressing cells, indicating that absence of Put might result in suboptimal levels of protein expression. To test this hypothesis, we used as a control a nuclear GFP-tagged protein, 6xmyc, which is not directly affected by TGF-β signalling. When *put*RNAi2 is expressed, the fluorescence intensity of 6xmyc-GFP also decreases in relation to control (Figure 25).

These results demonstrate that TGF-β signalling not only interacts with nucleolar structural proteins, but also affects the localization and levels of ribosomal proteins. Moreover, disruption of Put negatively affects the efficiency of cell in protein production, possibly due to impairment in ribosome biogenesis.

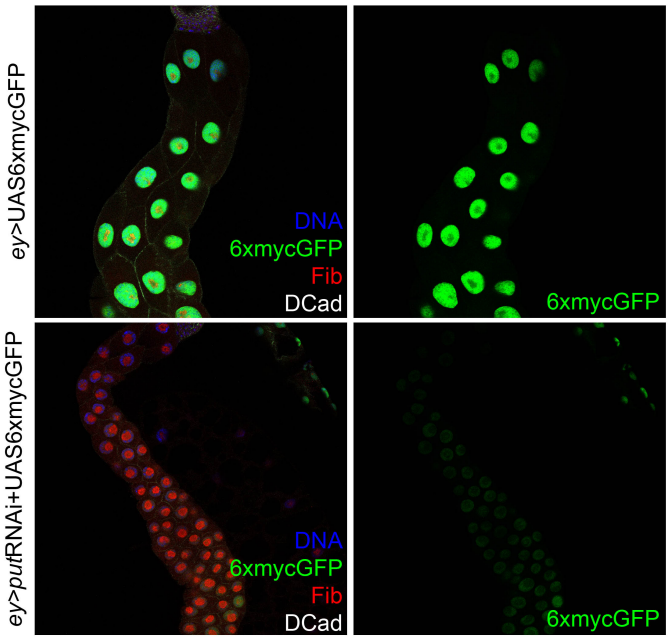

Figure 25- Expression of Put RNAi results in suboptimal levels of protein expression. The 6xmycGFP protein was used as a control to test the effect of depletion of TGF-β signalling in general protein expression. Simultaneous expression of UAS*put*RNAi and UAS6xmycGFP (*ey*G4/UAS6xmyc-GFP;UAS*put*RNAi/+) diminishes the GFP fluorescence intensity (green), in relation to the control expressing only UASGFP6xmyc (*ey*G4/UAS6xmyc-GFP;+). Third instar salivary glands were stained with Fibrillarin (Fib, red), D-Cadherin (DCad, white) and DAPI (DNA, blue).

Disruption of TGF-β signalling results in defective ribosome biogenesis

The deficit of growth observed in *put*RNAi-expressing cells, along with the mis-localization of ribosomal proteins and the decreased protein synthesis strongly suggest that absence of TGF-β signalling affects nucleolar function, resulting in defective ribosome biogenesis.

To test this hypothesis, we used an antibody to mark rRNA in salivary gland cells. The ribosomal RNA is transcribed at nucleolus and suffers rounds of processing and maturation, being quickly translocated to nucleoplasm and then exported to the cytoplasm. This process is extremely dynamic and requires several proteins to give rise the mature 28S, 5.8S and 18S rRNAs. Moreover, it must happen in a short period of time in order to supply the cellular demand of protein synthesis (Raska et al., 2004; Xue and Barna, 2012b). Thus, the passage of the rRNA in the nucleolus is transitory, and is not detected in the control salivary gland cells (Figure 26, upper panel). However, in *put*RNAi2-expressing cells, the ribosomal RNA can be detected in small aggregates within the nucleolus (Figure 26, bottom panel). Interestingly, when we analysed the localization of the homologue human exonuclease Nol12 (Vito), we found that it accumulates in the same regions of rRNA, whereas in control cells it is uniformly distributed trough nucleoli, nuclei and cytoplasm (Figure 26).

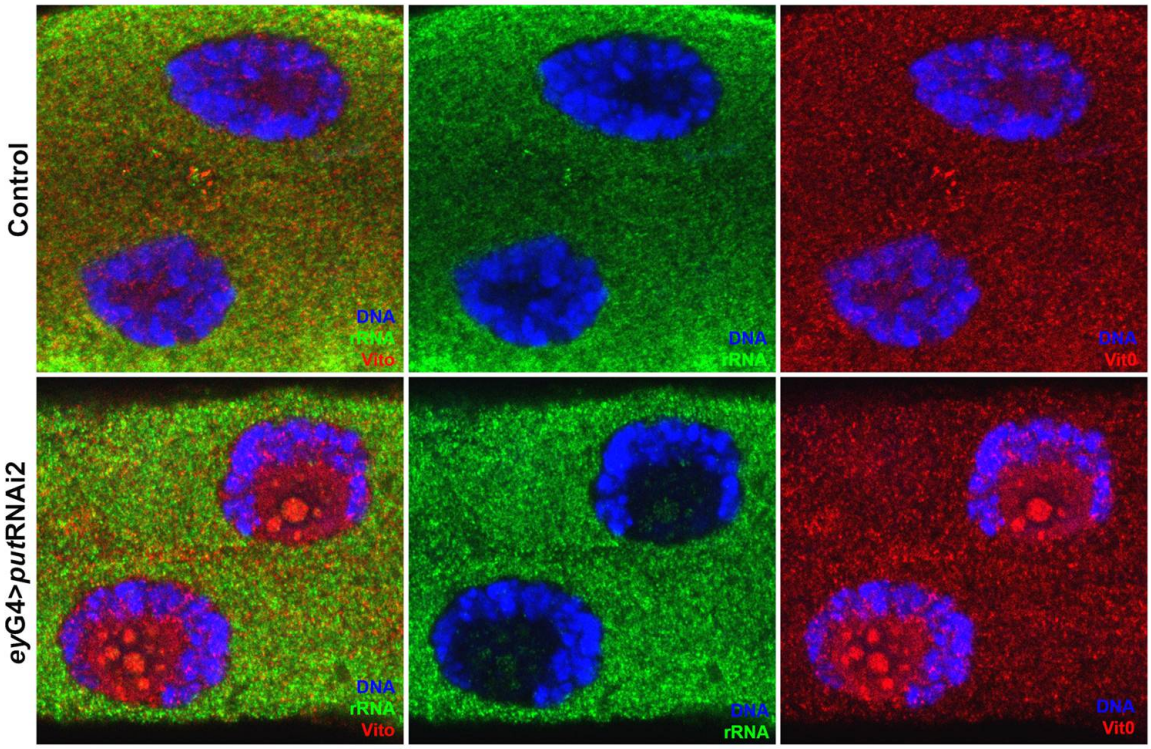

Figure 26- Disruption of TGF-β signalling results in nucleolar accumulation of rRNA, which co-localize with Vito. In control salivary gland cells, rRNA (green) is not detected at nucleoli, whereas Vito (red) is uniformly expressed in nucleoli, nuclei and cytoplasm. Expression of *put*RNAi2 results in small aggregates of rRNA at nucleoli. In these cells, Vito accumulates specifically at the ribosomal aggregates.

These results suggest that absence of TGF-β signalling results in a defective ribosome biogenesis, which possibly causes retention of immature

rRNA particles at nucleolus. Indeed, when we isolated the total RNA of third instar salivary glands of control genotype (*ey*Gal4/UAS*lacZ*;+) and *put*RNAi (*ey*Gal4/+;UAS*put*RNAi2/+), the amount of mature rRNA (18S and 28S) was decreased in *put*RNAi-expressing salivary glands (Figure 27), suggesting that the accumulation of immature rRNA at nucleolus is due to its defective processing and maturation.

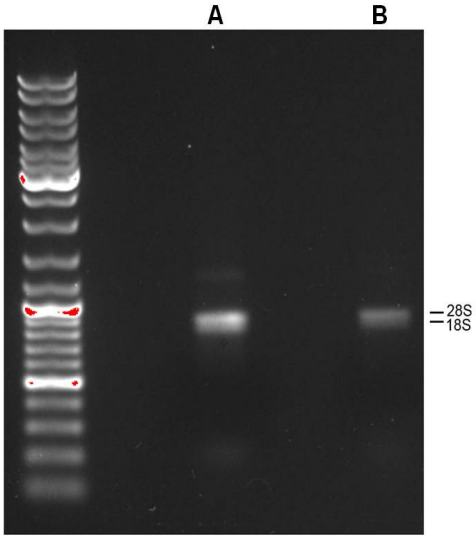

Figure 27- Absence of TGF-β signalling results in a decrease of mature rRNA. RNA extraction from third instar salivary glands of the control genotype (*ey*G4/UAS*lacZ*;+) (A) and *put*RNAi2 (*ey*G4/+;UAS*put*RNAi2/+) (B), showing that TGF-β signalling depletion leads to decreased amounts of mature 28S and 18S rRNAs in relation to control salivary glands. Ribosomal RNA bands are indicated and the total load RNA amount for each condition was 250ng.

To further evaluate functional and structural effects of Put at nucleoli in higher magnification, we used Transmission Electron Microscopy (TEM). As previously described, *Drosophila* nucleoli is not divided in sub-regions, as happens in vertebrates (Orihara-Ono et al., 2005). Control salivary gland cells display uniformly compacted nucleoli (Figure 28, upper panel). In contrast, *put*RNAi2-expressing cells exhibit a nucleolus that occupies most of nuclear area and contains vacuolar structures inside. In concordance with the previous indirect results, it is visible using this technique an abnormal accumulation of small particles, pre-ribosomes, near the nucleolus-nucleus boundary, and occasionally within the vacuolar structures (Figure 28, middle panel). Conversely, salivary glands overexpressing Put displayed a low contrast nucleolus, an organization in accord with our previous data where it was shown that nucleolar proteins barely localize at nucleolus (Figure 28, bottom panel).

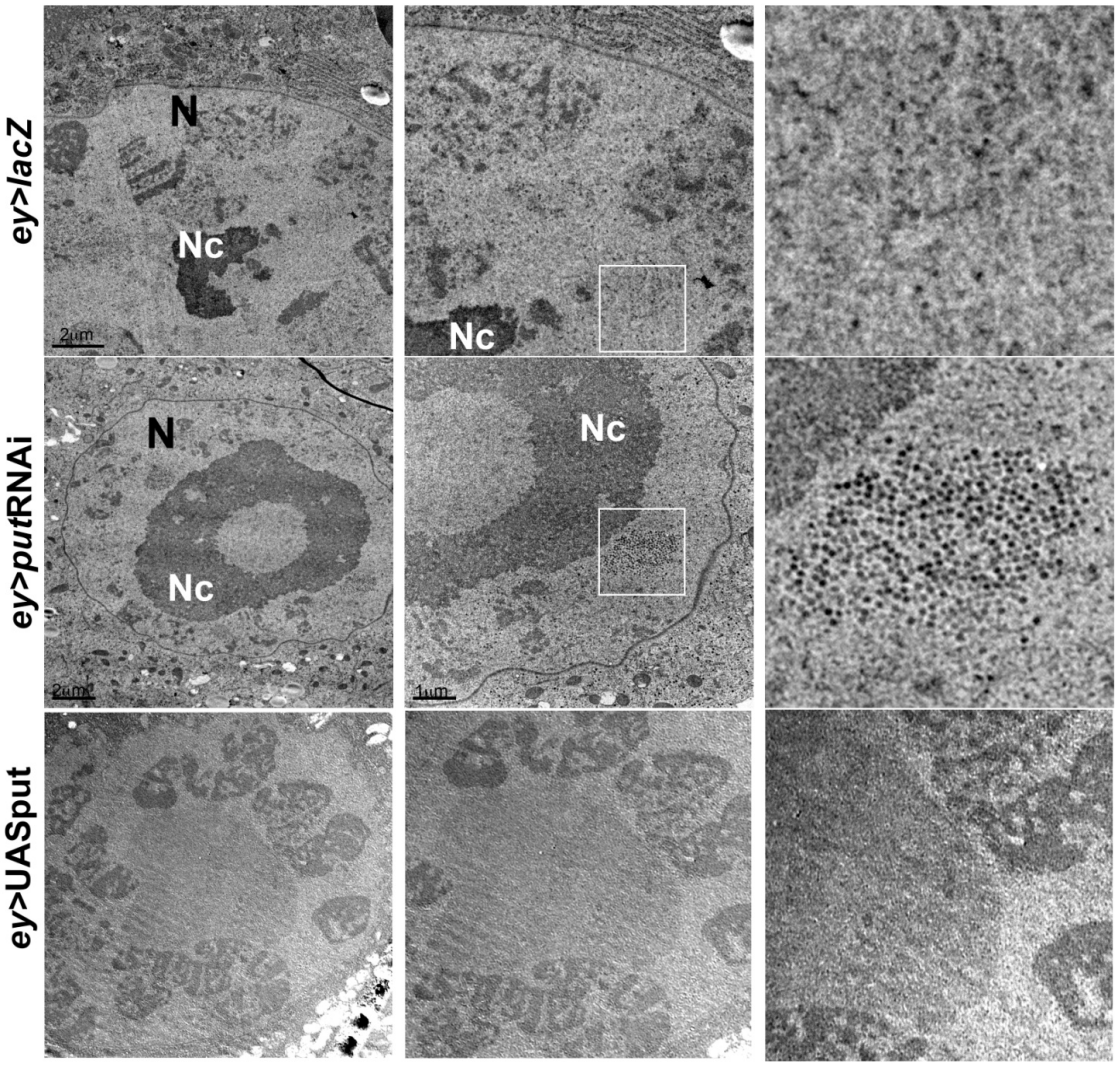

Figure 28- TGF-β signalling regulates nucleolar structure. Transmission electron microscopy (TEM) micrographs of nuclear regions from third instar salivary gland cells and correspondent magnifications are shown. Control cells expressing lacZ (*ey*G4/UASlacZ;+) display compact and uniform nucleolus (upper panel). Salivary gland cells expressing *put*RNAi2 (*ey*G4/+;UAS*put*RNAi2/+) exhibit bigger nucleolus containing vacuolar structures and accumulation of pre-ribosomes (middle panel). Conversely, overexpression of Put (*ey*G4/+;UASPut) results in less intense nucleolus (bottom panel). N, Nucleus; Nc, Nucleolus.

These results show that nucleolar morphology is profoundly affected by the variation of Put levels, and thus demonstrate a direct effect of TGF-β signalling in the regulation of nucleolar architecture and integrity. Moreover, the accumulation of ribosome immature particles at the nucleoplasm observed in the absence of Put strongly supports that disruption of TGF-β signalling results in a defective nucleolar function in ribosome biogenesis.

*put*RNAi2 phenotype is mainly due to downregulation of Put levels

The main disadvantage of using RNAi is the possibility of occurring non-specific interactions and the resulting off-target effect, which could originate false-positives results. Several approaches can be applied to overcome this problem, ensuring the specificity of the observed phenotype (Echeverri and Perrimon, 2006).

Since *put*RNAi2 is the strongest RNAi targeting Put, we used it as the phenotypic reference to represent the depletion of TGF-β signalling (Figure 12). One approach that can be applied to further confirm that the phenotypic effects of *put*RNAi2 are specific is the use of alternative RNAis targeting different regions of the same gene. For Put, this could be achieved using *put*RNAi4 or *put*RNAi5 (Figure 29). However, these RNAis were generated in vectors that are mainly effective in the germline (VALLIUM 21 and 22, from TRiP collection), and thus not so efficient in silencing Put expression on somatic cells (Figure 12).

One of the main limitations in using the *put*RNAi2 is that it is very difficult to modulate its strong phenotype and every attempt that we did to modulate it, always failed or just slightly differ from the phenotype of *put*RNAi2 alone. Nevertheless, if the *put*RNAi2 phenotype is indeed target gene-specific, we could expect to get a similar phenotype with the combination of less effective alternative tools that silence *put*. Thus, we decided to use an effective but less strong RNAi for *put* (*put*RNAi3). Previous results have shown a significant increase in the RpL41-YFP nucleolar fluorescence in *put*RNAi3, although not so pronounced as *put*RNAi2 (Figure 15B). In the eye, expression of this RNAi results in a mild reduction in the eye size (Figure 12). Taking advantage of this intermediate severity of *put*RNAi3, we expressed it in a Put mutant background, increasing the efficacy in silencing the target gene.

Approximately 90% of the flies expressing *put*RNAi3 in the wild-type, w^{1118}, background born with both retinas and exhibit a reduction in the eye size of around 40% in relation to control (Figure 30). As expected, expression of the *put*RNAi3 in the put^{88} mutant background significantly reduces the retina size relatively to control (Figure 30A and C). However, the strongest phenotypic severity is reached when the RNAi is expressed in flies together with a chromosome deficiency that lacks *put* gene, we named it as Def(*put*).

Approximately 50% of these flies were born without both retinas, thereby resembling *put*RNAi2 phenotype (Figures 30A and B).

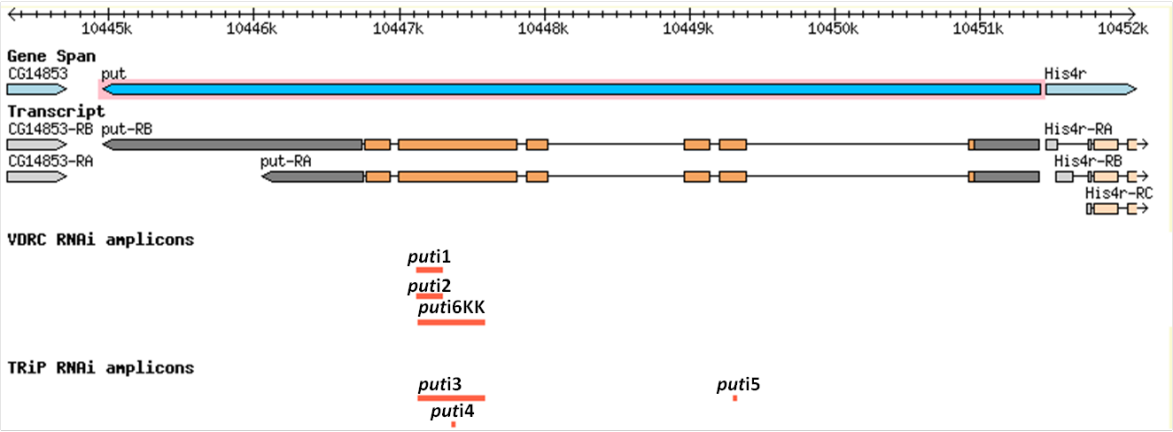

Figure 29- Put gene, transcripts and RNAis targeting sequence. Exons are represented in orange, intercalated by the intronic regions (lines). RNAi-targeting regions are in red, for the indicated RNAis.

Another approach to verify the specificity of the RNAi is the phenotypic rescue under silencing conditions, by the overexpression of the target gene. Ideally, this experiment should be achieved with an orthologue of the target gene from related species, with enough sequence degeneracy over the targeted region to avoid its recognition and consequently silencing by the RNAi. Since a Put orthologue was not available at this moment, we overexpressed Put transgene in flies expressing *put*RNAi3 (Figure 30A). Put expression in these flies significantly increases the retina size, although it does not reach the wild-type size (Figure 30C). This partial rescue of the phenotype further indicates that *put* is the main gene affected by these RNAis.

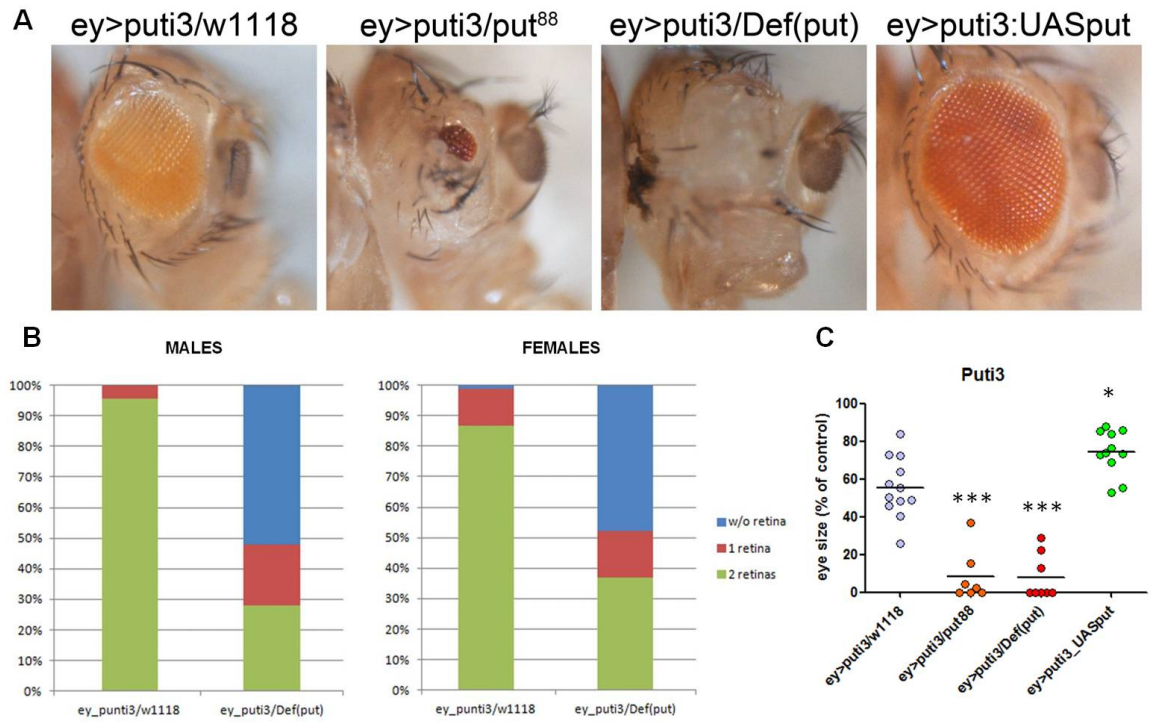

Figure 30- Expression of *put*RNAi3 in a mutant background increase the Put silencing efficacy. (A) Lateral views of adult retinas of flies with the indicated genotypes. **(B)** Quantification of the percentage of male and female flies that born with one, both or without retinas in flies expressing *put*RNAi3 in a wild-type background (*ey*G4;UAS*put*RNAi3/w^{1118}) and in a *put* deficiency background (*ey*G4;UAS*put*RNAi3/Def(*put*)) **(C)** Scatter plots comparing the retina size of the indicated genotypes. Expression of *put*RNAi3 results in a reduction in about 40% in the eye size, in relation to w^{1118} control. When this RNAi is expressed in a mutant background of put^{88} or in flies deficient for Put, Def(*put*), the eye size is significantly reduced, in relation to *ey*G4;*put*RNAi3/w^{1118}. Overexpression of Put results in partial rescue of the *put*RNAi3 phenotype. Statistics were done using ANOVA one way analysis (*, p<0.05; ***, p<0.0001).

In salivary glands, expression of *put*RNAi3 either in w^{1118} or Def(*put*) background does not significantly alter the cellular and nuclear areas in relation to control cells, contrary to what happens in *put*RNAi2-expressing cells, in which the nuclear and cellular areas are significantly decreased (Figure 31A, data not shown). Nevertheless, a significant increase in the ratio between nucleolar and nuclear areas is observed in these cells, although less accentuated than in *put*RNAi2 expression (Figure 31B). A more detailed analysis shows that although *put*RNAi2-expressing cells exhibit a nucleolus with a similar size to control cells, the cellular area is significantly smaller. In fact, these cells rarely reach the cellular area of control cells (Figure 31C). On the other hand, *put*RNAi3-expressing cells are similar in size to control cells but display larger nucleolus (Figure 31C). We also analysed hemizygous flies containing the *put* mutation (put^{135}) and the deficiency for *put* gene. Salivary glands of these flies display nucleoli occasionally fragmented (Figure 32A) and a significant increase in the ratio between the nucleolar and nuclear areas (Figure 32B). As observed to

*put*RNAi3, these cells require a large nucleolus to attain the same cell size of control cells (Figure 32C).

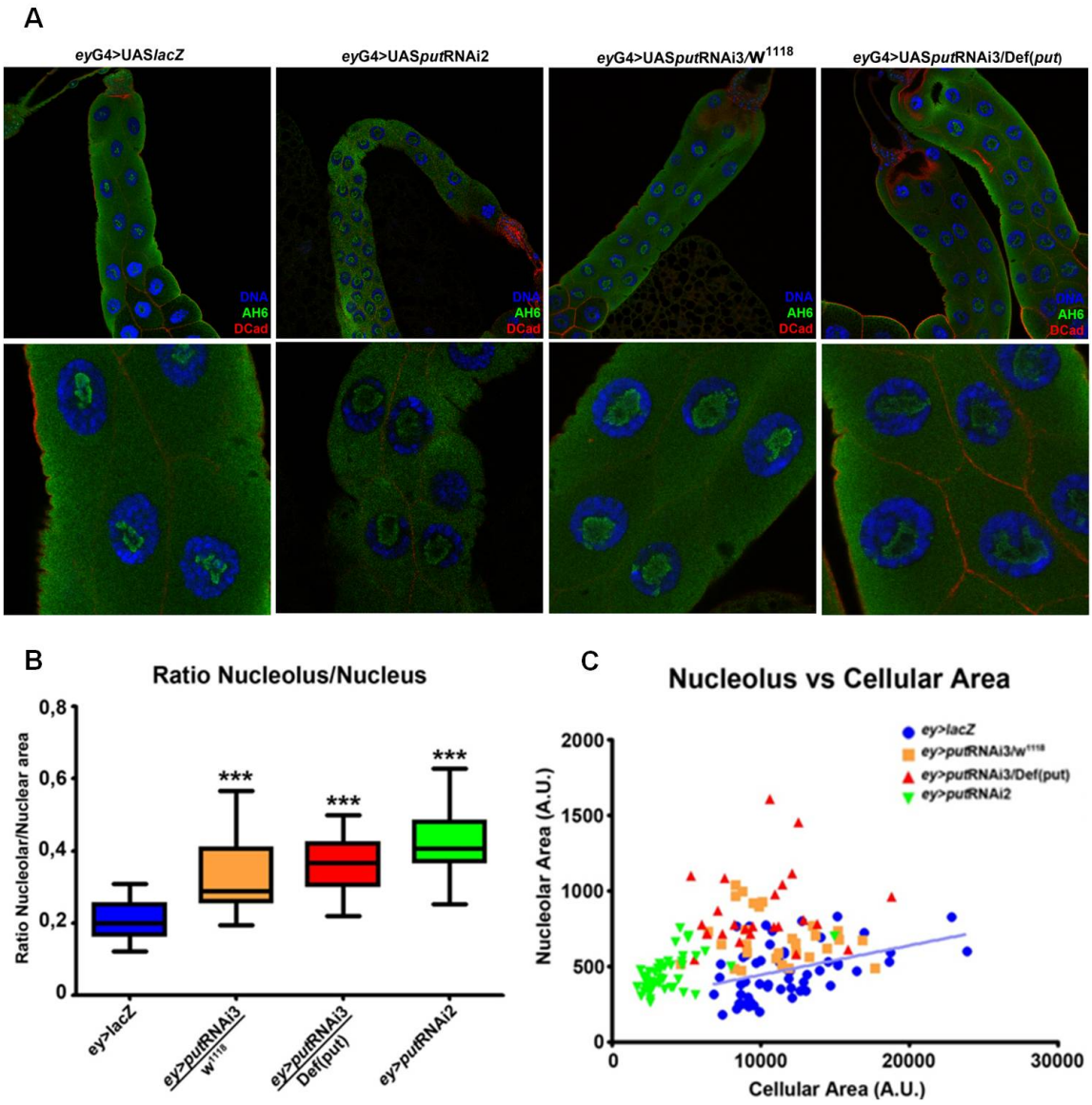

Figure 31- *put*RNAi3-expressing cells have an increased ratio between nucleolar and nuclear areas. (A) Third instar salivary glands and correspondent magnifications (4x zoom), for the control genotype (*ey*G4/UAS*lacZ*;+), *put*RNAi2 (*ey*G4/+;UAS*put*RNAi2/+), *put*RNAi3 (*ey*G4:UAS*put*RNAi3/w^{1118}) and the expression of *put*RNAi3 in deficient flies (*ey*G4/+;UAS*put*RNAi3/Def(*put*)). Salivary glands were stained for the nucleolar marker, AH6, a membrane protein D-Cadherin (DCad, red) and DNA (DAPI, blue) **(B)** Box plots comparing the ration between nucleolar and nuclear areas for the indicated genotypes. Cells expressing *put*RNAi3 display a significant increase in the ratio, as happens with *put*RNAi2-expressing cells. **(C)** Scatter plots showing the relation between nucleolar and cellular areas, for the indicated genotypes. Expression of *put*RNAi2 causes the most severe phenotype, in which cells rarely reach the cellular size of normal control cells. Statistics were done using ANOVA one way analysis (***, p<0.0001).

These results show that, although *put*RNAi2 produce the severe phenotype, both in the eye and in salivary glands, comparable phenotypes can be obtained by expression of a weak RNAi targeting Put, *put*RNAi3, in a Put mutant

background or by the combination of a mutation (*put*^{135}) and a deficiency in *put* gene. Flies with these genotypes display the same trend to nucleolar expansion in relation to the nuclear and cellular areas in salivary gland cells. Those cells require a larger nucleolus to reach the same cellular area of control cells. We conclude that *put*RNAi2 phenotypic effects are, in fact, target gene-specific.

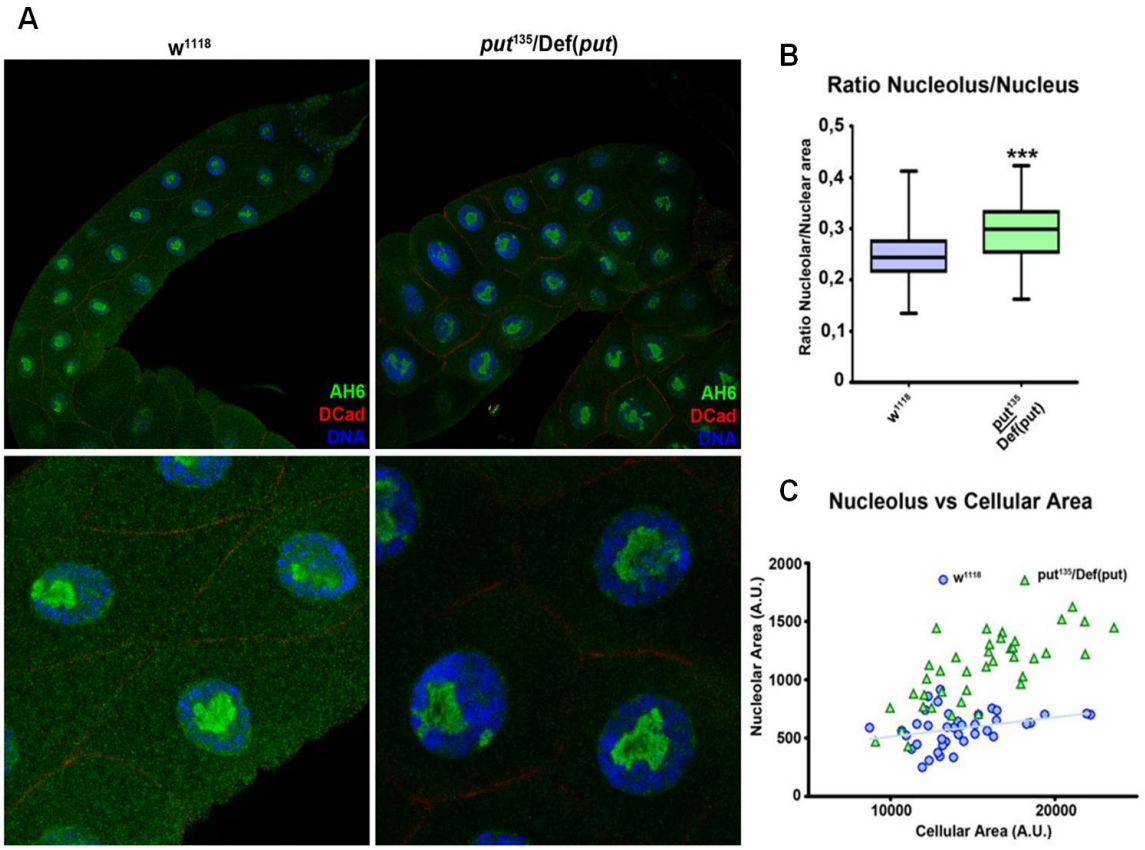

Figure 32- Put depletion results in expanded nucleolus, in relation to nuclear and cellular areas. (A) Third instar salivary gland cells and correspondent magnifications (4x zoom), for the control genotype (w^{1118}) and depletion of put (*put*^{135}/Def(*put*)). The cross was raised at 18ºC. Salivary glands were stained for the nucleolar marker, AH6, a membrane protein D-Cadherin (DCad, red) and DNA (DAPI, blue) **(B)** Box plots representing the ratio between nucleolar and nuclear areas for the same genotypes. Salivary glands of hemizygous flies, containing a mutation and a deficiency in put gene, display a significant increase in the ration between nucleolar and nuclear areas, in relation to control. **(C)** Scatter plots representing the relation between nuclear and cellular areas for the indicated genotypes. Salivary glands of hemizygous flies require larger nucleolus to reach the same cellular area of control cells. Statistics were done using student *t*-test analysis (***, p<0.0001).

TGF-β signalling disruption impairs regulation of the miRNA Bantam

Since its discovery, miRNAs are seen as important players in the regulation and modulation of several pathways (Winter et al., 2009). The reciprocal activity

was also found, as TGF-β was described to promote the maturation of microRNAs by facilitating its processing by Drosha through Smad proteins (Davis et al., 2010). Moreover, a relevant study showed that Yki and Mad can form a transcriptional complex to regulate specifically *ban* expression (Brennecke et al., 2003; Oh and Irvine, 2011). Bantam (Ban) is a miRNA that is directly related with growth, as it induces proliferation and inhibits apoptosis (Brennecke et al., 2003). Therefore, we decided to investigate the behaviour of Ban when TGF-β signalling is depleted by the expression of *put*RNAi2. For that, we took advantage of a sensor of Bantam activity (Brennecke et al., 2003). This sensor consists in a GFP-tagged transgene containing *bantam* target sequences. When present, Ban bind to the sensor, inducing its degradation and therefore reducing the GFP levels.

In eye imaginal discs, Bantam sensor is strongly detected in the differentiated photoreceptors, meaning that *bantam* is not expressed in those cells (Figure 36, upper and far right panel). This result is in accordance with previous studies demonstrating that Ban is mainly required for the proliferative state and surviving of the anterior cells in the eye disc, where the sensor is not detected (Peng et al., 2009). When Put is depleted by expression of *put*RNAi2, retinal differentiation does not occur, and the GFP-tagged sensor levels are downregulated in the whole disc, suggesting that Ban is active in the whole eye disc (Figure 33, bottom and far right panel).

The expression of *ban* in salivary gland cells seems to be dependent on the developmental stage, as in early L3 salivary glands the Ban sensor is not detected at the proximal region of the gland, being strongly present in the more distal cells. But as the salivary glands develop, the GFP become readily detectable at the most proximal cells (Figure 33, upper left and middle panels). This dynamic behaviour suggests that Ban is required for the early growth of the salivary glands but it becomes dispensable when the salivary glands reach the final size. Interestingly, when TGF-β signalling is depleted, the Ban sensor is not detected in the salivary gland cells, with a small exception of the most proximal three cells, a feature that may be related with other complex regulation (Figure 33, bottom left and middle panels).

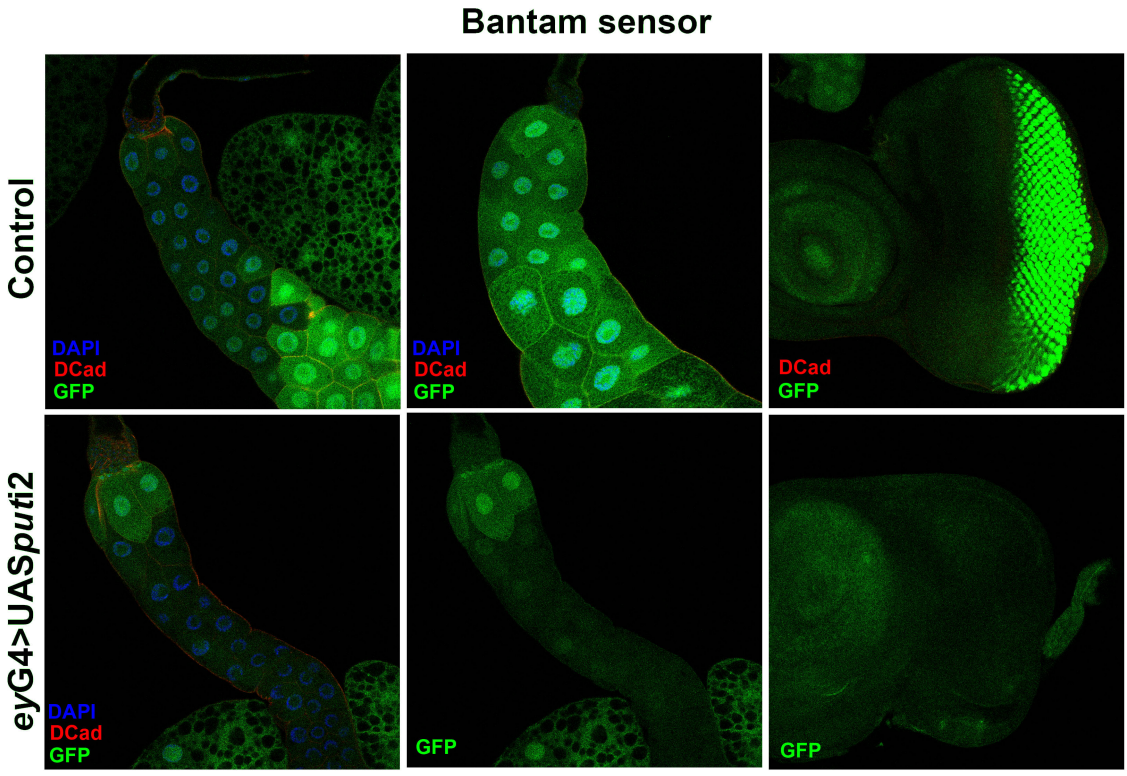

Figure 33- Bantam activity depends on TGF-β signalling. Third instar salivary glands (left and middle panels) and eye-antennal imaginal discs (far right panels) are shown, for the indicated genotypes. A GFP-tagged bantam sensor (green) was used to monitor Ban activity, in control cells expressing LacZ and *put*RNAi2-expressing cells. Salivary glands and eye discs were also stained for membrane protein D-Cadherin (DCad, red) and DNA (DAPI, blue).

As Bantam activity seems to be regulated by TGF-β, we decided to follow if TGF-β affects its expression pattern. For that propose, we monitored *ban* expression using the ban5'-lacZ reporter. In accordance with the previous results, in the control eye discs *ban* expression is detected in the anterior region of the disc, at the margins of the disc that give rise to the adult fly head, and also in photoreceptors supporting cells (Figure 34, upper far right panel). When Put is depleted, *ban* expression is detected in whole disc, although at higher levels in the anterior region (Figure 34, bottom far right panel). In L3 control salivary glands, *ban* expression is observed at the proximal region (Figure 34, far left and middle panels), but when TGF-β signalling is depleted, its expression is detected in the all gland (Figure 34, bottom far left and middle panels).

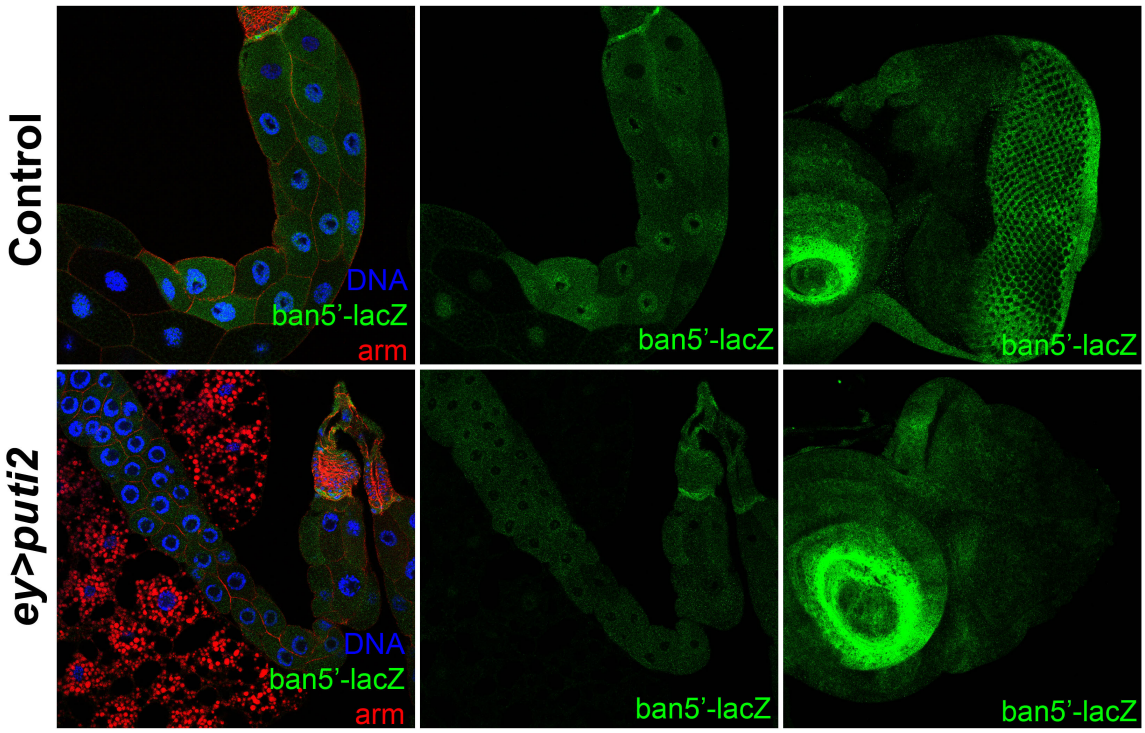

Figure 34- The expression patterns of *ban* are modified in the absence of TGF-β signalling. Third instar salivary glands (left and middle panels) and eye-antennal imaginal discs (far right panels) are shown, for the indicated genotypes. To monitor *ban* expression, the tissues were stained with anti-β-galactosidase (green), to detect the ban5'-lacZ reporter in the control genotype (*ey*G4/+;UAS*ban5'-lacZ*/+) and *put*RNAi2 (*ey*G4/+;UAS*put*RNAi2/UAS*ban5'-lacZ*). Salivary glands and eye discs were also stained for armadillo (arm, red) and DAPI (DNA, blue).

As it was shown for the Bantam sensor, *ban* expression seems to be regulated by TGF-β, as salivary glands without *put* do not downregulate *ban* expression. This may reflect one of two hypotheses, or cells must attain a certain size to downregulate *ban* expression or *ban* expression may be directly downregulated by TGF-β signalling. Another important aspect is that in late L3 control salivary glands Ban is not detected by the sensor but its expression seems to be present, however this may reflect that miRNA stability may be lower than the reporting protein LacZ. Therefore, the signal that is detected using the ban5'-lacZ may be a result of the LacZ perdurance.

Our data suggests that TGF-β signalling regulates directly or indirectly *ban* expression dynamics during salivary glands development. When this signal is absent, *ban* expression becomes detected in uniform levels along the tissue, independently of the larvae stage. To further investigate the relation between TGF-β signalling and *ban* expression, we overexpressed *bantam* in *put*RNAi-expressing eye discs. Interestingly, *ban* expression rescues at least one retina for

most of the born flies (Figure 35). Approximately 20% of males and about 70% of females were born with both retinas. These results further support a regulation of *ban* expression by TGF-β signalling, although this interaction seems to be extremely complex and may be dependent on the interplay with other factors.

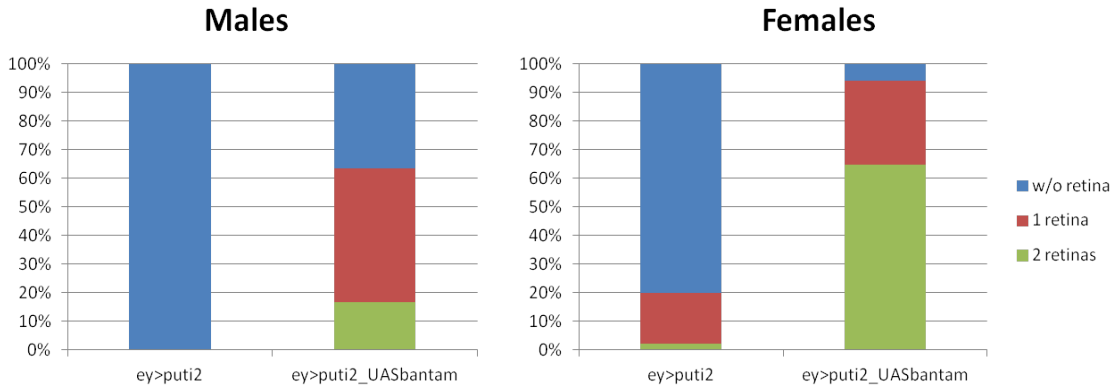

Figure 35- Overexpression of Bantam rescues the retina formation in *put*RNAi2-expressing eye discs. Quantification of the percentage of male and female flies that born with none, one or both retinas, for the indicated genotypes of absence of *put* (*ey*G4/+;UAS*put*RNAi2/+) and overexpression of Bantam in *put*RNAi-expressing cells (*ey*G4/+;UAS*put*RNAi2/UASBantam).

Discussion and Final Remarks

Previous studies in our laboratory have identified Viriato (Vito), the *Drosophila* homologue of the Nol12 conserved family of proteins. This protein is a key regulator of nucleolar morphology, and is required for tissue growth and survival during *Drosophila* development (Marinho et al., 2011). Our targeted double RNAi genetic screen to identify *vito* interactors during eye development, reveal a strong interaction between *vito* and TGF-β signalling pathway components. This interaction proved to be important not only for the eye disc growth, but also for the retinal differentiation, pointing to a possible interplay between Vito or in general, nucleolar proteins, and TGF-β signalling.

In fact, looking in more detail for eye disc nucleoli, we observed that as retinal differentiation progresses, it reduces the accumulation of the nucleolar marker AH6 in surrounding cells. Interestingly, eye discs expressing the strongest RNAi targeting Put, *put*RNAi2, completely lack differentiation and exhibit accumulation of AH6 and the ribosomal protein RpL41 all over the tissue. These results indicate a functional interdependency between nucleolar function and TGF-β signalling, in which nucleolar proteome and morphology seems to be altered in response to Dpp, whereas this signalling pathway requires a functional nucleolus to regulate differentiation and growth in the eye disc. Further experiments will be required to explore the biological significance of the Dpp-induced alteration of the nucleolar structure and the differentiation in the eye.

Due to their polyploidy, salivary gland cells display large nucleoli and a large capacity to grow, making this tissue an excellent system to study nucleolar function and structure. In these cells we found that TGF-β signalling interacts with nucleolar resident proteins, which support the structure of nucleolus and generate the proper microenvironment to its function (Raska et al., 2004). Nopp140 is a conserved phosphoprotein, which acts as a chaperone to the correct activity of snoRNPs, whereas Fibrillarin is a methyltransferase, associating with snoRNAs to guide 2'-*O*-methylation during rRNA processing. Surprisingly, we found that TGF-β signalling directly regulate the recruitment of Fibrillarin to nucleolus. This direct control of Fibrillarin nucleolar retention was also observed with Vito (Marinho et al., 2011), supporting recent findings in which is shown that Vito acts downstream of Dpp (Marinho et al., *submitted*). Nevertheless, in vertebrates, Fibrillarin co-localizes with transcriptionally active rDNA genes, at DFC region of nucleolus (Carmo-fonseca et al., 2000; Pliss et al., 2005). The observed accumulation of this protein when TGF-β signalling is disrupted might

be resultant from a mechanism of cellular compensation, due to impairment in rRNA processing. Consequently, Fibrillarin accumulates, surrounding the nascent rRNA transcripts, in an attempt to recovery the correct nucleolar function and supporting the nucleolar structure.

The retention of Nopp140 at nucleolus also seems to be dependent on Put-derived signals. However, Vito does not regulate the recruitment of this protein (Marinho et al., 2011), thereby suggesting that TGF-β signalling might regulate other nucleolar components independently of Vito. On the other hand, Nopp140 has shown to be required to the Dpp-induced differentiation in the eye. Expression of the strongest RNAi targeting Nopp140, results in a delay of MF at the margins of the eye disc although differentiation still occurs, a phenotype similar to the partial Dpp loss-of-function (Chanut and Heberlein, 1997). Thus, Nopp140 may act with Vito as mediators between TGF-β signalling and nucleolar function.

Besides resident nucleolar proteins, we demonstrated that absence of TGF-β signalling affects the localization and levels of several RPs belonging to both ribosome subunits (Figure 36). Ribosomal proteins are constantly synthesized at cytoplasm and transported to nucleolus, to assemble with rRNA and originate mature ribosome subunits. Unassembled proteins accumulate at nucleoplasm and are degraded in proteasomes (Raska et al., 2004; Andersen et al., 2005) (Figure 36A). Therefore, as previously observed, RPs localization patterns are mainly distributed between cytoplasm and nucleolus in control cells, being hardly detected at nucleoplasm (Robledo et al., 2008). Disruption of TGF-β signalling has shown to cause ectopic nucleolar accumulation of RpS6 and RpL10Ab, in complementary patterns. Possibly, due to impairment in rRNA processing, the levels of free RpL10Ab increase, surrounding immature rRNA particles and associated proteins, which include RpS6. On the other hand, RpL11 suffers mis-localization from nucleolus, being only occasionally detected at this sub-organelle.

In mammals it is well described that perturbation of any step of ribosome biogenesis results in nucleolar stress, leading to several nucleolar responses mediated by the tumour-suppressor protein p53. Translation of several RPs which contain a 5'-terminal oligopyrimidine (5'-TOP) sequence in their mRNA, is promoted, although global protein synthesis is reduced. These proteins are translocated from nucleolus to nucleoplasm, to stabilize p53, which trigger a

cascade of events to induce cell cycle arrest and growth inhibition (Zhang and Lu, 2009; Boulon et al., 2010). However, at nucleoplasm RPs are more susceptible to proteasomal degradation. It was observed that prolonged treatment with an inhibitor of RNA polymerase I, Actinomycin D, in mammalian cells results in decreased levels of RpL11, due to its re-localization and subsequent degradation at nucleoplasm (Sundqvist et al., 2009). Thus, although we did not see accumulation of RpL11 at nuclei, absence of this protein at nucleolus may be a result of its translocation to nucleoplasm, thereby stimulating p53-mediated stress response. Nevertheless, mammalian RpL11 mRNA contains the TOP sequence, suggesting that the observed decreased levels are probably due to increased degradation rates at nucleoplasm, than to a defective production.

Moreover, depletion of TGF-β signalling induces the accumulation of RpL26 at nucleoplasm. Mammalian RpL26 mRNA also contains the TOP sequence. It was shown that during nucleolar stress this RP binds to the 5' unstranslated region (5'UTR) of p53 mRNA, stimulating its translation (Takagi et al., 2005). The strong accumulation of this protein may be a recovery mechanism, in which the cell produces higher levels of RpL26 to increase p53 translation. However, although RPs are highly conserved proteins, the mechanisms underlying the nucleolar stress-induced responses in *Drosophila* remain poorly understood.

The defective ribosome synthesis is corroborated by the observed decrease in GFP intensity of a control protein, 6xMyc, when Punt is depleted. In fact, *put*RNAi2-expressing cells display small aggregates of rRNA within nucleolus. Ribosomal RNA is transcribed from rDNA and is subjected to multiple steps of processing and maturation, being quickly translocated to cytoplasm, to form functional ribosomes (Raska et al., 2004). As a result, the presence of rRNA in the nucleolus is transient, and is not detected in normal cells. Accordingly, *put*RNAi2-expressing salivary glands have reduced amounts of ribosome mature precursors, 18S and 28S, in relation to control. These results were confirmed in more detail by TEM, in which *put*RNAi2-expressing cells display internal vacuolar structures and accumulation of what appears to be immature ribosomal particles at nucleoplasm and occasionally within the vacuoles.

Interestingly, Vito co-localizes with the small aggregates of rRNA observed within nucleolus. This could be explained by the finding that Vito homologue in yeast, Rrp17p, has 5'-3' exonucleolytic activity, crucial for 60S rRNA processing (Oeffinger et al., 2009), and also supports the regulation of Vito by TGF-β. It

seems that *put*RNAi2-expressing cells accumulate Vito in an attempt to recovery from the defective ribosome biogenesis, as a compensatory mechanism to rescue TGF-β activity.

Taken together, these observations confirm that absence of Put-derived signals results in nucleolar dysfunction, probably due to defective ribosomal biogenesis. The main function of nucleolus is to produce functional ribosomes, thereby ensuring the maintenance of a sufficient pool of mature subunits to support the cellular protein requirements (Boisvert et al., 2007). Therefore, nucleolar function is tightly controlled, to coordinate cell growth and division. Mutations in a wide range of ribosomal proteins causes the Drosophila Minute phenotype, characterized by a developmental delay, resultant from a suboptimal protein synthesis (Marygold et al., 2007). On the other hand, hypertrophy of nucleoli is commonly associated with neoplastic transformation (Montanaro et al., 2008). The analysis by TEM also showed important differences in nucleolar morphology after variation of Put levels, which might reflect the regulation of nucleolar structural proteins by TGF-β signalling. Nevertheless, altered Put levels, either by expression of RNAi or by overexpression, seem to change the nucleolar proteome equilibrium, modifying nucleolar function and limiting overall tissue growth. These results support the described function of nucleolus as the major regulator of cell growth and corroborate a novel mechanism, in which TGF-β-stimulated growth is mediated by the nucleolar function.

We confirmed that *put*RNAi2 phenotypic effects are specific. Combination of a weak RNAi targeting Put, putRNAi3, with *put* mutations/deficiency resembles some aspects of the phenotype obtained in *put*RNAi2. All the combined genotypes have demonstrated the similar trend to a nucleolar expansion in relation to the nuclear area. In fact, we noticed that without *put* expression, cells require a larger nucleolus to reach the normal control cellular size. Nevertheless, expression of *put*RNAi2 causes the most severe condition, in which expressing cells rarely reach the normal size. Probably, the severity of *put*RNAi2 limits the nucleolar-mediated response to stress, thereby those cells have more difficulties the recover its protein synthesis.

Finally, we found that Put levels also affect the dynamics of the microRNA *bantam* expression in salivary glands. Ban was shown to induce proliferation and inhibit apoptosis, exerting an important role in tissue growth. In normal salivary glands *ban* expression seems to be required early in development, as L3 salivary

glands do not have detectable Ban expression. When TGF-β signalling is disrupted, *ban* expression is maintained throughout the gland. The regulation of the expression of *ban* in salivary gland cells might be due to cellular ability to growth, therefore *ban* expression is maintained in proximal cells as those cells are the last ones to increase its ploidy during development.

In the eye disc, the expression of *ban* in the anterior proliferative region is in accordance with previous studies (Peng et al., 2009). However, we observed that ban is also expressed in the tissue surrounding differentiated photoreceptors, possibly promoting tissue growth and survival in the posterior region of the disc. When *put*RNAi2 is expressed, eye discs lack differentiation and *ban* is expressed in the whole disc.

It was recently demonstrated that Mad and Yki can form a transcriptional complex to activate *ban* expression and promote growth, in the wing disc (Oh and Irvine, 2011). Moreover, it was shown that TGF-β signalling can facilitate processing of miRNAs, through Smads (Davis et al., 2010). Interestingly, overexpression of Ban rescues the retina differentiation in *put*RNAi2-expressing cells. It seems that Ban levels when Put is depleted are not sufficient to restore differentiation, indicating that TGF-β induction of *ban* expression is necessary for the onset of differentiation. However, the regulation of *ban* expression seems to be complex, and also depend on other factors. Therefore, these data are very preliminary.

In conclusion, we have demonstrated an interaction between TGF-β signalling and the regulation of nucleolar function. Nucleolus has been described as a key player in growth, being the central factory of ribosome production (Boisvert et al., 2007). Recently, it was proposed a model in which the ribosomal heterogeneity defines specialized activity of different cell types. In a developmental context, specific ribosome profiles can define the pool of proteins present in the cell in a given moment, therefore representing a new spatio-temporal control of gene expression at the translational level (Xue and Barna, 2012a). Our results suggest that TGF-β signalling may be one of the developmental signals that regulate nucleolar function and components, defining specific ribosomal profiles. Importantly, this interaction have shown to be not only required for differentiation but also for growth control, presenting a real breakthrough in the current knowledge about how morphogens drive tissue growth.

However, many questions remain to be answered. The recent finding that Babo also can phosphorylate Mad increased the complexity of the regulatory network mediated by TGF-β signalling (Peterson et al., 2012). As we used the shared receptor of both pathways, additional studies are required to understand the role of each branch. Moreover, absence of Put was shown to cause impairment in rRNA processing, but it remains unclear which step is altered, and if it is the cause or the consequence of the observed mis-localization of important nucleolar components, as Nopp140. To finish, we also left open another possible growth regulatory interaction, mediated by the microRNA Bantam.

Deregulation of TGF-β signalling has been linked with several diseases, particularly cancer (Wharton and Derynck, 2009). We hope that our work open more perspectives on the understanding of the enormous puzzle of developmental network involving TGF-β signalling, during animal organogenesis.

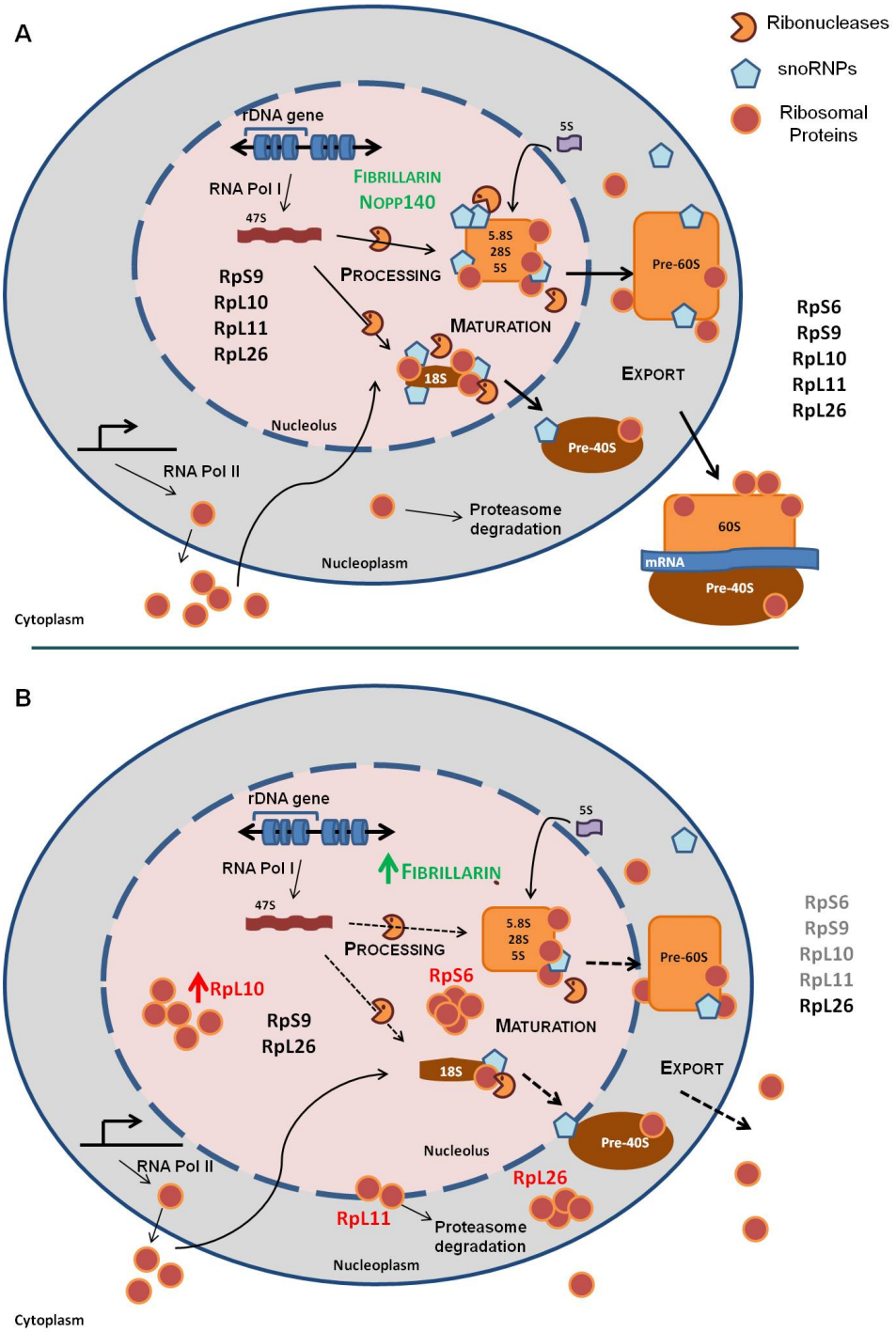

Figure 36- Absence of Put results in nucleolar stress. (A) The correct ribosomal biogenesis requires the interaction between several proteins, such as ribosomal proteins (RPs) and nucleolar resident proteins, such as Fibrillarin and Nopp140. In control cells RPs are transcribed by polymerase II and translocated from cytoplasm to assemble in the rRNA particles at nucleolus. Unassembled proteins are degraded at nuclear proteasomes. Fibrillarin and Nopp140 are nucleolar structural proteins also crucial for processing of rRNA. Vito might be involved in the processing of rRNA. **(B)** When Put is depleted, nucleolar levels and localization of several RPs are altered, probably due to a defective ribosome biogenesis. These cells display an expansion of nucleolus in relation to the nuclear area and accumulation of immature ribosome particles at nucleoplasm. Vito and some RPs accumulate in the same regions, probably in a compensation mechanism of the cell. Due to the impairment in ribosome biogenesis and subsequent decrease of the number of functional ribosomes, general protein expression levels are diminished. Resident nucleolar proteins are represented at green, and mis-localized RPs in red. RPs with reduced cytoplasmic levels are denoted in grey. The arrows represent accumulation of the correspondent protein.

References

Adams, M.D., SE, C., RA, H., CA, E., JD, G., PG, A., SE, S., PW, L., RA, H., RF, G., et al. (2000). The Genome Sequence of *Drosophila* melanogaster. Science *287*, 2185–2195.

Affolter, M., and Basler, K. (2007). The Decapentaplegic morphogen gradient: from pattern formation to growth regulation. Nature Reviews. Genetics *8*, 663–674.

Amore, G., and Casares, F. (2010). Size matters□: The contribution of cell proliferation to the progression of the specification *Drosophila* eye gene regulatory network. Developmental Biology *344*, 569–577.

Andersen, J.S., Lam, Y.W., Leung, A.K.L., Ong, S.-E., Lyon, C.E., Lamond, A.I., and Mann, M. (2005). Nucleolar proteome dynamics. Nature *433*, 77–84.

Arias, A.M. (2008a). Chapter 1-*Drosophila melanogaster* and the Development of Biology in the 20th century. In Methods in Molecular Biology, pp. 1–25.

Arias, A.M. (2008b). Chapter 2- Getting started: An overview on raising and handling *Drosophila*. In Methods in Molecular Biology, pp. 27–44.

Arias, A.M. (2008c). Chapter 5- The GAL4 System: A versatile system for the expression of genes. In Methods in Molecular Biology, pp. 79–95.

Atkins, M., and Mardon, G. (2009). Signaling in the third dimension: the peripodial epithelium in eye disc development. Developmental Dynamics: an Official Publication of the American Association of Anatomists *238*, 2139–2148.

Audas, T.E., Jacob, M.D., and Lee, S. (2012). Immobilization of proteins in the nucleolus by ribosomal intergenic spacer noncoding RNA. Molecular Cell *45*, 147–157.

Basler, K., and Struhl, G. (1994). Compartment boundaries and the control of *Drosophila* limb pattern by hedgehog protein. Nature *368*, 208 – 214.

Bessa, J., Gebelein, B., Pichaud, F., Casares, F., and Mann, R.S. (2002). Combinatorial control of *Drosophila* eye development by eyeless, homothorax, and teashirt. Genes & Development *16*, 2415–2427.

Boisvert, F.-M., van Koningsbruggen, S., Navascués, J., and Lamond, A.I. (2007). The multifunctional nucleolus. Nature Reviews. Molecular Cell Biology *8*, 574–585.

Boulon, S., Westman, B.J., Hutten, S., Boisvert, F.-M., and Lamond, A.I. (2010). The nucleolus under stress. Molecular Cell *40*, 216–227.

Brand, a H., and Perrimon, N. (1993). Targeted gene expression as a means of altering cell fates and generating dominant phenotypes. Development *118*, 401–415.

Brennecke, J., Hipfner, D.R., Stark, A., Russell, R.B., and Cohen, S.M. (2003). bantam encodes a developmentally regulated microRNA that controls cell proliferation and regulates the proapoptotic gene hid in *Drosophila*. Cell *113*, 25–36.

Brummel, T., Abdollah, S., Haerry, T.E., Shimell, M.J., Merriam, J., Raftery, L., Wrana, J.L., and O'Connor, M.B. (1999). The *Drosophila* Activin receptor Baboon signals through dSmad2 and controls cell proliferation but not patterning during larval development. Genes & Development *13*, 98–111.

Burke, R., and Basler, K. (1996). Dpp receptors are autonomously required for cell proliferation in the entire developing *Drosophila* wing. Development *122*, 2261–2269.

Capdevila, J., and Guerrero, I. (1994). Targeted expression of the signaling molecule decapentaplegic induces pattern duplications and growth alterations in *Drosophila* wings. The EMBO Journal *13*, 4459–4468.

Carmo-fonseca, M., Mendes-soares, L., and Campos, I. (2000). To be or not to be in the nucleolus. Nature Cell Biology *2*,.107-112

Chanut, F., and Heberlein, U. (1997). Role of decapentaplegic in initiation and progression of the morphogenetic furrow in the developing *Drosophila* retina. Development *124*, 559–567.

de la Cova, C., Abril, M., Bellosta, P., Gallant, P., Johnston, L.A., and Street, W. (2004). Size by Inducing Cell Competition. Cell *117*, 107–116.

de la Cova, C., and Johnston, L. A. (2006). Myc in model organisms: a view from the flyroom. Seminars in Cancer Biology *16*, 303–312.

Czerny, T., Halder, G., Kloter, U., Souabni, A., Gehring, W.J., and Busslinger, M. (1999). twin of eyeless , a Second Pax-6 Gene of *Drosophila* , Acts Upstream of eyeless in the Control of Eye Development. Molecular Cell *3*, 297–307.

Dai, M.-S., Arnold, H., Sun, X.-X., Sears, R., and Lu, H. (2007). Inhibition of c-Myc activity by ribosomal protein L11. The EMBO Journal *26*, 3332–3345.

Davis, B.N., Hilyard, A.C., Nguyen, P.H., Lagna, G., and Hata, A. (2010). Smad proteins bind a conserved RNA sequence to promote microRNA maturation by Drosha. Molecular Cell *39*, 373–384.

Dekanty, A., and Milán, M. (2011). The interplay between morphogens and tissue growth. EMBO Reports *12*, 1003–1010.

Dietzl, G., Chen, D., Schnorrer, F., Su, K.-C., Barinova, Y., Fellner, M., Gasser, B., Kinsey, K., Oppel, S., Scheiblauer, S., et al. (2007). A genome-wide transgenic RNAi library for conditional gene inactivation in *Drosophila*. Nature *448*, 151–156.

Domínguez, M., and Casares, F. (2005). Organ specification-growth control connection: new in-sights from the *Drosophila* eye-antennal disc. Developmental Dynamics: an Official Publication of the American Association of Anatomists *232*, 673–684.

Duffy, J.B. (2002). GAL4 system in *Drosophila*: a fly geneticist's Swiss army knife. Genesis *34*, 1–15.

Echeverri, C.J., and Perrimon, N. (2006). High-throughput RNAi screening in cultured cells: a user's guide. Nature Reviews. Genetics *7*, 373–384.

Edgar, B.A. (2006a). From cell structure to transcription: Hippo forges a new path. Cell *124*, 267–273.

Edgar, B.A. (2006b). How flies get their size: genetics meets physiology. Nature Reviews. Genetics *7*, 907–916.

Edgar, B.A., and Orr-weaver, T.L. (2001). Endoreplication Cell Cycles: More for Less. Cell *105*, 297–306.

Emmott, E., and Hiscox, J. A. (2009). Nucleolar targeting: the hub of the matter. EMBO Reports *10*, 231–238.

Entchev, E.V., Schwabedissen, A., and González-Gaitán, M. (2000). Gradient formation of the TGF-beta homolog Dpp. Cell *103*, 981–991.

Fankhauser, G. (1945). The effects of changes in chromosome number on amphibian development. The Quarterly Review of Biology *20*, 20–78.

Feng, X.-H., and Derynck, R. (2005). Specificity and versatility in tgf-beta signaling through Smads. Annual Review of Cell and Developmental Biology *21*, 659–693.

Ferguson, E.L., and Anderson, K.V. (1992). Decapentaplegic acts as a morphogen to organize dorsal-ventral pattern in the *Drosophila* embryo. Cell *71*, 451–461.

Fire, A., Xu, S., Montgomery, M.K., Kostas, S.A., Driver, S.E., and Mello, C.C. (1998). Potent and specific genetic interference by double-stranded RNA in Caenorhabditis elegans. Nature *391*, 806–811.

Gadal, O., Strauß, D., Kessl, J., Tollervey, D., Hurt, E., Trumpower, B., and Hurt, E.D. (2001). Nuclear Export of 60S Ribosomal Subunits Depends on Xpo1p and Requires a Nuclear Export Sequence-Containing Factor , Nmd3p , That Associates with the Large Subunit Protein Rpl10p. Molecular and Cellular Biology *21*, 3405–3415.

Greenwood, S., and Struhl, G. (1999). Progression of the morphogenetic furrow in the *Drosophila* eye□: the roles of Hedgehog , Decapentaplegic and the Raf pathway. Development *126*, 5795–5808.

Grewal, S.S., Li, L., Orian, A., Eisenman, R.N., and Edgar, B. A. (2005). Myc-dependent regulation of ribosomal RNA synthesis during *Drosophila* development. Nature Cell Biology *7*, 295–302.

Halder, G., Callaerts, P., and Gehring, W.J. (1995). Induction of ectopic eyes by targeted expression of the eyeless gene in *Drosophila* . Science *267* , 1788–1792.

Halder, G., and Johnson, R.L. (2011). Hippo signaling: growth control and beyond. Development *138*, 9–22.

Harvey, K.F., Pfleger, C.M., and Hariharan, I.K. (2003). The *Drosophila* Mst ortholog, hippo, restricts growth and cell proliferation and promotes apoptosis. Cell *114*, 457–467.

Hogan, B.L.M., and Kolodziej, P. a (2002). Organogenesis: molecular mechanisms of tubulogenesis. Nature Reviews. Genetics *3*, 513–523.

Huang, J., Wu, S., Barrera, J., Matthews, K., and Pan, D. (2005). The Hippo signaling pathway coordinately regulates cell proliferation and apoptosis by inactivating Yorkie, the *Drosophila* Homolog of YAP. Cell *122*, 421–434.

Huminiecki, L., Goldovsky, L., Freilich, S., Moustakas, A., Ouzounis, C., and Heldin, C.-H. (2009). Emergence, development and diversification of the TGF-beta signalling pathway within the animal kingdom. BMC Evolutionary Biology *9*, 1-17.

Johnston, L.A. (2009). Competitive interactions between cells-death, growth and geography. Science 1679–1682.

Johnston, L.A., Prober, D.A., Edgar, B.A., Eisenman, R.N., and Gallant, P. (1999). *Drosophila* myc Regulates Cellular Growth during Development. Cell *98*, 779–790.

Kenyon, K.L., Ranade, S.S., Curtiss, J., Mlodzik, M., and Pignoni, F. (2003). Coordinating proliferation and tissue specification to promote regional identity in the *Drosophila* head. Developmental Cell *5*, 403–414.

Kulkarni, M.M., Booker, M., Silver, S.J., Friedman, A., Hong, P., Perrimon, N., and Mathey-prevot, B. (2006). Evidence of off-target effects associated with long dsRNAs in *Drosophila melanogaster* cell-based assays. Nature Methods *3*, 833–838.

Lafontaine, D.L., and Tollervey, D. (2001). The function and synthesis of ribosomes. Nature Reviews. Molecular Cell Biology *2*, 514–520.

Lam, Y.W., Lamond, A.I., Mann, M., and Andersen, J.S. (2007). Analysis of nucleolar protein dynamics reveals the nuclear degradation of ribosomal proteins. Current Biology: *17*, 749–760.

Lecuit, T., and Le Goff, L. (2007). Orchestrating size and shape during morphogenesis. Nature *450*, 189–192.

Lindström, M.S. (2009). Emerging functions of ribosomal proteins in gene-specific transcription and translation. Biochemical and Biophysical Research Communications *379*, 167–170.

Lo, S.J., Lee, C.-C., and Lai, H.-J. (2006). The nucleolus: reviewing oldies to have new understandings. Cell Research *16*, 530–538.

Lopes, C.S., and Casares, F. (2010). hth maintains the pool of eye progenitors and its downregulation by Dpp and Hh couples retinal fate acquisition with cell cycle exit. Developmental Biology *339*, 78–88.

Marinho, J., Casares, F., and Pereira, P.S. (2011). The *Drosophila* Nol12 homologue viriato is a dMyc target that regulates nucleolar architecture and is required for dMyc-stimulated cell growth. Development *138*, 349–357.

Marinho, J., Martins T., Neto, M., Casares, F., and Paulo, S. An eye-targeted double-RNAi screen identifies a modulatory role for Vito / Nol12 in *Drosophila* Dpp signaling. *Submitted.*

Martín, F. a, Pérez-Garijo, A., Moreno, E., and Morata, G. (2004). The brinker gradient controls wing growth in *Drosophila*. Development *131*, 4921–4930.

Marygold, S.J., Roote, J., Reuter, G., Lambertsson, A., Ashburner, M., Millburn, G.H., Harrison, P.M., Yu, Z., Kenmochi, N., Kaufman, T.C., et al. (2007). The ribosomal protein genes and Minute loci of *Drosophila melanogaster*. Genome Biology *8*, R216.

Massagué, J. (1998). TGF-beta signal transduction. Annual Review of Biochemistry *67*, 753–791.

Massagué, J., Blain, S.W., and Lo, R.S. (2000). TGFbeta signaling in growth control, cancer, and heritable disorders. Cell *103*, 295–309.

Metcalf, D. (1963). the Autonomous Behaviour of Normal Thymus Grafts. The Australian Journal of Experimental Biology and Medical Science *41*, 437–47.

Metcalf, D. (1964). Restricted Growth Capacity of Multiple Spleen Grafts. Transplantation *2*, 387–392.

Montanaro, L., Treré, D., and Derenzini, M. (2008). Nucleolus, ribosomes, and cancer. The American Journal of Pathology *173*, 301–310.

Moreno, E., Basler, K., and Zu, C. (2004). dMyc Transforms Cells into Super-Competitors. Cell *117*, 117–129.

Moustakas, A., and Heldin, C.-H. (2009). The regulation of TGFbeta signal transduction. Development *136*, 3699–3714.

Myat, M.M. (2005). Making tubes in the *Drosophila* embryo. Developmental Dynamics : an Official Publication of the American Association of Anatomists *232*, 617–632.

Müller, B., Hartmann, B., Pyrowolakis, G., Affolter, M., and Basler, K. (2003). Conversion of an extracellular Dpp/BMP morphogen gradient into an inverse transcriptional gradient. Cell *113*, 221–233.

Nellen, D., Burke, R., Struhl, G., and Basler, K. (1996). Direct and long-range action of a DPP morphogen gradient. Cell *85*, 357–368.

Neto-Silva, R.M., de Beco, S., and Johnston, L. A.(2010). Evidence for a growth-stabilizing regulatory feedback mechanism between Myc and Yorkie, the *Drosophila* homolog of Yap. Developmental Cell *19*, 507–520.

Neto-Silva, R.M., Wells, B.S., and Johnston, L. A.(2009). Mechanisms of growth and homeostasis in the *Drosophila* wing. Annual Review of Cell and Developmental Biology *25*, 197–220.

Oeffinger, M., Zenklusen, D., Ferguson, A., Wei, K.E., Hage, A.E., Tollervey, D., Chait, B.T., Singer, R.H., and Route, M.P. (2009). Rrp17p Is a Eukaryotic Exonuclease Required for 5′ End Processing of Pre-60S Ribosomal RNA.pdf. Molecular Cell *36* 768–781.

Oh, H., and Irvine, K.D. (2010). Yorkie: the final destination of Hippo signaling. Trends in Cell Biology *20*, 410–417.

Oh, H., and Irvine, K.D. (2011). Cooperative regulation of growth by Yorkie and Mad through bantam. Developmental Cell *20*, 109–122.

Olson, M.O., Dundr, M., and Szebeni, A (2000). The nucleolus: an old factory with unexpected capabilities. Trends in Cell Biology *10*, 189–196.

Orihara-Ono, M., Suzuki, E., Saito, M., Yoda, Y., Aigaki, T., and Hama, C. (2005). The slender lobes gene, identified by retarded mushroom body development, is required for proper nucleolar organization in *Drosophila*. Developmental Biology *281*, 121–133.

Padgett, R.W., St. Johnston, R.D., and Gelbart, W.M. (1987). A transcript from a *Drosophila* pattern gene predicts a protein homologous to the transforming growth factor-[beta] family. Nature *325*, 81–84.

Parker, L., Stathakis, D.G., and Arora, K. (2004). Regulation of BMP and Activin signaling in *Drosophila*. Prog Mol Subcell Biol *34*, 73–101.

Peng, H.W., Slattery, M., and Mann, R.S. (2009). Transcription factor choice in the Hippo signaling pathway: homothorax and yorkie regulation of the microRNA bantam in the progenitor domain of the *Drosophila* eye imaginal disc. Genes & Development *23*, 2307–2319.

Peterson, A.J., Jensen, P. a, Shimell, M., Stefancsik, R., Wijayatonge, R., Herder, R., Raftery, L. a, and O'Connor, M.B. (2012). R-Smad competition controls activin receptor output in *Drosophila*. PloS One *7*, 1-12

Pichaud, F., and Casares, F. (2000). homothorax and iroquois-C genes are required for the establishment of territories within the developing eye disc. Mechanisms of Development *96*, 15–25.

Pierce, S.B., Yost, C., Anderson, S. a R., Flynn, E.M., Delrow, J., and Eisenman, R.N. (2008). *Drosophila* growth and development in the absence of dMyc and dMnt. Developmental Biology *315*, 303–316.

Pierce, S.B., Yost, C., Britton, J.S., Loo, L.W.M., Flynn, E.M., Edgar, B.A., and Eisenman, R.N. (2004). dMyc is required for larval growth and endoreplication in *Drosophila*. Development *131*, 2317–2327.

Pliss, A., Koberna, K., Vecerová, J., Malínský, J., Masata, M., Fialová, M., Raska, I., and Berezney, R. (2005). Spatio-temporal dynamics at rDNA foci: global switching between DNA replication and transcription. Journal of Cellular Biochemistry *94*, 554–565.

Prasanth, K.V. (2012). Policing cells under stress: noncoding RNAs capture proteins in nucleolar detention centers. Molecular Cell *45*, 141–142.

Raska, I., Koberna, K., Malínský, J., Fidlerová, H., and Masata, M. (2004). The nucleolus and transcription of ribosomal genes. Biology of the Cell *96*, 579–594.

Reddy, B.V.V.G., and Irvine, K.D. (2008). The Fat and Warts signaling pathways: new insights into their regulation, mechanism and conservation. Development *135*, 2827–2838.

Reichow, S.L., Hamma, T., Ferré-D'Amaré, A.R., and Varani, G. (2007). The structure and function of small nucleolar ribonucleoproteins. Nucleic Acids Research *35*, 1452–1464.

Reiter, L.T., Potocki, L., Chien, S., Gribskov, M., and Bier, E. (2001). A systematic analysis of human disease-associated gene sequences in *Drosophila melanogaster*. Genome Research *11*, 1114–1125.

van Riggelen, J., Yetil, A., and Felsher, D.W. (2010). MYC as a regulator of ribosome biogenesis and protein synthesis. Nature Reviews. Cancer *10*, 301–309.

Roberts, D.B. (2006). *Drosophila melanogaster*: the model organism. Entomologia Experimentalis et Applicata. *121*, 93–103.

Robledo, S., Idol, R. a, Crimmins, D.L., Ladenson, J.H., Mason, P.J., and Bessler, M. (2008). The role of human ribosomal proteins in the maturation of rRNA and ribosome production. RNA *14*, 1918–1929.

Sander, V., Eivers, E., Choi, R.H., and De Robertis, E.M. (2010). *Drosophila* Smad2 opposes Mad signaling during wing vein development. PloS One *5*, 1–10.

Schwank, G., and Basler, K. (2010). Regulation of organ growth by morphogen gradients. Cold Spring Harbor Perspectives in Biology *2*, 1-16.

Schwank, G., Restrepo, S., and Basler, K. (2008). Growth regulation by Dpp: an essential role for Brinker and a non-essential role for graded signaling levels. Development *135*, 4003–4013.

Schwank, G., Tauriello, G., Yagi, R., Kranz, E., Koumoutsakos, P., and Basler, K. (2011). Antagonistic growth regulation by Dpp and Fat drives uniform cell proliferation. Developmental Cell *20*, 123–130.

Shi, Y., and Massagué, J. (2003). Mechanisms of TGF-β Signaling from Cell Membrane to the Nucleus. Cell *113*, 685–700.

Silver, S.J., and Rebay, I. (2005). Signaling circuitries in development: insights from the retinal determination gene network. Development *132*, 3–13.

Smith, a V., and Orr-Weaver, T.L. (1991). The regulation of the cell cycle during *Drosophila* embryogenesis: the transition to polyteny. Development *112*, 997–1008.

Sundqvist, A., Liu, G., Mirsaliotis, A., and Xirodimas, D.P. (2009). Regulation of nucleolar signalling to p53 through NEDDylation of L11. EMBO Reports *10*, 1132–1139.

Takagi, M., Absalon, M.J., McLure, K.G., and Kastan, M.B. (2005). Regulation of p53 translation and induction after DNA damage by ribosomal protein L26 and nucleolin. Cell *123*, 49–63.

Thompson, B.J., and Cohen, S.M. (2006). The Hippo pathway regulates the bantam microRNA to control cell proliferation and apoptosis in *Drosophila*. Cell *126*, 767–774.

Tomlinson, A. (1985). The cellular dynamics of pattern formation in the eye of *Drosophila*. Journal of Embryology and Experimental Morphology *89*, 313–331.

Treisman, J.E., and Rubin, G.M. (1995). wingless inhibits morphogenetic furrow movement in the *Drosophila* eye disc. Development *121*, 3519–3527.

Tschochner, H., and Hurt, E. (2003). Pre-ribosomes on the road from the nucleolus to the cytoplasm. Trends in Cell Biology *13*, 255–263.

Twitty, V.C., and Schwind, J.L. (1931). The growth of eyes and limbs transplanted heteroplastically between two species of Amblystoma. Journal of Experimental Zoology *59*, 61–86.

Udan, R.S., Kango-Singh, M., Nolo, R., Tao, C., and Halder, G. (2003). Hippo promotes proliferation arrest and apoptosis in the Salvador/Warts pathway. Nature Cell Biology *5*, 914–920.

Wang, H., Boisvert, D., Kim, K.K., Kim, R., and Kim, S.H. (2000). Crystal structure of a fibrillarin homologue from Methanococcus jannaschii, a hyperthermophile, at 1.6 A resolution. The EMBO Journal *19*, 317–323.

Wang, S., Huang, J., He, J., Wang, A., Xu, S., Huang, S.-F., and Xiao, S. (2010). RPL41 , a Small Ribosomal Peptide Deregulated in Tumors , Is Essential for Mitosis and Centrosome Integrity. Neoplasia *12*, 284–293.

Warner, J.R., and McIntosh, K.B. (2009). How common are extraribosomal functions of ribosomal proteins? Molecular Cell *34*, 3–11.

Wartlick, O., Mumcu, P., Kicheva, a, Bittig, T., Seum, C., Jülicher, F., and González-Gaitán, M. (2011). Dynamics of Dpp signaling and proliferation control. Science *331*, 1154–1159.

Wharton, K., and Derynck, R. (2009). TGF-beta family signaling: novel insights in development and disease. Development *136*, 3691–3697.

Winter, J., Jung, S., Keller, S., Gregory, R.I., and Diederichs, S. (2009). Many roads to maturity: microRNA biogenesis pathways and their regulation. Nature Cell Biology *11*, 228–234.

Xu, N., Bagumian, G., Galiano, M., and Myat, M.M. (2011). Rho GTPase controls *Drosophila* salivary gland lumen size through regulation of the actin cytoskeleton and Moesin. Development *138*, 5415–5427.

Xue, S., and Barna, M. (2012a). Specialized ribosomes: a new frontier in gene regulation and organismal biology. Nat Rev Mol Cell Biol *13*, 355–369.

Xue, S., and Barna, M. (2012b). Specialized ribosomes: a new frontier in gene regulation and organismal biology. Nature Reviews. Molecular Cell Biology *13*, 355–369.

Zamore, P.D., and Haley, B. (2005). Ribo-gnome: the big world of small RNAs. Science *309*, 1519–1524.

Zecca, M., Basler, K., and Struhl, G. (1995). Sequential organizing activities of engrailed, hedgehog and decapentaplegic in the *Drosophila* wing. Development *121*, 2265–2278.

Zhang, H., Stallock, J.P., Ng, J.C., Reinhard, C., and Neufeld, T.P. (2000). Regulation of cellular growth by the *Drosophila* target of rapamycin dTOR. Genes & Development . 14, 2712–2724.

Zhang, Y., and Lu, H. (2009). Signaling to p53: ribosomal proteins find their way. Cancer Cell *16*, 369–377.

Zheng, X., Wang, J., Haerry, T.E., Wu, A.Y.-H., Martin, J., O'Connor, M.B., Lee, C.-H.J., and Lee, T. (2003). TGF-beta signaling activates steroid hormone receptor expression during neuronal remodeling in the *Drosophila* brain. Cell *112*, 303–315.

Zheng, X., Zugates, C.T., Lu, Z., Shi, L., Bai, J., and Lee, T. (2006). Baboon/dSmad2 TGF-beta signaling is required during late larval stage for development of adult-specific neurons. The EMBO Journal *25*, 615–627.

Zhu, C.C., Boone, J.Q., Jensen, P. a, Hanna, S., Podemski, L., Locke, J., Doe, C.Q., and O'Connor, M.B. (2008). *Drosophila* Activin- and the Activin-like product Dawdle function redundantly to regulate proliferation in the larval brain. Development *135*, 513–521.

Ziosi, M., Baena-López, L.A., Grifoni, D., Froldi, F., Pession, A., Garoia, F., Trotta, V., Bellosta, P., Cavicchi, S., and Pession, A. (2010). dMyc functions downstream of Yorkie to promote the supercompetitive behaviour of hippo pathway mutant cells. PLoS Genetics *6*,. 1-11